

**FLUID REPLACEMENT MODEL (FRM) ANALYSIS
OF TELISA SAND RESERVOIR :
YM FIELD, SOUTH SUMATRA BASIN**

THESIS

**YOESE MARIAM
0706171636**



**PHYSICS GRADUATE PROGRAM
FACULTY OF MATHEMATIC AND NATURAL SCIENCE
JAKARTA
JULY, 2009**

PAGE OF APPROVAL

JUDUL : FLUID REPLACEMENT MODEL ANALYSIS OF TELISA
SAND RESERVOIR : YM FIELD, SOUTH SUMATRA BASIN

NAMA : YOESE MARIAM

NPM : 0706171636

APPROVED AS TO STYLE AND CONTENT BY :

Prof. Dr. Suprajitno Munadi
Supervisor

Dr. Ricky Adi Wibowo
Examiner

Dr. Waluyo
Examiner

Dr. Abdul Haris
Examiner

PHYSICS GRADUATE PROGRAM
FACULTY OF MATHEMATIC AND NATURAL SCIENCE

Dr. Dedi Suyanto

NIP. 130 935 271

Date of Final Examination : July 3, 2009

Abstract

Rock physics data is a tool for fluid identification and quantification in reservoir, and also plays an important part in any fluid substitution study that may provide a valuable tool for modeling various fluid scenarios. This thesis presents the results of the two well cases where the effect of rock and fluid properties on seismic response are illustrated. Both of wells (YM-232 and YM-247) show the effect of replacing hydrocarbons with brine. This effect illustrates how rock and fluid properties along with reflection amplitudes can be used to estimate fluid type in YM field. First synthetic using the original case. And the other synthetic by using FRM case, with an assumption that the fluid was brine/oil and the mineralogy was clean sand. These amplitude was extracted to be correlated with the real seismic data. Finally, a good correlation was obtain from a model to estimate the fluid type in prospect based on amplitude information in seismic data. In other word, we can understand the effect of hydrocarbon saturation on synthetic offset gathers. This analysis can be use as one of parameter to improve seismic 3D interpretation and to reduce drilling risk.

Abstrak

Data *Rock Physics* adalah alat untuk identifikasi fluida, perhitungan dalam reservoir, dan bagian penting dalam studi substitusi fluida untuk memodelkan berbagai macam fluida. Thesis ini merupakan hasil dari penelitian dua sumur untuk melihat pengaruh dari batuan dan properti fluida terhadap respon seismik. Kedua sumur tersebut adalah (YM-232 dan YM-247) merupakan *oil well* yang menunjukkan pengaruh dari substitusi hidrokarbon dengan air. Akibat dari substitusi fluida terhadap batuan dan properti fluida menunjukkan respon tertentu pada refleksi amplitude, variasi amplitude tersebut dapat digunakan sebagai *guide* untuk memperkirakan penyebaran jenis fluida pada lapangan YM. Pertama dengan melakukan sintetik pada keadaan insitu. Diikuti dengan sintetik pada kondisi tersaturasi (*FRM*), dengan menganggap bahwa fluida adalah air/minyak dan mineral adalah batu pasir bersih. Amplitude ini akan diekstrak untuk dikorelasikan dengan data seismic yang sebenarnya. Koefisien korelasi yang memiliki nilai tinggi (~ 1) dijadikan sebagai model untuk memprediksi tipe fluida pada area prospek yang didasarkan pada informasi amplitude dari data seismic. Dengan kata lain, kita dapat memahami efek dari saturasi hidrokarbon terhadap *synthetic offset gathers*. Analisis ini digunakan sebagai salahsatu parameter untuk mengembangkan interpretasi data seismic 3D & untuk menekan/mengurangi resiko pengeboran.

Foreword

All praise be to ALLAH SWT for His blessing & mercy, so that I can accomplish my thesis.

I sincerely thank my supervisor, Profesor Suprajitno Munadi, for his guidance and his patience. The arguments with him helped me to clear my thoughts and remember the concepts that I forgot. Without his insistence, I would not have gone this far into FRM seismogram.

I also want to thank my friends for helping me and giving me helpful suggestions and also the examiner team. The discussion with them is very helpful for my progress.

Finally, the support of my parents should not be understated. Particularly, I dedicated my thesis to my beloved mother for her patience and endless prayer.

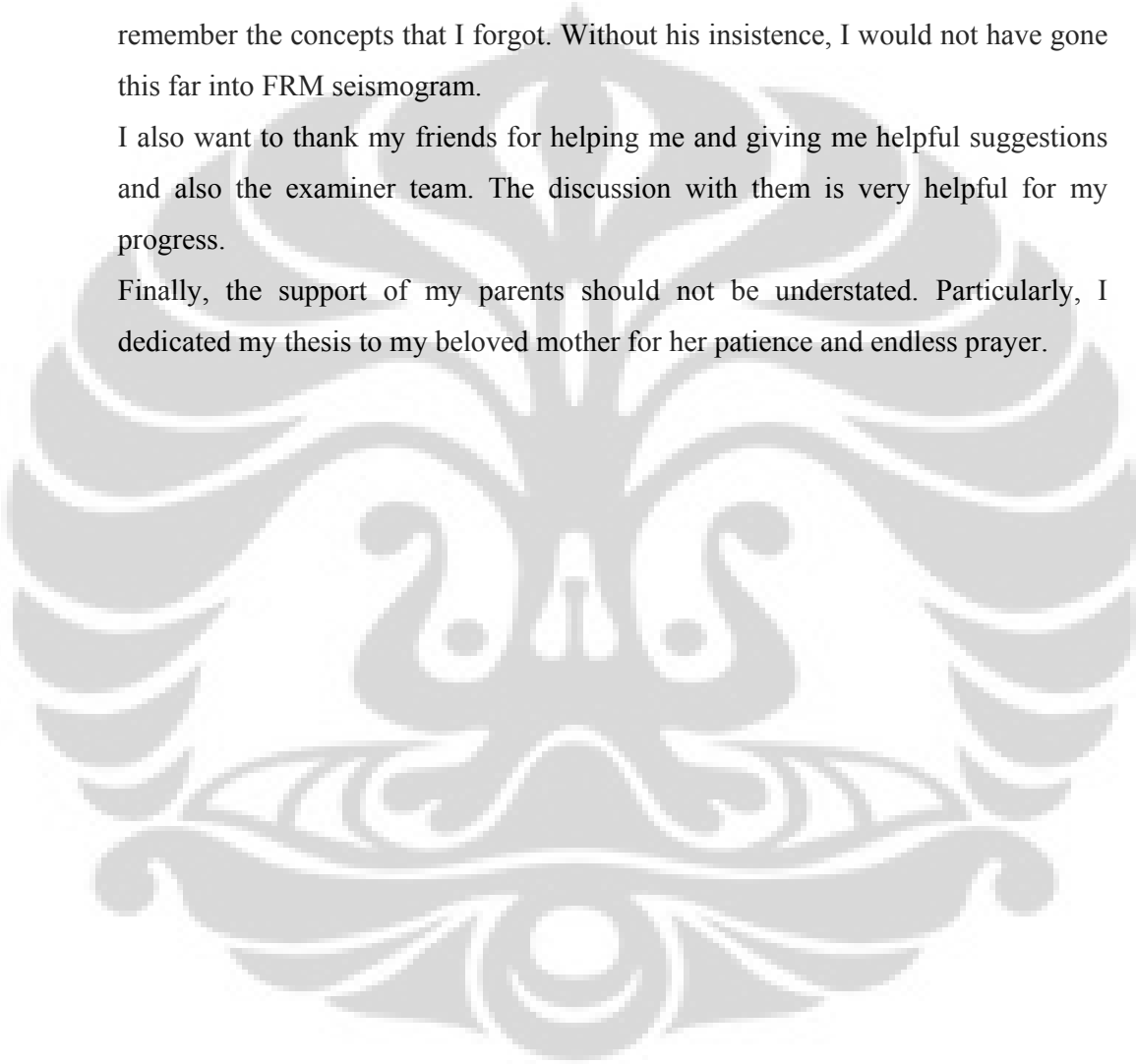


Table of Contents

	Page
Title page.....	i
Approval page	ii
Abstract	iii
Foreword	iv
Table of Contents	v
Table of figures.....	vi
Chapter 1. Introduction	1
1.1. Background	1
1.2. Objectives	2
1.3. Study Area	2
Chapter II. Theoretical Background.....	2
2.1. Regional Geology Setting.....	2
2.1.1 Structure & Tectonic.....	4
2.1.2 Tectonostratigraphy.....	4
2.2. Telisa Sandstone Characterizations.....	4
2.3. Rock Physics Theory.....	5
2.3.1 Rock Physics Properties of Shaly Sand.....	6
2.4. Fluid Substitutiton – Gassmann.....	9
2.4.1 Rock Properties.....	10
2.4.2 Using Gassmann’s Equation.....	13
2.4.3 Porosity.....	13
2.4.4 Fluid Properties.....	14
2.4.5 Matrix Properties.....	14
2.4.6 Frame Properties.....	14
2.4.7 Calculating Velocities.....	15
2.4.8 Dry Frame Bulk Modulus, K^*	15
2.5. Effect of Fluid Saturation on Seismic Properties.....	16
2.6. Theoretical Model.....	16
2.6.1 Internal Consistency & Saturation Modeling.....	16
Chapter III. Data and Methodology	16

3.1	Methodology.....	17
3.1.1	Fluid Substitution.....	20
3.2	Data.....	20
3.3	Wavelet Extraction & Well Seismic Tie.....	21
Chapter IV. Analysis and Interpretation		22
4.1	Data Processing.....	22
4.2	Sensitivity Analysis.....	25
4.3	Fluid Substitution.....	25
4.4	Wavelet Extraction & Well Seismic Tie.....	26
4.5	Rock Physics Analysis & Synthetic Offset Gathers.....	35
4.5.1	The Analysis of The Telisa Sand Reservoir at YM- 232 Well.....	36 35
4.5.2	The Analysis of The Telisa Sand Reservoir at YM- 247 Well.....	46
4.6	Comparison between Model Amplitude & Real Seismic...	58
Chapter V. Conclusions & Recommendation.....		69
	References.....	71

Table of Figures

	Page
Figure 1.1. Map showing the area of the thesis in YM Block at South Sumatra Basin	3
Figure 2.1. Stratigraphy of South Sumatra.....	5
Figure 2.2. Lines of Vp vs Pore for Shales with varying silt content....	11
Figure 2.3 Pore & P-wave Velocity vs Clay Content for Shaly Sands & Sandy Shales.....	12
Figure 3.1 Work Flowchart.....	24
Figure 4.1 Composite Log YM-232 Well.....	25
Figure 4.2. Composite Log YM-247 Well.....	26
Figure 4.3. Porosity vs Sw & Porosity vs Vclay at YM-232 Well.....	27
Figure 4.4. Porosity vs Sw & Porosity vs Vclay at YM-247 Well.....	27
Figure 4.5 Crossplot Gamma Ray vs VpVs_Ratio with Color Key Gamma Ray.....	28
Figure 4.6 Crossplot Gamma Ray vs VpVs_Ratio with Color Key Porosity.....	29
Figure 4.7 Crossplot Gamma Ray vs VpVs_Ratio with Color Key Saturasi.....	30
Figure 4.8 Fluid Substitution at YM-232 Well.....	32
Figure 4.9 Fluid Substitution at YM-247 Well.....	33
Figure 4.10 Frequency Dominant at 40 Hz & Wavelet Extraction.....	34
Figure 4.11 Correlation with Ricker 40 Hz at YM-232 Well.....	34
Figure 4.12 Correlation with Ricker 40 Hz at YM-247 Well.....	35
Figure 4.13 Crossplot Velocity – Water Saturation (10%)_YM-232 Well.....	37
Figure 4.14 Crossplot Velocity – Water Saturation (100%)_YM-232 Well.....	38
Figure 4.15 Crossplot Velocity – Water Saturation (40% & 70%)_YM-232 Well.....	39
Figure 4.16 Crossplot Velocity – Water Saturation (80% & 90%)_YM-232 Well.....	39

Figure 4.17 Crossplot Density – Water Saturation (10% & 100%)_YM-232 Well.....	40
Figure 4.18 Crossplot Density – Water Saturation (40% & 70%)_YM-232 Well.....	41
Figure 4.19 Crossplot Velocity – Porosity (10% & 100% water saturaton)_YM-232 Well.....	42
Figure 4.20 Crossplot Density – Water Saturation (80% & 90%)_YM-232 Well.....	43
Figure 4.21 Crossplot Velocity – Porosity (40% & 70% water saturaton)_YM-232 Well.....	44
Figure 4.22 Crossplot P-impedance – Porosity YM-232 Well.....	44
Figure 4.23 Crossplot P-impedance – Water Saturation YM-232 Well..	45
Figure 4.24 Crossplot Velocity – Water Saturation (10% & 100%)_YM-247 Well.....	47
Figure 4.25 Crossplot Velocity – Water Saturation (40% & 70%)_YM-247 Well.....	48
Figure 4.26 Crossplot Density – Water Saturation (10% & 100%)_YM-247 Well.....	49
Figure 4.27 Crossplot Density – Water Saturation (40% & 70%)_YM-247 Well.....	50
Figure 4.28 Crossplot Velocity – Porosity (10% & 100% water saturaton)_YM-247 Well.....	51
Figure 4.29 Crossplot Velocity – Porosity (40% & 70% water saturaton)_YM-247 Well.....	52
Figure 4.30 Crossplot P-impedance – Porosity YM-247 Well.....	52
Figure 4.31 Crossplot P-impedance – Water Saturation YM-247 Well..	53
Figure 4.32 Synthetic Seismic at YM-232 Well with 2000 ft Offset (Insitu Case & Saturated Case).....	53
Figure 4.33 AVO Crossplot at YM-232 Well with 2000 ft Offset.....	54
Figure 4.34 Synthetic Seismic at YM-247 Well with 2000 ft Offset (Insitu Case & Saturated Case).....	54
Figure 4.35 AVO Crossplot at YM-247 Well with 2000 ft Offset.....	55
Figure 4.36 The Behavior of Sonic Transit Time in The Reservoir	

Rock as Fluid Content Increases. Red Indicates Oil & Blue Indicates Water. (Suprajitno Munadi, 2007).....	56
Figure 4.37 AVO Analysis (Intercept & Gradient of Top & Bottom Telisa Sand) for Synthetic of YM-232 Well (insitu case & substituted with 10%water saturation).....	56
Figure 4.38 AVO Analysis (Intercept & Gradient of Top & Bottom Telisa Sand) for Synthetic of YM-232 Well (substituted with 70% & 100% water saturation).....	57
Figure 4.39 AVO Analysis (Intercept & Gradient of Top & Bottom Telisa Sand) for Synthetic of YM-247 Well (insitu case & substituted with 10% water saturation).....	57
Figure 4.40 AVO Analysis (Intercept & Gradient of Top & Bottom Telisa Sand) for Synthetic of YM-247 Well (substituted with 70% & 100% water saturation).....	58
Figure 4.41 The Correlation Coefficient Real Amplitude to Model after Substituted Insitu Case YM-232 Well.....	59
Figure 4.42 ρ , V_p , & V_s _Synthetic Offset Gathers (insitu case, substituted with 10%, & 100% water saturation)_YM-232 Well.....	59
Figure 4.43 The Correlation Coefficient Real Amplitude to Model after Substituted with 10% Water Saturation YM-232 Well.....	60
Figure 4.44 The Correlation Coefficient Real Amplitude to Model after Substituted with 70% Water Saturation YM-232 Well.....	60
Figure 4.45 ρ , V_p , & V_s _Synthetic Offset Gathers (insitu case, substituted with 40%, & 70% water saturation)_YM-232 Well.....	61
Figure 4.46 The Correlation Coefficient Real Amplitude to Model after Substituted with 90% Water Saturation YM-232 Well.....	61
Figure 4.47 The Correlation Coefficient Real Amplitude to Model after Substituted with 100% Water Saturation YM-232 Well.....	62
Figure 4.48 ρ , V_p , & V_s _Synthetic Offset Gathers (insitu case, substituted with 80%, & 90% water saturation)_YM-232	

Well.....	62
Figure 4.49 The Correlation Coefficient Real Amplitude to Model Amplitude after Normalized YM-232 Well.....	63
Figure 4.50 The Correlation Coefficient Real Amplitude to Model Amplitude for Insitu Case YM-247 Well.....	63
Figure 4.51 The Correlation Coefficient Amplitude Model to Real Amplitude after Substituted with 10% Water Saturation YM-247 Well.....	64
Figure 4.52 The Correlation Coefficient Amplitude Model to Real Amplitude after Substituted 40% Water Satruation YM- 247 Well.....	64
Figure 4.53 ρ , V_p , & V_s _Synthetic Offset Gathers (insitu case, substituted with 10%, & 100% water saturation)_YM-247 Well.....	65
Figure 4.54 The Correlation Coefficient Amplitude Model to Real Amplitude after Substituted with 70% Water Saturation....	65
Figure 4.55 ρ , V_p , & V_s _Synthetic Offset Gathers (insitu case, substituted with 40%, & 70% water saturation)_YM-247 Well.....	66
Figure 4.56 The Correlation Coefficient Amplitude to Real Amplitude after Substituted with 100% Water Satruation _YM-247 Well.....	66
Figure 4.57 The Correlation Coefficient between Real Amplitude & Model Amplitude after Normalized _YM-247 Well.....	67
Figure 4.58 The Amplitude Distribution from Real Seismic.....	68

Abstract

Rock physics data is a tool for fluid identification and quantification in reservoir, and also plays an important part in any fluid substitution study that may provide a valuable tool for modeling various fluid scenarios. This thesis presents the results of the two well cases where the effect of rock and fluid properties on seismic response are illustrated. Both of wells (YM-232 and YM-247) show the effect of replacing hydrocarbons with brine. This effect illustrates how rock and fluid properties along with reflection amplitudes can be used to estimate fluid type in YM field. First synthetic using the original case. And the other synthetic by using FRM case, with an assumption that the fluid was brine/oil and the mineralogy was clean sand. These amplitude was extracted to be correlated with the real seismic data. Finally, a good correlation was obtain from a model to estimate the fluid type in prospect based on amplitude information in seismic data. In other word, we can understand the effect of hydrocarbon saturation on synthetic offset gathers. This analysis can be use as one of parameter to improve seismic 3D interpretation and to reduce drilling risk.

Abstrak

Data *Rock Physics* adalah alat untuk identifikasi fluida, perhitungan dalam reservoir, dan bagian penting dalam studi substitusi fluida untuk memodelkan berbagai macam fluida. Thesis ini merupakan hasil dari penelitian dua sumur untuk melihat pengaruh dari batuan dan properti fluida terhadap respon seismik. Kedua sumur tersebut adalah (YM-232 dan YM-247) merupakan *oil well* yang menunjukkan pengaruh dari substitusi hidrokarbon dengan air. Akibat dari substitusi fluida terhadap batuan dan properti fluida menunjukkan respon tertentu pada refleksi amplitude, variasi amplitude tersebut dapat digunakan sebagai *guide* untuk memperkirakan penyebaran jenis fluida pada lapangan YM. Pertama dengan melakukan sintetik pada keadaan insitu. Diikuti dengan sintetik pada kondisi tersaturasi (*FRM*), dengan manganggap bahwa fluida adalah air/minyak dan mineral adalah batu pasir bersih. Amplitude ini akan diekstrak untuk dikorelasikan dengan data seismic yang sebenarnya. Koefisian korelasi yang memiliki nilai tinggi (~1) dijadikan sebagai model untuk memprediksi tipe fluida pada area prospek yang didasarkan pada informasi amplitude dari data seismik. Dengan kata lain, kita dapat memahami efek dari saturasi hidrokarbon terhadap *synthetic offset gathers*. Analisis ini digunakan sebagai salahsatu parameter untuk mengembangkan interpretasi data seismic 3D & untuk menekan/mengurangi resiko pengeboran.

Chapter 1

Introduction

1.1. Background

One of the productive reservoirs in South Sumatra Basin, is sandstones of the Telisa formation. Now, reservoir pressure decreases, gas comes out of solution, remaining oil phase changes, net stress increases, and rock stiffens. To maintain the production rate, exploration efforts continue with new ideas and concepts. The Telisa sandstone, consists of very fine to fine grained sandstones with minor shales, deposited in a shallow marine shoreface setting during both sea level lowstand and transgression.

Rock physics data allow us to make an analysis, which provides a tool for fluid identification and quantification in reservoir, and also plays an important role in any fluid substitution study that may provide a valuable tool for modeling various fluid scenarios.

According to Castagna (2001), an objective of seismic analysis is to quantitatively extract lithology, porosity, and pore fluid content directly from seismic data. Rock physics provides the fundamental basis for seismic lithology determination. The ultimate question in rock physics for direct hydrocarbon indication is 'How do velocities change when pore fluid content changes?'. More specifically, we need a rock physics model that can transform velocities from one saturation state to another.

A simple example combines Gassmann's deterministic equation for fluid substitution with statistics inferred from log, core, and seismic data to detect hydrocarbons from observed seismic velocities. The formulation is applied to a well log example for detecting the most likely pore fluid and quantifying the associated uncertainty from observed sonic and density logs. The formulation offers a convenient way to implement deterministic fluid substitution equations in the realistic case when natural geologic variations cause the reference porosity and velocity to span a range of values.

1.2. Objectives

The objectives of this thesis are :

- 1) To predict the elastic behaviour of rock property by the fluid replacement methods.
- 2) To understand the effect of hydrocarbon saturation on synthetic offset gathers
- 3) To get a model as the best practice of quantitative and qualitative predictions, the model is expected could be applied and tested to other exploration and/or development field in South Sumatra.

1.3. Study Area

The study area is located in South Sumatra basin. The largest oil field in the region is the YM oil field. It is believed that one of the potential candidates is sandstone of the Telisa formation. Telisa sandstone contributes significant additional reserves at YM field where production after hydraulic fracturing of 20 wells could reach 4,000 BOPD. While in Old YM, production of 7 wells (after hydraulic fracturing) reached 750 BOPD.

The Telisa Sandstone, which includes the sandstones in the lower part of the Telisa formation, consists of very fine to fine-grained sandstones with minor shales, deposited in a shallow marine shoreface setting during both sea level lowstand and transgression. The acoustic impedance contrast between the sandstones and the overlying and underlying “Telisa” shales is very small because of highly argillaceous content of the sandstone. The hydrocarbon potential in this “Telisa” sandstone play remains unknown, but the results are encouraging. Several successful tests have been conducted through the hydraulic fracturing efforts. Although most of the sandstones are relatively tight, the reservoir flows oil.

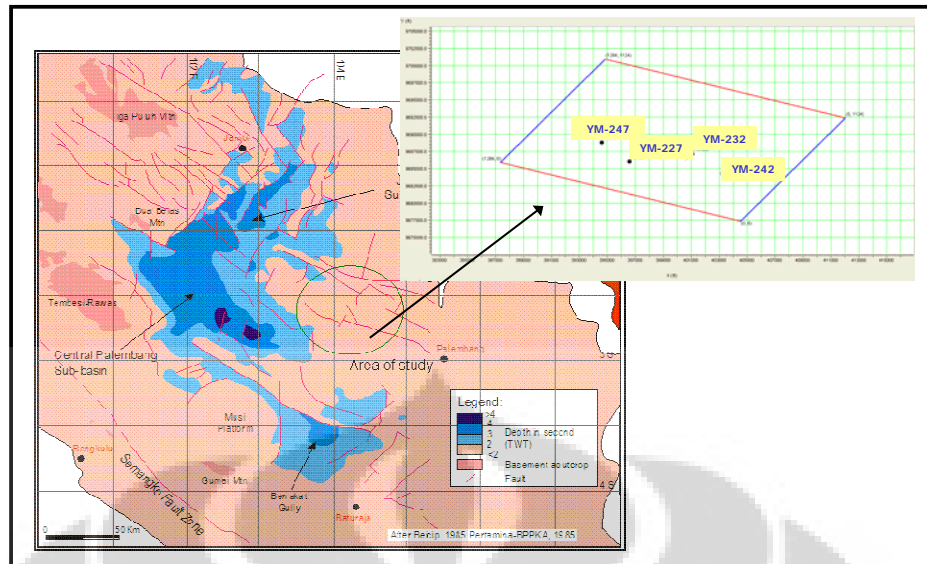
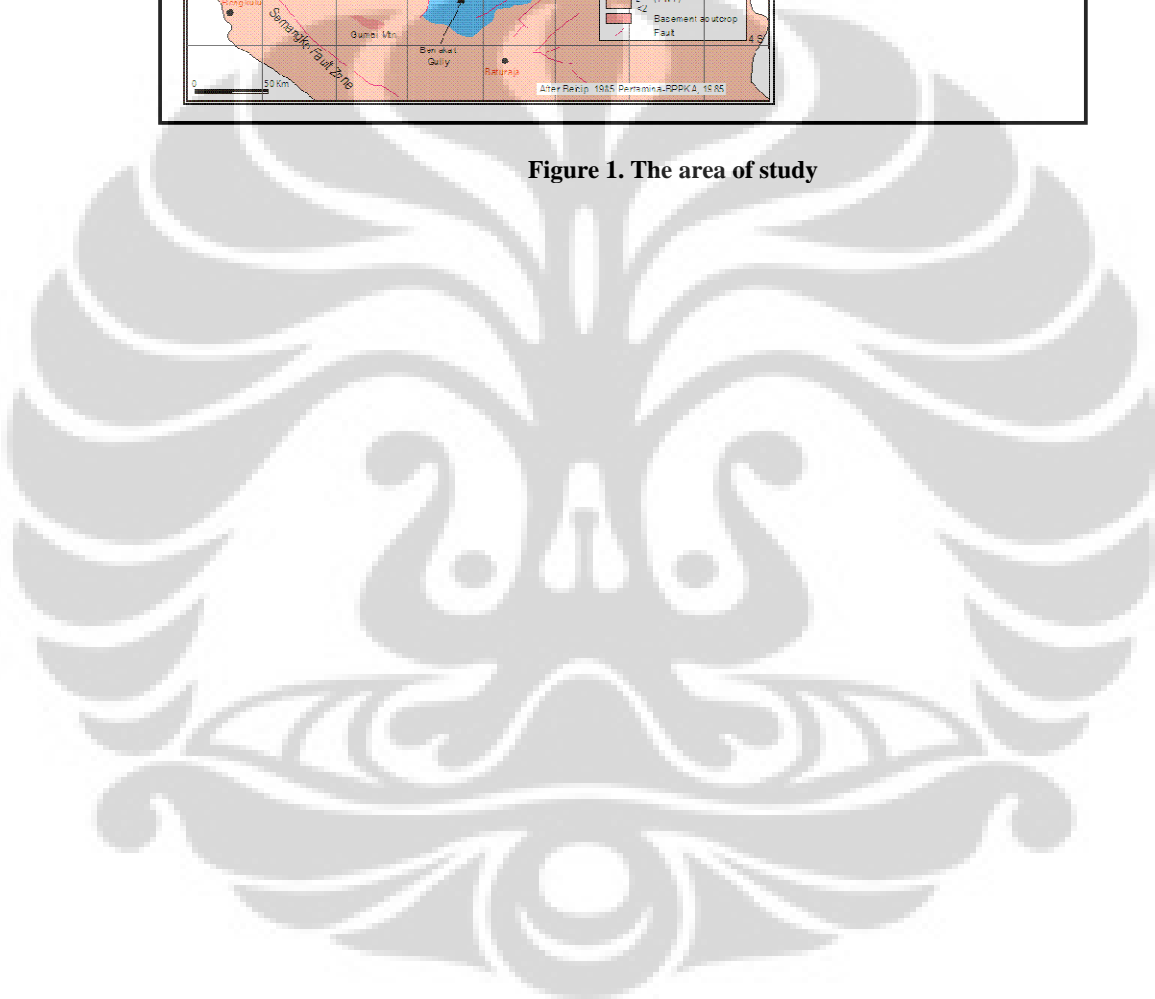


Figure 1. The area of study



Chapter 2

Theoretical Background

2.1 Regional Geology Setting

2.1.1 Structure & Tectonic

The study area is part of the YM Block, within South Sumatra Basin in Palembang Province, Indonesia. The South Sumatra Basin was formed as a result of crustal extension at Paleogene time. The basins is divided into three sub-basins : Jambi sub-basin, Central Palembang sub-basin, and South Palembang sub-basin. The dominant structure within the basin are : : WNW-ESE, N-S, NW-SE and $\pm N 30^{\circ}E$ (Pulunggono et. al., 1992), which were generated by both Australian Plate and Sundaland interaction.

The WNW-ESE strike slip system is the oldest structure generated during tectonic compression phase in Pre-Tertiary time. The lithology of the basement complexes consist of the Mesozoic igneous rock as wells as Paleozoic and Mesozoic metamorphic and carbonate.

During early Tertiary time (Eocene to Oligocene), tectonic stress and extension (resulting from northward movement of the Australian plate) formed rift or half-graben complexes along much of southern margin of the Sunda Shelf plate (Hall, 1997; Longley, 1997; Sudarmono, et. al., 1997). The half-graben complexes were formed by N-S trend normal fault and reactivated WNW-ESE growth fault. In this event, deposits began to fill the basin in response to the half-graben architectural style and basin subsidence (Bishop, 1988). Additional synrift deposits of tuffaceous sands, conglomerates, breccias and clays have deposited in fault and topographic low by alluvial, fluvial and lacustrine processes. The sediments were deposited in a transgressive-regressive cycles.

Many of the normal faults that formed the depositional basin in South Sumatra have been reactivated and some have been reversed during Miocene to Plio-Pleistocene compression and basin inversion (Sudarmono et. al., 1997).

The Plio-Pleistocene compression created the NW-SE trending, a normal type fault with some lateral displacement as the most prominent feature, and some other small faults and folds (Hutapea, 1998).

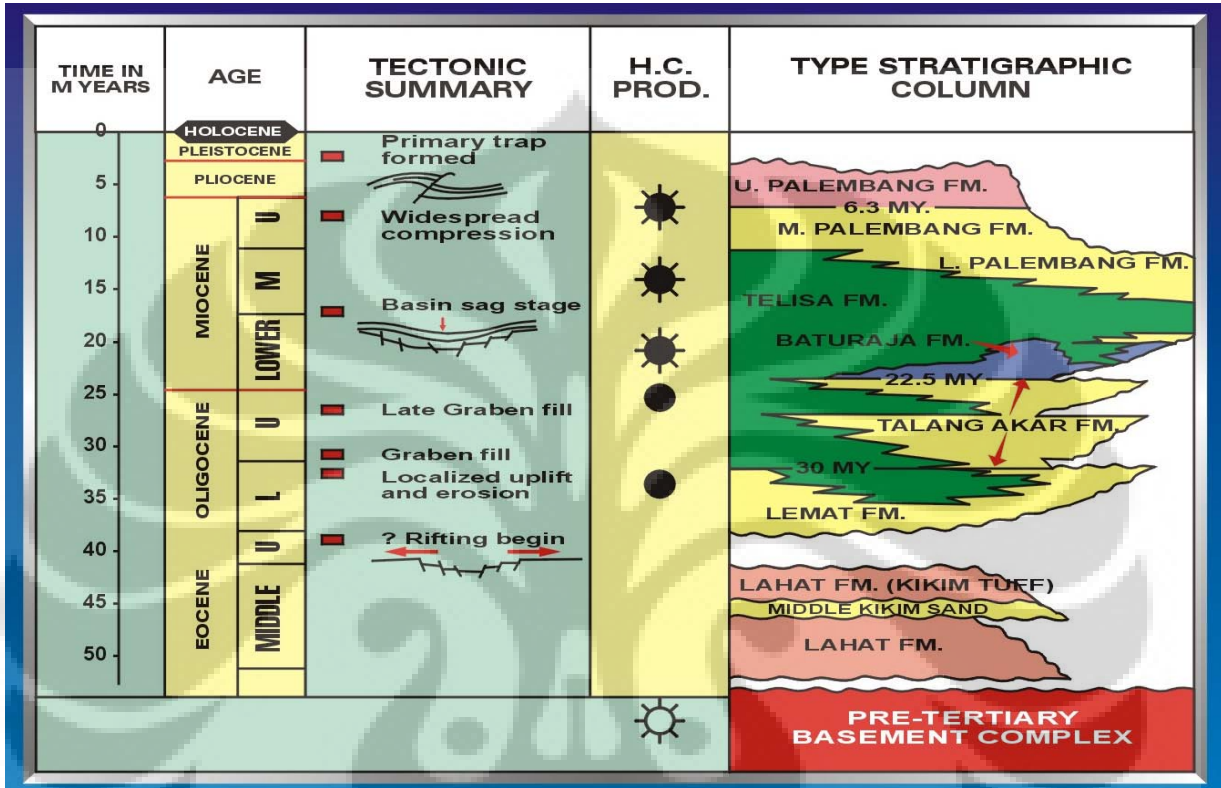


Figure 2.1. Stratigraphy South Sumatera

2.1.2 Tectonostratigraphy

The Lemat Formation has been deposited in a continental environment during Paleocene to Early Oligocene time. This formation is normally bounded at its base and top by an unconformity (Guruh et. al, 2003). The coarse clastic member of the Lemat Formation is composed of sandstones, clays, rock fragment, breccias, granite wash.

Sedimentation was renewed in the Upper Oligocene to Lower Miocene with the deposition of the Talangakar marine clastic (TAF) during transgressive cycle in deltaic to shallow marine environment.

Widespread marine transgression in the Late Oligocene to Early Miocene resulted in clastic deposits overlying Talangakar Formation and in developments of platform carbonates and carbonate build-up of the Baturaja Formation (BRF) above the TAF.

Maximum transgression in the Middle Miocene deposited the clastic shallow marine of the Gumai (Telisa) Formation across the region. It is characteristically fossiliferous, marine shale, containing occasional thin beds of glauconitic limestone.

Development of the Barisan Mt., and possible volcanic islands to the south and southeast during Mid. Miocene – Plio Pleistocene, further decreased and then cut off and overwhelmed marine influence and added new clastic and volcano clastic sources from those directions (Hamilton, 1979).

The Formation which has been deposited during regressive cycle is Airbenakat Formation and Muaraenim Formation. The Airbenakat Formation composed of shale with glauconitic sandstones and occasional limestone, deposited in a neritic environment at the base grading to a shallow marine environment at the top. The Muaraenim Formation has been deposited in shallow marine-brackish (at the base), paludal, deltaplain, and non-marine environment and are composed of sandstones, mudstones and coal (Guruh et, al, 2003).

2.2 Telisa Sandstone Characterizations

The telisa sandstone is the lower part of The Gumai Formation which has been deposited during Early Miocene (NN4-NN3; Geoservices, 2001). It is bounded by Top BRF at the lower part.

The lithology of the telisa sand interval consists of shale, glauconitic calcareous sandstone, calcareous sandstone and thin bed limestone. Interbedded limestone and shale present in the lower part of the telisa sand interval. This lithology shows coarsening upward and it can be recognized from the cores and log character. It is overlaid by hummocky cross stratification calcareous sandstone. The hummocky sandstone is overlaid by shale with thin intercalated fine sand.

The telisa Sandstone, which includes the sandstones in the lower part of the Telisa formation, consists of very fine to fine grained sandstones with minor

shales, deposited in a shallow marine shoreface setting during both sea level lowstand and transgression. The acoustic impedance contrast between the sandstones and the overlying and underlying “telisa” shales is very small because of highly argillaceous content of the sandstone.

The Telisa formation is lithostratigraphically defined as shallow to deep open marine, dark grey shales. The shallow marine shales have been observed in the Palembang High area. In this region, the lower part of the formation usually contains thin reservoir sandstones called “Telisa Sandstone” and has thicknesses ranging from 20 to 80 feet.

Wireline log motifs of the Telisa sandstone sequence varies significantly from well to well. The sequence in the YM wells generally shows a blocky motif, occasionally coarsening upward in the lower portion and fining upward in the upper part, with an erosional surface in between. Based on this log shape and core descriptions, the sandstones can be subdivided into several more detailed facies lobes. In general, the sandstones are light olive gray, all fine and very fine grained, claceros, angular to subrounded, very well sorted lithic arenites with feldspar and substantial numbers of globigerinids, small benthic foraminifers, small echinoid spines, and splinters of vertebrate bone. It is a mix of sediment particles, created in a fully marine environment (pelagic skeletal materials) with detrital particles (fine sand and some clay mud) wafted in from the nearby coast. Wavy lamination and ripple bedding, and bioturbated to various degrees, suggest deposition below the fair weather wave base but it could be close to the storm wave base.

The overall Telisa sandstone sequence in the Palembang High region was deposited during N5-N6 (middle Early Miocene). The water depth is increasing from the top Baturaja to the shales overlying the Telisa sandstone : middle neritic to upper bathyal. This is consistent with the major transgression period during deposition of the Telisa formation. Following this transgression, a series of regional regression occurred when the Palembang Group (Lower, Middle, and Upper Palembang Formations) was deposited across the South Sumatra Basin.

The Telisa sandstone is present at shallow depths between 1700’ and 2500’. The sandstone generally has low permeability causing low production. To improve the production performance, the stimulation technique called “hydraulic

fracturing” has been employed. This technique uses hydraulic power to create crack or opening at the reservoir, followed by pumping sand to fill the crack to avoid closing.

Efforts to optimize the fracturing results have been made using six sigma (statistical approach) and analytical approaches. The goal is to focus on increasing oil gain from the fracturing job. The first step is to identify all factors that could impact oil gain. The candidate selection criteria include area (field), resistivity, and hydrocarbon pore thickness (HPT). Fracturing design includes fracturing length, fracturing conductivity, propan size, and propan loads. Each of these factors is evaluated using statistical analysis.

The second step is to evaluate data using a statistical approach: hypothesis test, such as t-test and F-test. The t-test is to compare the mean of the two data sets while the F-test is to compare the standard deviation of the two data sets. By using these hypothesis tests the impact of the factors to the fracturing results can be predicted. The evaluation continues for all of the factors and is combined with the analytical approach using a fracturing simulator to determine the candidate selection criteria and fracturing design.

The third step is the execution plan and field trials in the YM wells to confirm the work results. The TSO fracturing design was applied in the Y Field wells and the long hydraulic fracturing design was applied in the M wells.

The fourth step is monitoring work. Initially the oil production, after the fracturing job, from the selected YM wells is high. There was significant oil gain improvement after the work. The mean oil gain after the work was 220 BOPD (35 m³/day) compared to the mean oil gain before the work of 168 BOPD (26.7 m³/day). Standard deviation also decreased from 186 BOPD (26.9 m³/day) to 130 BOPD (20.7 m³/day). The performance of the wells will have to be closely monitored.

There are some challenges in optimizing fracturing job results such as sand flow back to the well bore, production drop after production for 3-5 months, and high water cut. Sand flow back to the well bore will not only cause problems for the facilities such as pipe line and pumps, but will also result in productivity reduction. Both the causes of the problems and how to control them needs to be addressed. The application of resin-coated sand may be one suitable means of

preventing this happening in the future. The production drop after initially good production appears to happen in those wells that have extremely low permeability, as indicated by the low resistivity values. To develop the wells that have resistivity less than 5 ohm-m, will need further economic study will be required.

2.3 Rock Physics Theory

Rock physics reservoir characterization is based on applying rock physics relations, such as between velocity and porosity, to a volume of seismic velocity or impedance resulting from seismic inversion. The relevant rock physics laws are often derived from well log data. The spatial scale of log measurements is much smaller than the seismic scale. It is important to upscale rock physics relations used or to make sure that they hold at the seismic scale.

Physical properties of porous rocks, such as seismic velocity, depend on elastic properties of the porous frame and the pore-space filling material. The elastic properties such as velocity, density, impedance, and V_p/V_s ratio take an important role in reservoir characterization because they are related to the reservoir properties. To analyze these elastic properties, rock physics knowledge is a bridge that links the elastic properties to the reservoir properties such as water saturation, porosity, and shale volume.

Rock physics is an indispensable tool for an efficient interpretation, providing the basic relationship between the lithology, fluid, and geological deposition environment of the reservoir. Also, rock physics modeling can be utilized to build a template for efficient reservoir characterization (Ødegaard and Avseth, 2004; Avseth et al., 2006; Andersen and Wijngaarden, 2007). In reservoir property analysis, the lithology and fluid content or saturation can not be predicted efficiently by identifying different clusters in the cross plot of elastic properties. In contrast, the elastic properties inverted from seismic data can be efficiently interpreted in conjunction with a rock physics template, which in turn can be used to predict lithology and fluid content.

Gassmann's equation is applied to estimate the fluid substitution effect in a rock physics template and thereby the elastic modulus of dry and saturated rock.

The pore fluid properties are controlled by reservoir pressure, temperature, and water saturation.

Usually, upon water saturation from the dry state, P-wave increases slightly and S-wave decrease slightly. The velocity response to water saturation is rather complex and physically controlled by the influence of the pore fluid on the rock moduli :

$$V_p = \sqrt{\frac{K_u + \frac{4}{3}\mu}{\rho_u}}$$

$$V_s = \sqrt{\frac{\mu}{\rho_u}}$$

Compressional (P) velocity.....equation (2.1)

Shear (S) velocity.....equation (2.2)

First equation is the compressional (or P) velocity, which is the velocity for the particle motion parallel to the direction of propagation. The second equation is the shear (or S) velocity which is the velocity for the particle motion perpendicular to the direction of propagation.

2.3.1. Rock Physics Properties of Shaly Sand

By analogy with the friable-sand model, we use the modified Hashin Shtrikman lower bound to model constant-clay lines for shaly sands. These lines can be used to define subfacies of sands where the facies changes associated with varying clay content. Alternatively, we can use the more empirical Vp-porosity-clay trends of Han (1986), or the lithology lines of Vernik (1992).

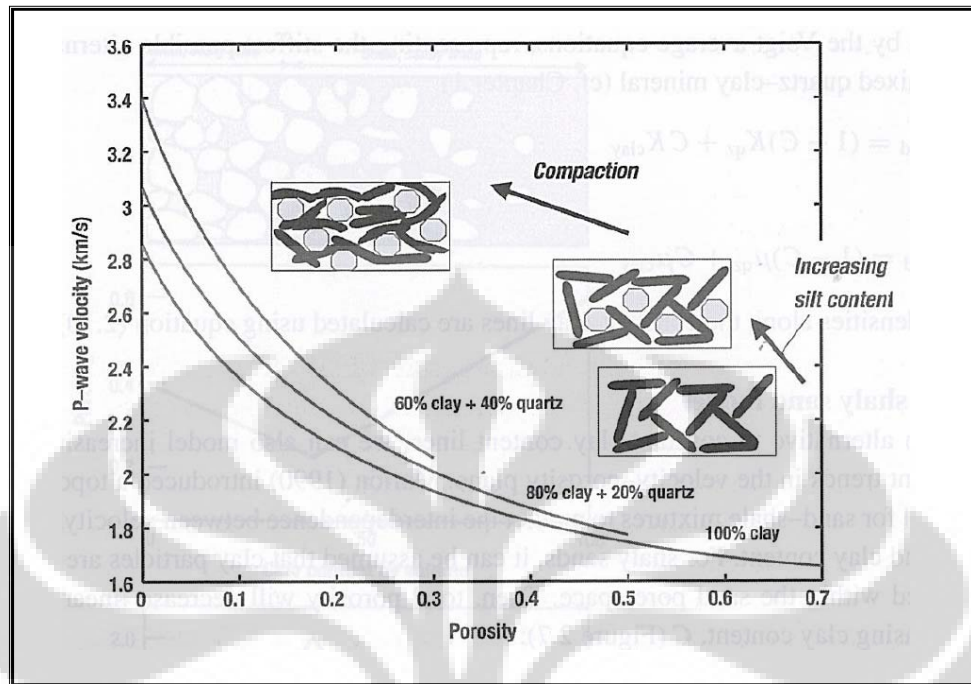


Figure 2.2 Lines of V_p versus porosity for shales with varying silt content. The lines are modeled using modified lower bound Hashin-Shtrikman combined with Hertz-Mindlin theory

In shaly sands, we can assume that the clay particles fill in the pores between the sand grains. Assuming shaly sands to be uncemented, we can apply the friable-sand model (i.e. Hertz-Mindlin plus modified lower bound Hashin-Shtrikman) to calculate constant-clay content lines for friable shaly sands. We obtain K_{dry} and μ_{dry} for the mixed lithology, and using Gassmann's equation we can calculate the corresponding water-saturated moduli. The critical porosity will be lower for shaly sands than for sands (10-40%), depending on the clay content. The higher the clay content, the lower the critical porosity will be. The critical porosity will never reach zero since the clay particles have internal porosity. The next input parameters to consider are the mineral moduli. Since we are mixing quartz and clay particles, we need to calculate effective mineral moduli, just like we did for the silty shales. The mineral moduli represent the projections of the frame moduli, given by the modified lower Hashin-Shtrikman bound, at zero porosity. The moduli calculated from Voight or Reuss should be approximately the same for most mineral mixtures. However, if we have very soft clays (e.g. smectite or illite)

mixed with relatively stiff quartz, the difference between the two methods can be significant. We assume that the effective mineral moduli are given by the Voight average equations, representing the stiffest possible alternative of the mixed quartz-clay mineral :

$$K_{\text{mixed}} = (1-C)K_{\text{qz}} + CK_{\text{clay}}$$

And

$$\mu_{\text{mixed}} = (1-C)\mu_{\text{qz}} + C\mu_{\text{clay}}$$

Voight average equations.....equation (2.3)

As an alternative to constant-clay content lines, we can also model increasing clay content trends in the velocity-porosity plane. Marion (1990) introduced a topological model for sand-shale mixtures to predict the interdependence between velocity, porosity, and clay content. For shaly sands, it can be assumed that clay particles are strictly located within the sand pore space. Then, total porosity will decrease linearly with increasing clay content. When clay content exceeds the sand porosity, the addition of clay will cause the sand grains to become disconnected, as we go from grain-supported to clay-supported sediments (i.e shales). The total porosity evolution of a sand-shale mixture, as a function of increasing clay content.

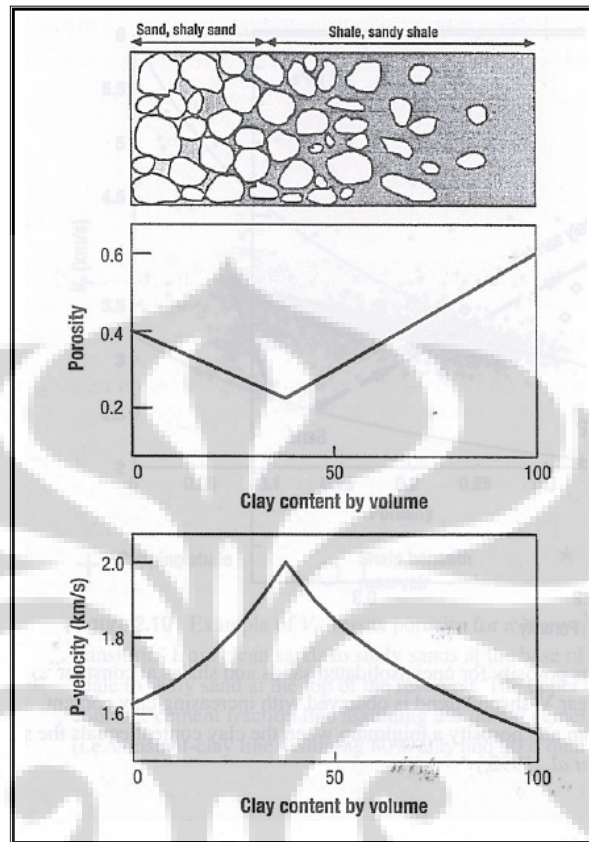


Figure 2.3 Porosity and P-wave velocity versus clay content for shaly sands and sandy shales.

Note the porosity minimum and velocity maximum at the transition from grain-supported sediment to clay-supported sediment. (Adapted from Marion, 1990)

Marion applied Gassmann's equations to calculate the velocities of shaly sand. We can use Gassmann to replace porous fluids with pore-filling clay (treating clay like a liquid). When clay content is less than the sand porosity, clay particles are assumed to be located within the pore space of the load-bearing sand. The clay will stiffen the pore-filling material, without affecting the frame properties of the sand. Therefore, increasing clay content will increase the stiffness and velocity of the sand-shale mixture as the elastic moduli of the pore-filling material (fluid and clay) increases.

2.4. Fluid Substitution – Gassmann

Prior to delving into Gassmann, we must first define and briefly discuss the bulk and shear moduli of the rock, as well as the bulk modulus of the pore-filling fluid.

2.4.1 Rock Properties

Gassmann's equation relates the saturated bulk modulus of the rock (K_{sat}) to its porous frame properties and the properties of the pore-filling fluid. The bulk modulus, or incompressibility, of an isotropic rock is defined as the ratio of hydrostatic stress to volumetric strain. Values for bulk modulus can be obtained either by dynamic laboratory measurements of velocities or from analysis of wireline log data (typical static measurements for the moduli violate the assumption of infinitesimal strain, and should be avoided for fluid substitution purposes). Whether from dynamic velocity measurements or from wireline log data, we can relate the bulk modulus of a rock, K_{sat} , to its compressional velocity, shear velocity, and bulk density.

2.4.2. Using Gassmann's Equation

Before begin fluid substitution using equation , first must determine the porosity of the rock, Φ , the properties of the fluids (K_{fl} , ρ_{fl}) that occupy the pore space, the bulk modulus of the mineral matrix (K_o) , and the bulk modulus of the porous rock frame (K^*). All four components may be defined or inferred through laboratory measurement or analysis of wireline log data.

Gassmann's equation relates the bulk modulus of a rock to its pore, frame, and fluid properties, as follows :

$$K_{sat} = K_{frame} + \frac{\left(1 - \frac{K_{frame}}{K_{matrix}}\right)^2}{\frac{\phi}{K_{fl}} + \frac{(1-\phi)}{K_{matrix}} - \frac{K_{frame}}{K_{matrix}^2}}$$

Gassmann Formula.....equation (2.4)

2.4.3. Porosity

Porosity is routinely calculated from core data or from analysis of wireline log data is rewritten and solved for porosity. Because logging tools do not directly measure porosity or bulk density, calibration of the log-derived porosity to measured core porosity is highly desirable, and in some instances (e.g., when dealing with complex lithologies or low porosity rocks) may significantly alter the results of a fluid substitution. Core calibration may also be particularly important if the formation is invaded by drilling fluids.

2.4.5 Fluid Properties

Prior to performing a fluid substitution, three approaches are commonly used for determining the bulk modulus and density of the in-situ pore-filling fluid, as well as those of the new fluid to be model :

- 1) the properties are measured directly (at reservoir temperatures and pressures) from pore fluids recovered from the reservoir
- 2) the properties are calculated from equations of state (see McCain, 1990; Danesh, 1998)
- 3) the properties are calculated from an empirical calculator (e.g., Batzle and Wang, 1992)

Generally, the difference between the two is small unless the fluid has a relatively high gas-oil-ratio (GOR).

Because there typically are two or more fluid phases occupying the pore space of a reservoir rock, we must calculate a bulk modulus and density of the individual fluid end members, and then mix the fluids according to the following physical rules. Gassmann's equation assumes all the pore space is connected and pore pressure is equilibrated throughout the rock.

2.4.6 Matrix Properties

To calculate the bulk modulus of the mineral matrix, K_0 , information on the composition of the rock must be available. If core samples are available, mineral abundance may be determined using conventional laboratory techniques. In the absence of core data, lithology can be approximated from wireline logs by simple clay volume (V_{clay}) analysis and assuming the two

mineral end members are quartz and clay. For more complex lithologies, however, other techniques must be applied which allow the volumetric abundance of the mineral constituents to be estimated.

2.4.7 Frame Properties

Prior to applying Gassmann's equation, it is necessary to determine the bulk modulus of the porous rock frame, K^* . This is the low-frequency, drained bulk modulus of the rock. Once determined, K^* is held constant during the course of a fluid substitution. Note that the shear modulus, G , is also a frame property of the rock and is therefore also held constant during the typical fluid substitution process.

Mineral	Bulk Modulus (GPa)	Shear Modulus (GPa)	Density (g/cm ³)
Quartz	37	44	2.65
“Average” feldspar	37.5	15	2.62
Plagioclase feldspar	75.6	25.6	2.63
clay	variable	variable	variable
Pyrite	147.4	132.5	4.93
Hematite	100.2	95.2	5.24
Calcite	76.8	32	2.71
Dolomite	94.9	45	2.87
Siderite	123.7	51	3.96
Anhydrite	44.8	29.1	2.98

Table 2. Bulk modulus, shear modulus, and bulk density Of common rock forming minerals.* Values are from Carmichael (1989).

2.4.8 Calculating Velocities

Assume we have calculated porosity (ϕ) along with the matrix and frame properties of the rock (K_0 , K^* , and G). This allows us to calculate a new saturated bulk modulus for any desired fluid.

2.4.9 Dry Frame Bulk Modulus, K^*

Application of Gassmann's equation is dependent upon accurate determination of the porous frame properties of the rock (K^* and G). In order

to calculate the shear modulus, G , it is only necessary to know the bulk density and shear velocity of the information.

2.5 Effect of fluid saturation on seismic properties

The seismic response of reservoirs is directly controlled by compressional (P-wave) and shear (S-wave) velocities V_p and V_s respectively along with densities.

Clearly, bulk modulus is more sensitive to water saturation. The bulk-volume change and causes a pressure increase in pore fluid (water). This pressure increase stiffens the rock frame and causes an increase in bulk modulus. Shear deformation, however, does not produce a pore-volume change, and consequently different fluids do not affect shear modulus. Therefore, any fluid-saturation effect should correlate mainly to a change in bulk modulus.

Numerous assumptions are involved in the derivation and application of Gassmann's equation :

1. the porous material is isotropic, elastic, monomineralic, and homogenous;
2. the pore space is well connected and in pressure equilibrium (zero-frequency limit);
3. the medium is a closed system with no pore-fluid movement across boundaries;
4. there is no chemical interaction between fluids and rock frame (shear modulus remains constant)

2.6 Theoretical Models

The theoretical models are primarily continuum mechanics approximations of the elastic, viscoelastic, or poroelastic properties of rocks. Among the most famous are the poroelastic models of Biot (1956), who was among the first to formulate the coupled mechanical behavior of a porous rock embedded with a linear viscous fluid. The Biot equations reduce to the famous Gassmann (1951) relations at zero frequency; hence, we often refer to "Biot-Gassmann" fluid substitution. Biot (1962) generalized his formulation to include a viscoelastic frame, which was later pursued by Stoll and Bryan (1970). The "squirt model"

of Mavko and Nur (1975) and Mavko and Jizba (1991) quantified a grain-scale fluid interaction, which contributed to the frame viscoelasticity. Dvorkin and Nur (1993) explicitly combined Biot and squirt mechanisms in their “Bisq” model.

2.6.1 Internal Consistency and Saturation Modeling

Fluid substitution models should always be carefully evaluated for quality and internal consistency. For instance, when oil or gas is substituted into a brine sand, bulk densities should always decrease and shear velocities should always increase.

To aid as a quality-control check on fluid substitutions and in order to best understand how velocities and densities should vary for any given sand, it is often instructive to generate saturation models, where Gassmann’s relationships are used to calculate V_p , V_s , and ρ_B as a function of water saturation. These types of models are particularly important for understanding the rare case when compressional velocities for a gas sand are faster than those for oil in the same sand. This situation can occur when the bulk density decreases at a faster rate than the saturated bulk modulus as gas saturation is increased.

Fluid substitution is an important part of seismic attribute work, because it provides the interpreter with a tool for modeling and quantifying the various fluid scenarios. The most commonly used technique for doing this involves the application of Gassmann’s equations.

The objective of fluid substitution is to model the seismic properties (seismic velocities) and density of a reservoir at a given reservoir condition (e.g., pressure, temperature, porosity, mineral type, and water salinity) and pore fluid saturation such as 100% water saturation or hydrocarbon with only oil or only gas saturation.

Modeling the changes from one fluid type to another requires that the effects of the starting fluid first be removed prior to modeling the new fluid, and the moduli (bulk and shear) and bulk density of the porous frame are calculated. Once the porous frame properties are properly determined, the rock

is saturated with the new pore-fluid, and the new effective bulk modulus and density are calculated.

Gassmann fluid substitution can be performed by begin with an initial set of velocities and densities, V_p , V_s , and ρ corresponding to the rock with an initial set of fluids, which we call “fluid I”. These velocities often come from well logs, but might also be the result of an inversion or theoretical model.

The most common scenario is to begin with an initial set of velocities and densities, V_p , V_s , and ρ corresponding to the rock with an initial set of fluids, which we call “fluid 1”. These velocities often come from well logs, but might also be the result of an inversion or theoretical model.

When calculating fluid substitution, it is obviously critical to use appropriate fluid properties. To our knowledge, the Batzle and Wang (1992) empirical formulas are the state of the art.

- ✚ The density and bulk modulus of most reservoir fluids increase as pore pressure increases.
- ✚ The density and bulk modulus of most reservoir fluids decrease as temperature increases.
- ✚ The Batzle-Wang formulas describe the empirical dependences of gas, oil, and brine properties on temperature, pressure, and composition.
- ✚ The Batzle-Wang bulk moduli are the adiabatic moduli, which we believe are appropriate for wave propagation.
- ✚ In contrast, standart PVT data are isothermal. Isothermal moduli can be ~ 20% too low for oil, and a factor of 2 too low for gas. For brine, the two do not differ much.

Chapter 3

Data & Methodology

3.1. Methodology

Methodology used to achieve the goals of this study includes the main activities such as : selection and data validation, data processing and quality control (QC data), data processing and analysis. In principle, a series of major activities (work flow) in this study can be simplified as follows:

Phase 1 involves the selection zone or interval Telisa formation which is the target / goal of this study. The selection is done based on the consideration of completeness of data, scientific (geophysics, geology) and the expected results.

Phase 2 includes work-related classification the systematics raw data, download data, processes and tools help hardness and soft according with each type of data. Conversion work, corrections, and rarefaction (smoothing) of data is done in this phase 2.

Phase 3 will consist of the following jobs:

Computation, classification, and statistical data processing elastic properties and rock physical variables that other studies that are relevant to this. Of the output form of the various cross-plot, histogram, image, graphic and model. Relationships rock properties and ductile developed by previous researchers tested against the data set of research areas.

Phase 4 consists of the following work:

1. Develop and propose relationships quantitative and reasonable (reliable) between properties resilient, physical, and texture based on zone stratigraphy rock known in both these wells.
2. Comparing the results, the above results with previous studies of lithology similar to lithology of Telisa formation and compares with theory and models that have been universally accepted and that has been proposed by researchers in the latest other areas (models, between others:)

3. Discuss and investigate in detail the differences between the results of this study with the expected or with models and formulas that have been there. Propose alternative solutions and models as a result of these differences.
4. Workflow studies documenting the physical and rock properties of Telisa formation which may be applied to the formation of equivalent that there is oil in the field.

3.1.1 Fluid Substitution

Fluid substitution performed on two wells in the area of research focused on the Telisa sand, the reservoir (sandstone) is filled by fluid hydrocarbons that contain oil.

Fluid Substitution is carried out to investigate the changes of fluid saturation and its effect to V_p and V_s log in the presence of fluid of this reservoir. Fluid Substitution analysis was performed in YM#232 & YM#247 wells, based on the following data :

1. Gas gravity (gr/cc)
2. Oil gravity (gr/cc)
3. Formation pressure (reservoir) (psi)
4. Formation temperature (reservoir) (deg F)
5. Water salinity (ppm)
6. Gas Oil Ratio

This data can be obtained from the results of laboratory analysis of samples taken from welltest reports.

The data obtained are:

1. Formation Temperature (reservoir) : 284 deg F
2. Formation Pressure (reservoir) : 1100 psi
3. Salinity : 4000 ppm
4. Oil gravity : 35.2 API
5. Gas gravity : 0.8929
6. Gas Oil Ratio (GOR) : 296 SCF/STB

Input data required in this analysis is the fluid substitution velocity (V_p and V_s), or slowness, density, porosity, saturation of water (water saturation). Matrix

properties must also be used as input in the analysis this fluid substitution. For this study, quartz mineral is used as a default.

Based on the calculation of average Gassmann, fluid substitution can be made crossplot, with the assumption that the pore bulk modulus and dry rock poisson's ratio fixed (the same) although porosity changed rock.

3.2 Data

Main data used in this study is the result of measurement data in the field (raw data), in the form of data recording wells (Wireline log data) from four wells (YM-227, 232, 242 & 247) that consist of gamma ray, density, neutron, resistivity, SP, cali, and sonic (V_p & V_s).

Supporting data used in this study was results of the processing and interpretation of data from the two well cases (YM-232 & 247), which consist of:

- a. Petrophysical Analysis & Interpretation
- b. Seismic data (post stack)
- c. PVT data
- d. Mudlog report
- e. Report from Telisa Formation Study

3.3 Wavelet Extraction & Well Seismic Tie

The form of seismic signals (wavelet) influence the successfull of the benchmarking process models between the trace and data trace. This is because of the RC's precision anyway, but if the signal will result in a form and amplitude trace its model. Therefore, the signal that contain in the seismic waves can be extracted correctly. This process is called wavelet extraction.

There are 2 methods for extracting seismic signals (Prastianto, 1991):

1. Signal extraction from wells without information

In circumstances such as this, that the presumption applied RC truly random (random) so that the multiplication both of spectrum signal amplitude is the same as the multiplication both of amplitude seismic trace, as a result of this self-correlation spectrum of seismic trace, so that finally, to the conclusion that the spectrum amplitude signal proportional to the spectrum amplitude of the seismic

trace. From the amplitude spectrum of this signal can do with gained by reverse fourier transform.

2. Signal extraction wells with available data

In this case there are density and velocity data in the wells, so the AI can be calculated well. AI from this well revealed in the RC pit. RC in the wells is transformed first to the frequency area and the results are used to divide the spectrum of seismic trace through wells. To get the form of signals, the Fourier back transformation made from the results of this spectrum.

Wavelet extraction stage is the very success of the inverse set. Extraction is done with the wavelet method using the statistical seismic data only. The first stage of the extraction is conducted to analyze the spectrum amplitudo from seismic data and well log data and then taken the average. After that calculation is done on time and phase shift of the initial wavelet (wavelet amplitude spectrum) to produce an optimum correlation. Final stages of the wavelet extraction is the combination of spectrum amplitude with phase shift and time, so the best wavelet which has the highest price correlation between the synthetic seismogram.

The process of seismic well tie is a process to get the fitness reflektivitiy between the well data and seismic data. The first step that is done, apply the checkshot will the correct relationship between time and depth of the data well and or seismic. Then proceed with the wavelet to extract synthetic seismogram can be made that will dikorelasikan dnegan seismic data. Wavelet can be extracted from seismic data, log data and the accuracy synthetic specified price from the high correlation.

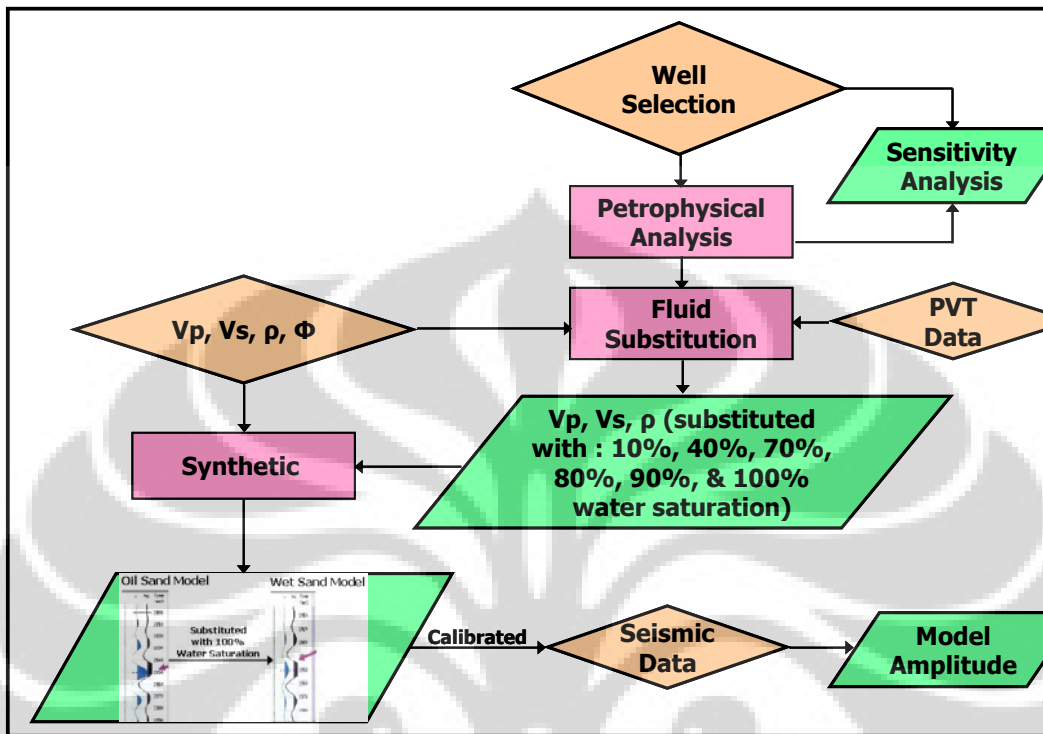


Figure 3. Work Flowchart

CHAPTER 4

Analysis & Interpretation

4.1. Data Processing

Processing data in this thesis has been done using the software Hampson Russel (HRS) because the data used are logs and seismic data. The steps of data processing which is done here consists of :

1. The petrophysical data from petrophysicist
2. Inputting data into software
3. Sensitivity analysis of rock properties by performing the calculation from YM-227, YM-232, YM-242, YM-247 wells as a data base and making some crossplot such as:
 1. VpVs_Ratio vs Gamma Ray with color key Gamma Ray
 2. VpVs_Ratio vs Gamma Ray with color key Saturation
 3. VpVs_Ratio vs Gamma Ray with color key Porosity

Only log data (figure 4.1 & 4.2) from YM-232 (with reservoir zone at 2322 – 2377 ft MD) and YM-247 (the reservoir zone at 2810 – 2873 ft MD) wells that will further analyze in this thesis.

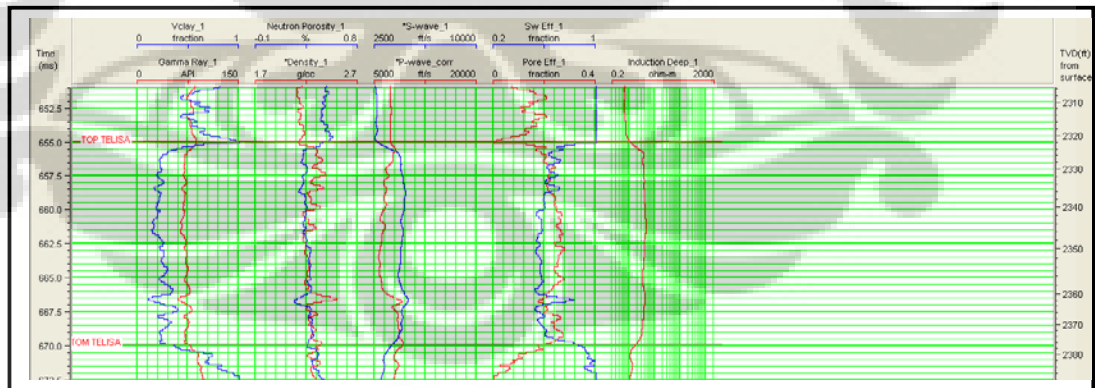


Figure 4.1 Composite Log YM-232 Well

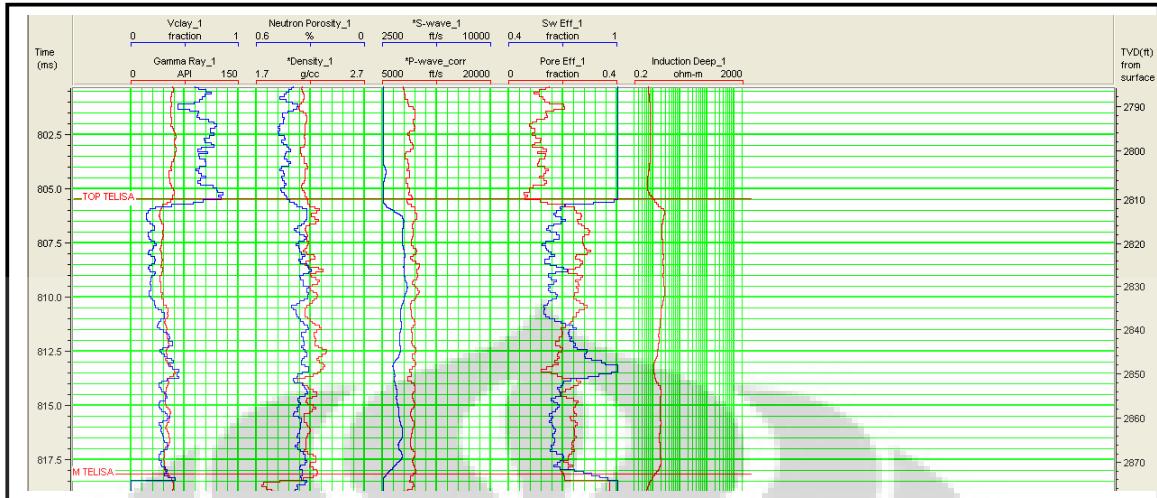


Figure 4.2 Composite Log YM-247 Well

4.2. Sensitivity Analysis

Sensitivity analysis has been conducted to explore the parameters that have a good correlation between petrophysics and seismic data. This parameter should be seen on the scale of seismic resolution. By using the well log data we can determine the type of reservoir rock, thickness of hydrocarbons zone (pay zone), type of fluid in the reservoir and petrophysical parameters such as porosity, saturation and others. The next crossplot was made by combining the well data to seismic data to determine the petrophysical parameters which correlates well with the seismic data.

The curve which are displayed has been selected only that related to thesis. This is to investigate the relationship between petrophysical parameters and sonic log. The cross plot has been limited only within the reservoir zone of the Telisa formation.

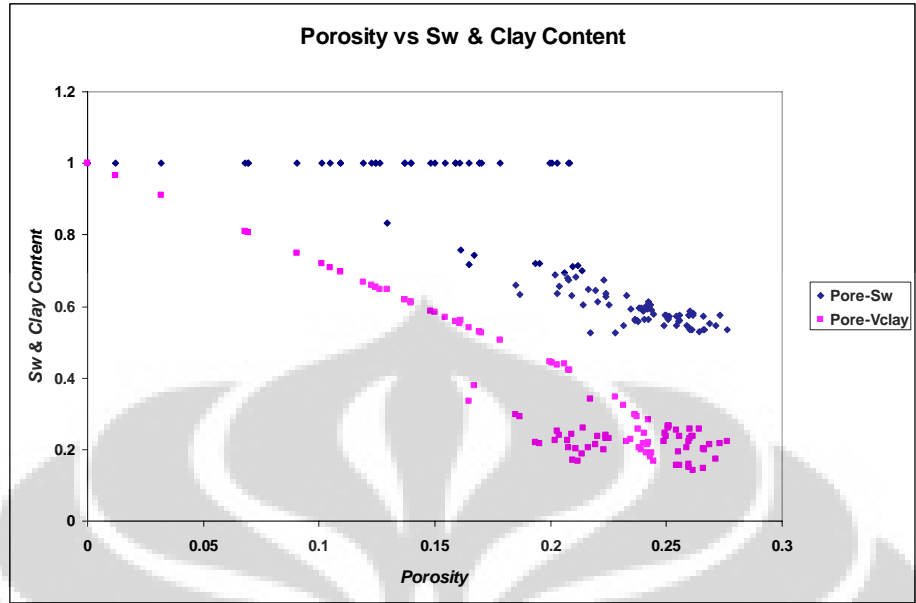


Figure 4.3 Porosity vs Sw & Porosity vs Vclay at YM-232 Well

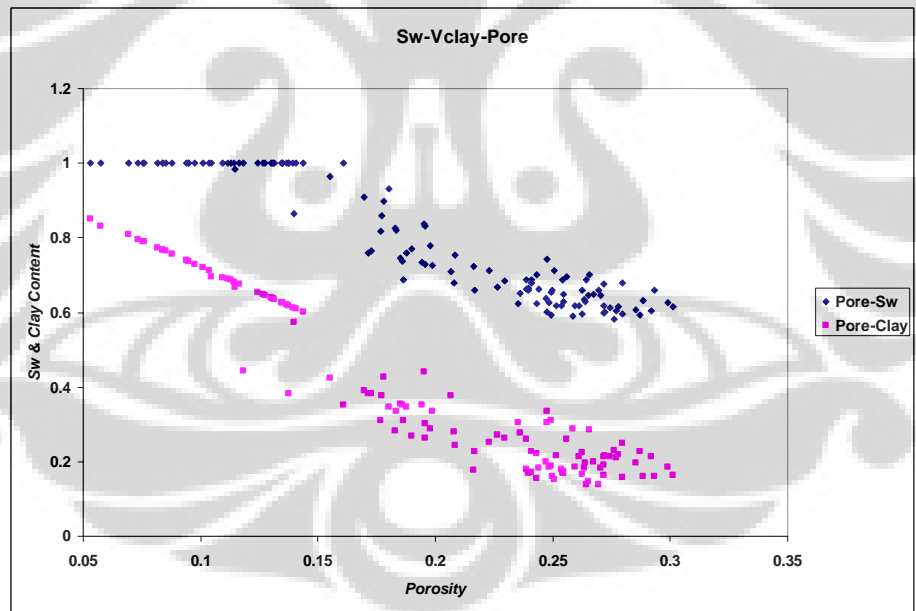


Figure 4.4 Porosity vs Sw & Porosity vs Vclay at YM-247 Well

The trend of petrophysical properties from YM-232 and YM-247 wells is that if the porosity increases, the saturation decreases (figure 4.3 & 4.4)

The crossplot was made from YM-227, YM-232, YM-242, and YM-247 wells as a data base. At the time Gamma Ray below 78 API within the yellow area as sandstone, while above 78 API within the green area as shale. Gamma Ray 78 API as a cut off to differentiate the lithology, while VpVs_Ratio at 2.7 as a cut off to distinguish pay and wet zone (figure 4.5, 4.6, & 4.7).

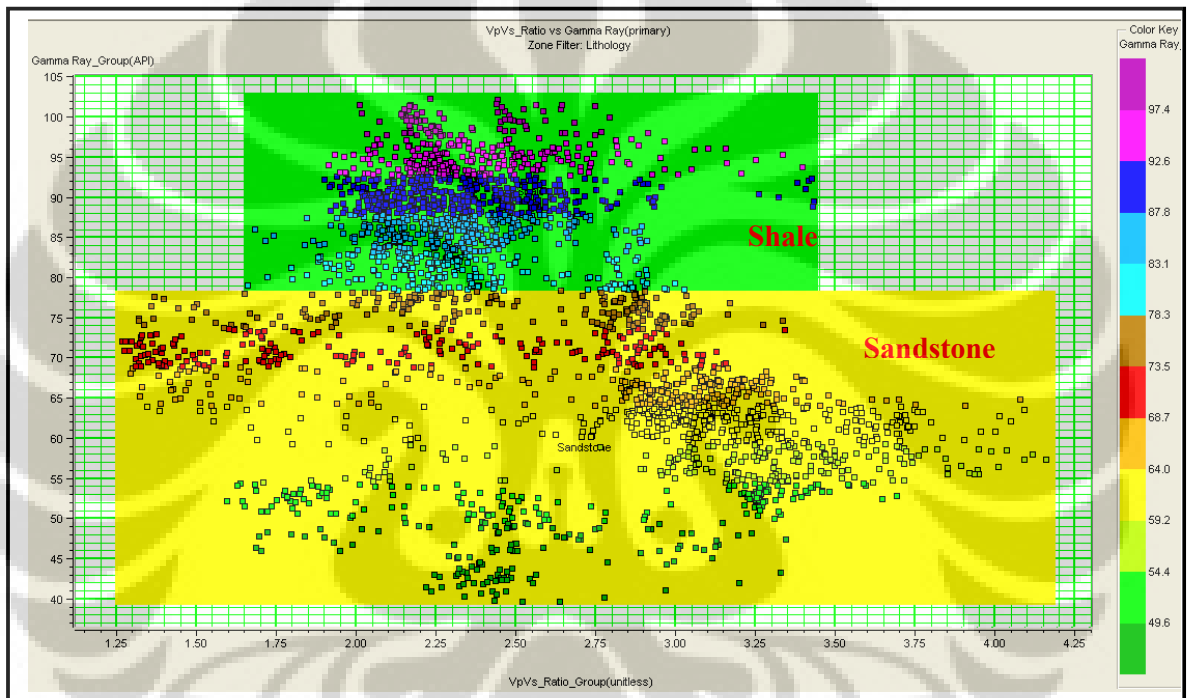


Figure 4.5 Crossplot (YM-227, 232, 242, & 247 Wells) Gamma Ray vs VpVs_Ratio with Color Key Gamma Ray

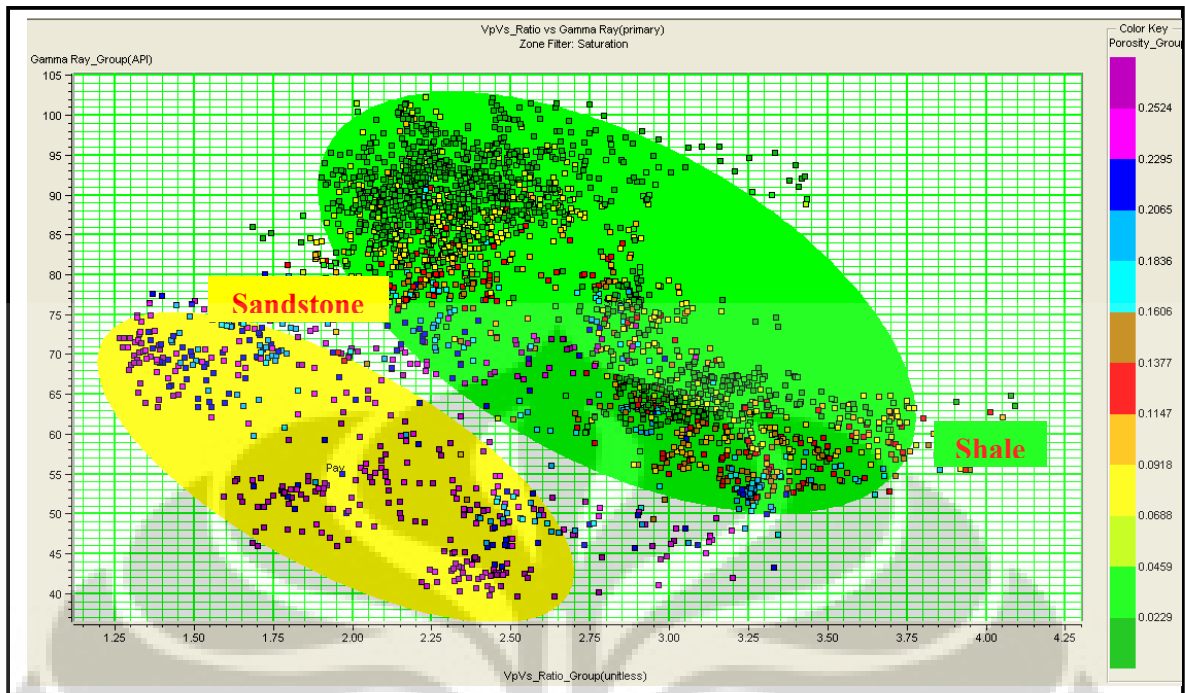


Figure 4.6 Crossplot (YM-227, 232, 242, & 247 Wells) Gamma Ray vs VpVs_Ratio with Color Key Porosity

Those figure 4.6 & 4.7, there's good correlation between porosity & saturation. The fourth well is sensitive to these parameter. Its can separate the pay zone and wet zone. The same trend can be seen at those crossplot.

4.3. Fluid Substitution

Shaly sands can be valuable reservoirs, so geophysical modeling of such sands, including fluid substitution, is useful. The model concentrates on seismic properties, i.e. density and velocity.

With the theory of fluid substitution proposed by Gassmann, we can predict the changes of seismic response by changing fluid which is done using oil with water. Theoretical calculations was performed by changing fluid saturation, and correlating with nature petrophysics in seismic response.

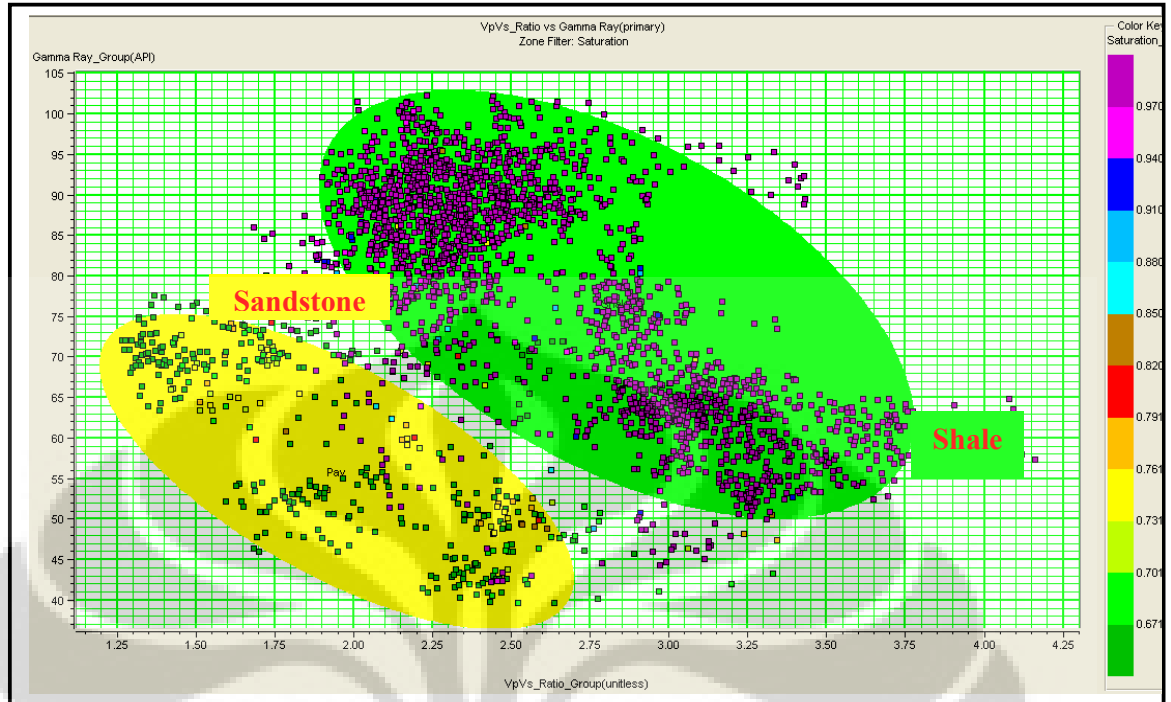


Figure 4.7 Crossplot (YM-227, 232, 242, & 247 Wells) Gamma Ray vs VpVs_Ratio with Color Key Saturation

By changing the fluid saturation (with S_w 10%, 40%, 70%, 80%, 90% and 100%), the Vp and density log will change. This Vp log together with density log can be used to construct the reflection coefficient. By convolving the reflection coefficient with the extracted wavelet from seismic trace, we get the FRM seismogram. FRM seismogram, this means that we know the synthetic which contains fluid. The FRM seismogram can be used to investigate the fluid content information in the field or real seismogram (seismic trace).

Fluid Substitution has been performed in two wells in the area of study and focused in the reservoir zone "Telisa Sand", the reservoir (sandstone) is filled by oil.

Fluid Substitution is carried out to investigate the changes of fluid saturation and its effect to density, Vp and Vs log in the presence of fluid of this reservoir.

Fluid Substitution analysis was performed in YM-232 & YM-247 wells, based on the following data (table 4.1) :

Property	Value
Formation Temp.	284 deg F
Formation Pres.	1100 psi
Salinity	4000 ppm
Oil Gravity	35.2 API
Gas Gravity	0.8929
GOR	296 SCF/STB

Table 4.1 Reservoir Properties

Input data needed in this analysis is the fluid substitution velocity (V_p and V_s) or slowness (DTA & DTSF/DTXX), density, porosity, saturation of water (water saturation). Matrix properties must also be used as input in the analysis of this fluid substitution. For this thesis, quartz mineral is used as a default.

To process for calculating of the above formula, can be executed using FRM module from HRS and the results can be seen in the logs above. Based on the picture above, it can be explained that for the reservoir “Telisa Sand” with the actual form of hydrocarbons in oil YM -232 & YM-247 wells, the changes of S_w value is more sensitive to the increases of V_p or in other words that V_p increases when it was completely oil saturated (figure 4.8 & 4.9).

The original saturation at YM-232 well is about 50% to 80%. It is substituted with water saturation 10%, 40%, 70%, 80%, 90%, & 100%. When it was completely oil saturated density decreases and V_p increases, while V_s increases. On the contrary, it was completely water saturated density increases and V_p decreases. While V_s is constant.

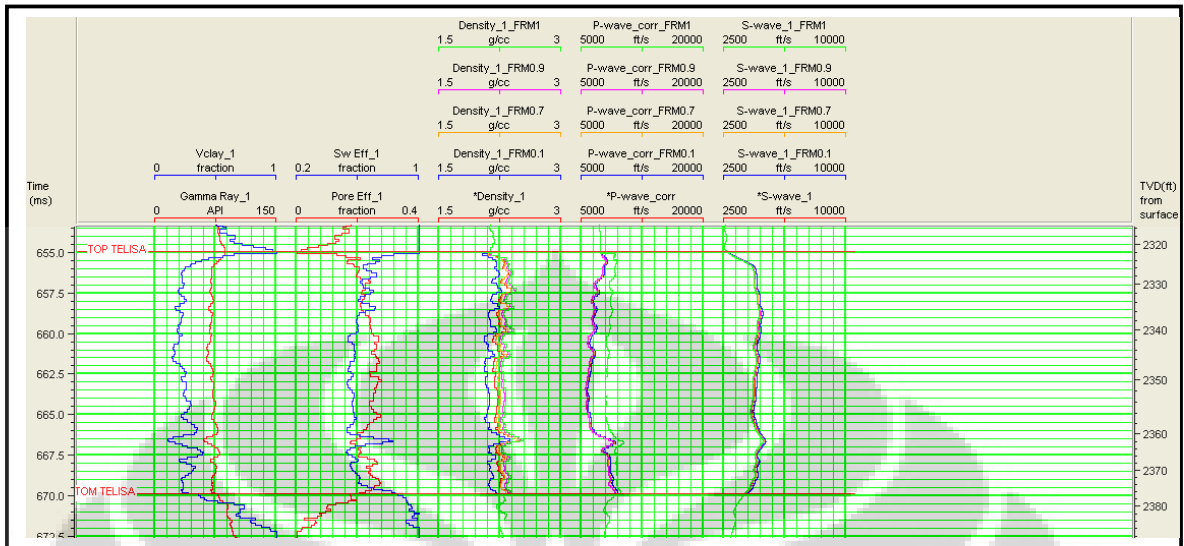


Figure 4.8 Fluid Substitution at YM-232 Well (Substitution with Sw 10%, 70%, 90%, & 100%)

YM-247 well has the saturation 50% to 80 %. The 10%, 40%, 70%, & 100% water saturation were applied for the substitution. The density decreases while Vp increases when it was completely oil saturated, and Vs is constant. On the contrary, the density increases, Vp decreases, and Vs is constant when it was completely water saturated.

4.4 Wavelet Extraction & Well Seismic Tie

Wavelet extraction process can be done using several methods. Firstly, we should find out the frequency dominant which is 40 Hz in this case. From the calculation, the tuning thickness is 62 ft and the reservoir thickness is 40 – 60 ft. However, the objective is above seismic resolution.

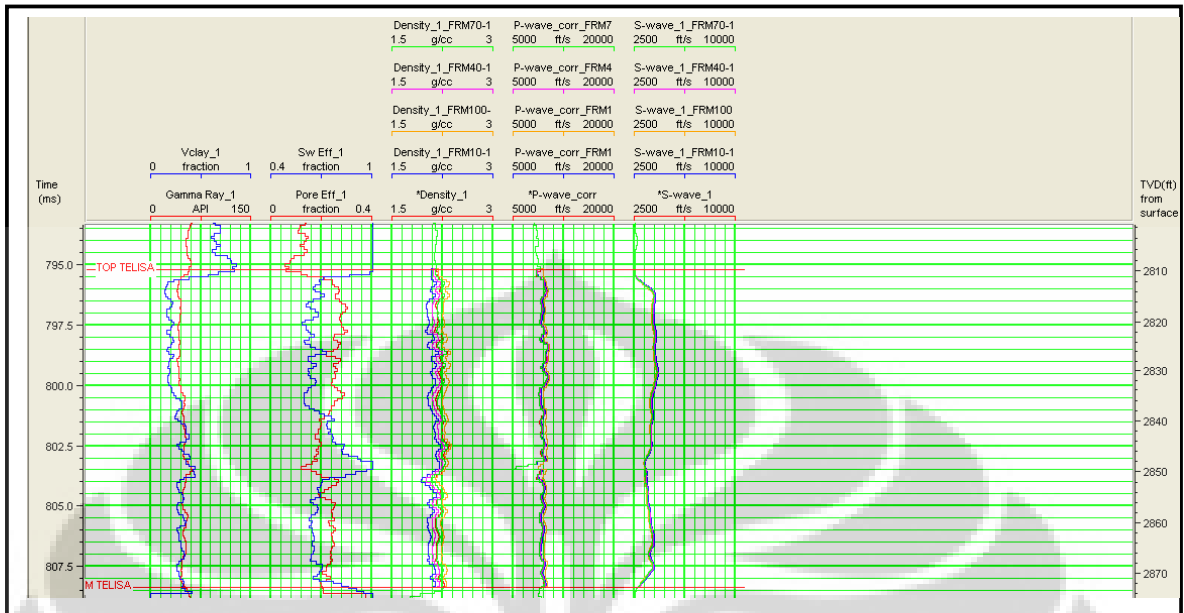


Figure 4.9 Fluid Substitution at YM-247 Well (Substitution with Sw 10%, 40%, 70%, & 100%)

In this research on wavelet extraction is done with several methods, including statistical methods (using the seismic data), using the data well, a combination of extraction from seismic data and wells and to wavelet Ricker and wavelet bandpass.

From several methods, we choose to use the wavelet obtained from Ricker. This wavelet extraction process is done repeatedly (try and error), with the fox-value wavelength and long taper to obtain the wavelet phase spectrum and the best.

Finally wavelet extraction on YM-232 & YM-247 wells applied Ricker 40 Hz, and the correlation each well is 0.698 for YM-232 well and 0.635 at YM-247 well (figure 4.11 & 4.12).

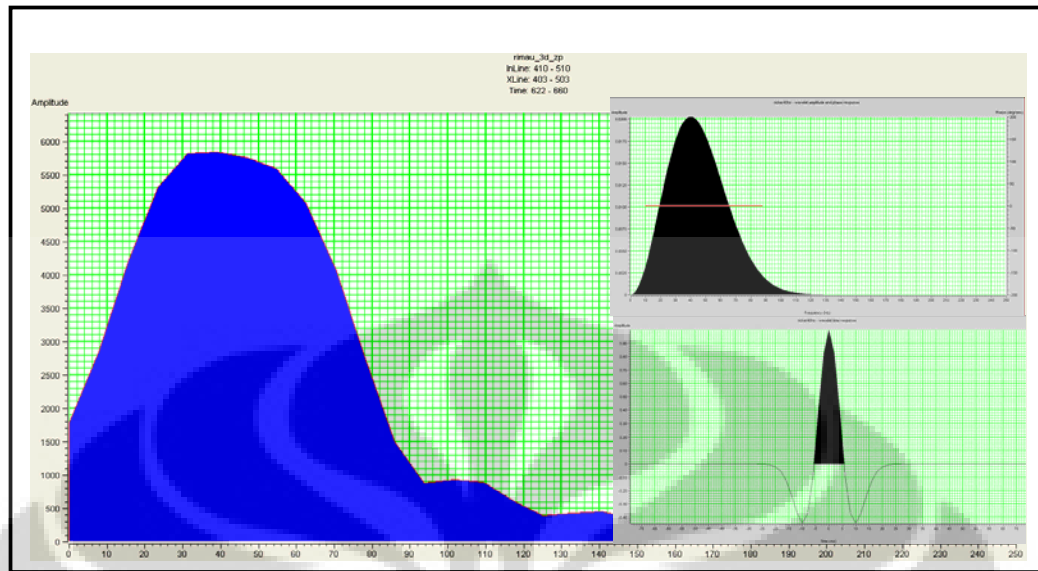


Figure 4.10 Frequency Dominant is 40 Hz & Wavelet Extraction

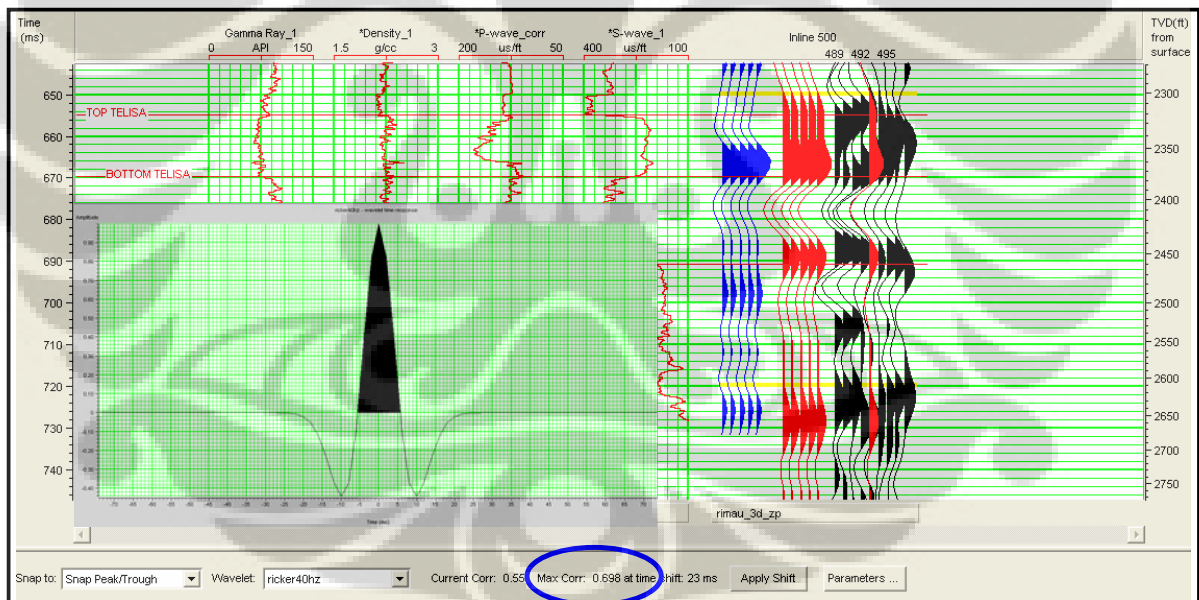


Figure 4.11 Correlation with Ricker 40 Hz at YM-232 Well

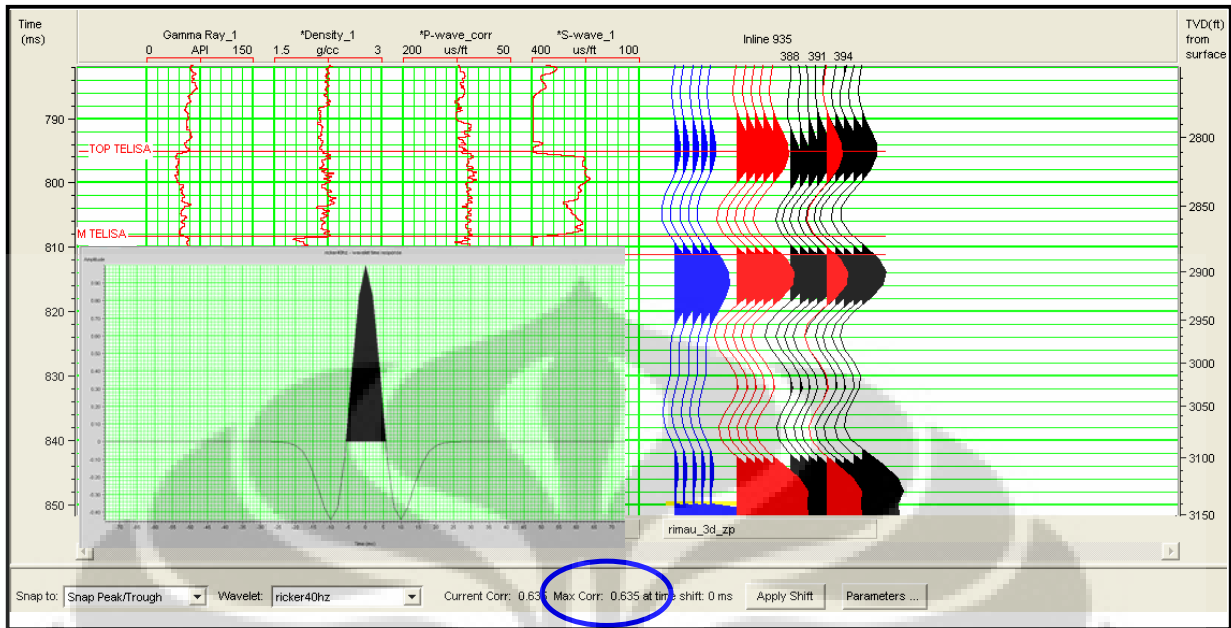


Figure 4.12 Correlation with Ricker 40 Hz at YM-247 Well

4.5. Rock Physics Analysis & Synthetic Offset Gathers

Rock physics is an indispensable tool for an efficient interpretation, providing the basic relationship between the lithology, fluid, and geological deposition environment of the reservoir. The elastic properties such as velocity, density, impedance, and V_p/V_s ratio take an important role in reservoir characterization because they are related to the reservoir properties such as water saturation, porosity, and shale volume.

This is the results of two well cases (YM-232 & YM-247) where the effects of rock and fluid properties on seismic are illustrated. This case is an example from YM field that shows the effect of hydrocarbons saturation on synthetic offset gathers. This well contains a hydrocarbon from about 2322 to 2377 ft at YM-232 well and 2810 ft to 2873 ft at YM-247 well. From the logs (GR-Density-Pwave_Swave), are able to construct a four layer model for the pay zone and its over-and under-lying horizons. The layers are shale, sandstone as reservoir, shale, and limestone. In other words, the reservoir is in between shale section.

4.5.1 The Analysis of The Telisa Sand Reservoir at YM-232 Well

Petrophysical analysis on YM-232 well in the Telisa Sand reservoir shows the porosity is 20% – 27%. Gamma Ray reading at this reservoir is high enough, shows 60 - 80 API. The reservoir is very fine to fine sandstone with streak of shale. The fluid contain in this reservoir is oil. Although the mudlog shows that high gas readings (720 units). Pressure data in this well was achieved from MDT (Modular Dynamic Tester).

The next rock properties analysis is P-impedance to perform calculations on the density and sonic logs. The range P-imp in the Telisa Sand reservoir is 12,200 to 18,500 gr / cc * ft / sec.

Then, the analysis of rock properties is VpVs_Ratio. This analysis involves the shear wave data recorded through the sonic log, called a shear DT (DTSF). The value of VpVs_Ratio in the Telisa Sand reservoir is 1.3 – 2.25. This value is correlate with the decrease of P-imp in this reservoir (figure 4.22 & 4.23).

From the figure that the P-imp value for insitu case, it is about 17000 ft/s*g/cc. Actually, when it was substituted with 100% water saturation, the AI is very high, it is about 19000 to 21000 ft/s*g/cc. And when it was completely oil saturated the AI is about 13000 to 17000 ft/s*g/cc. We used the porosity as a constant value (the original value).

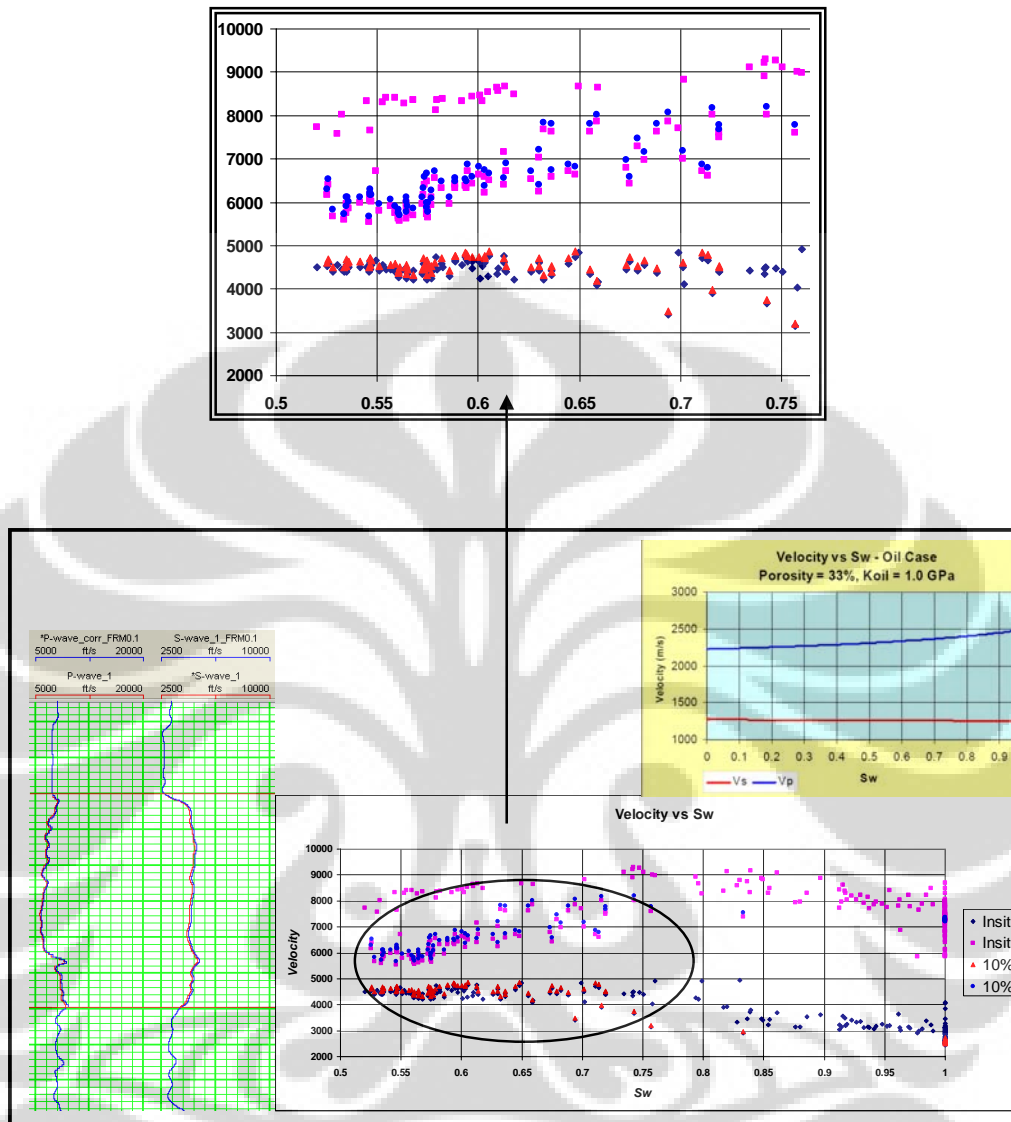


Figure 4.13 Crossplot Velocity – Water Saturation (10%)_YM-232 Well

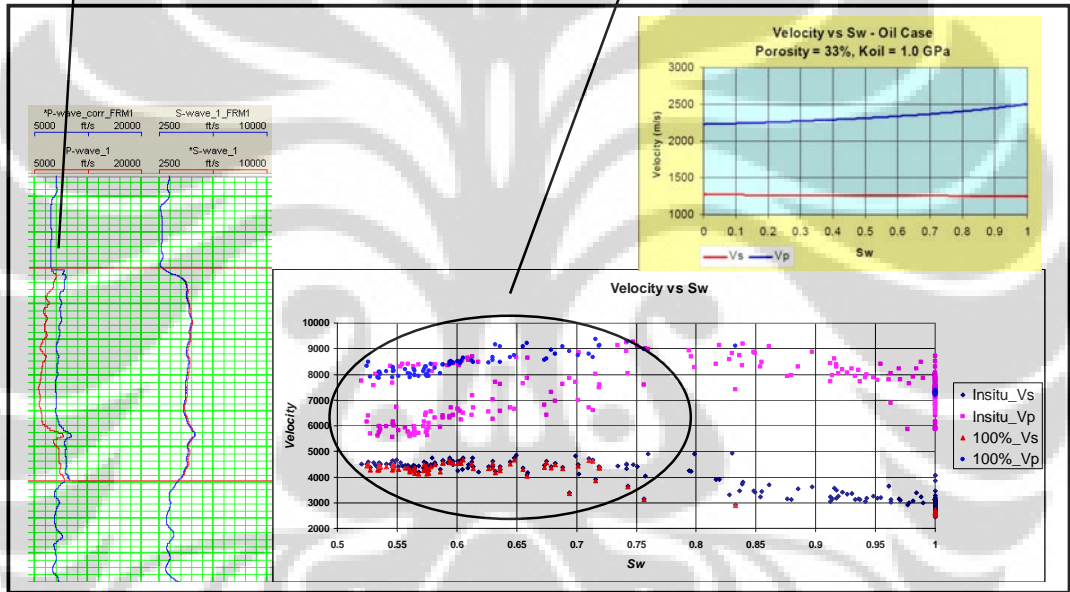
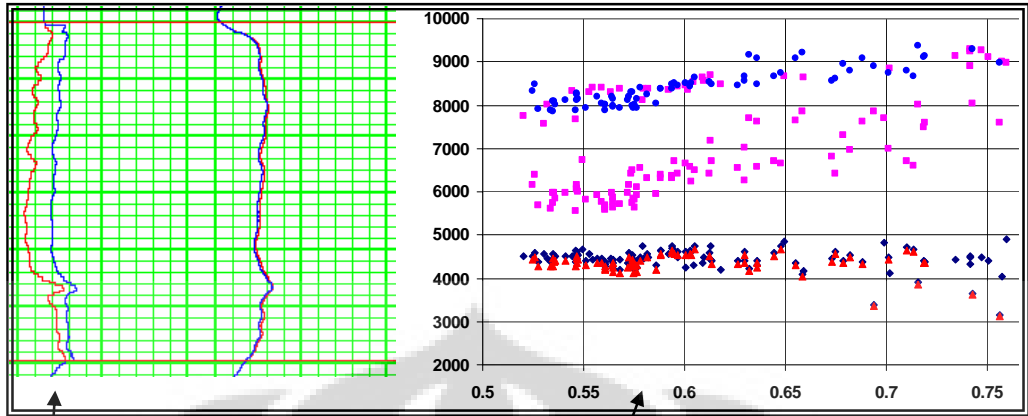


Figure 4.14 Crossplot Velocity – Water Saturation (100%)_YM-232 Well

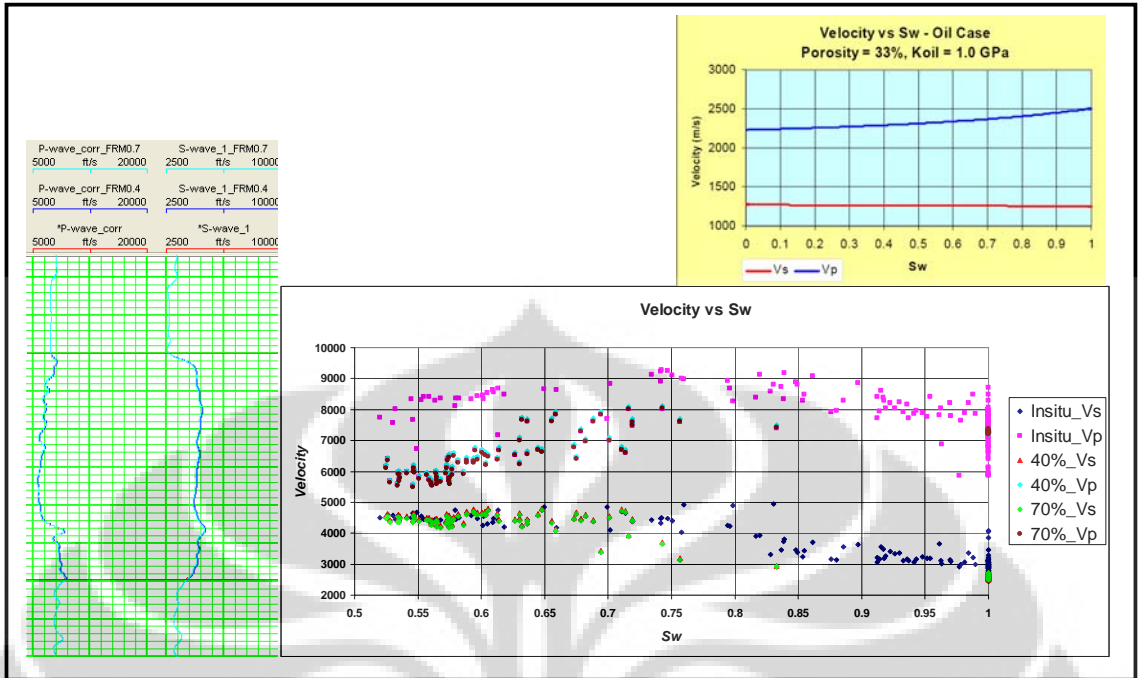


Figure 4.15 Crossplot Velocity – Water Saturation (40% & 70%) YM-232 Well

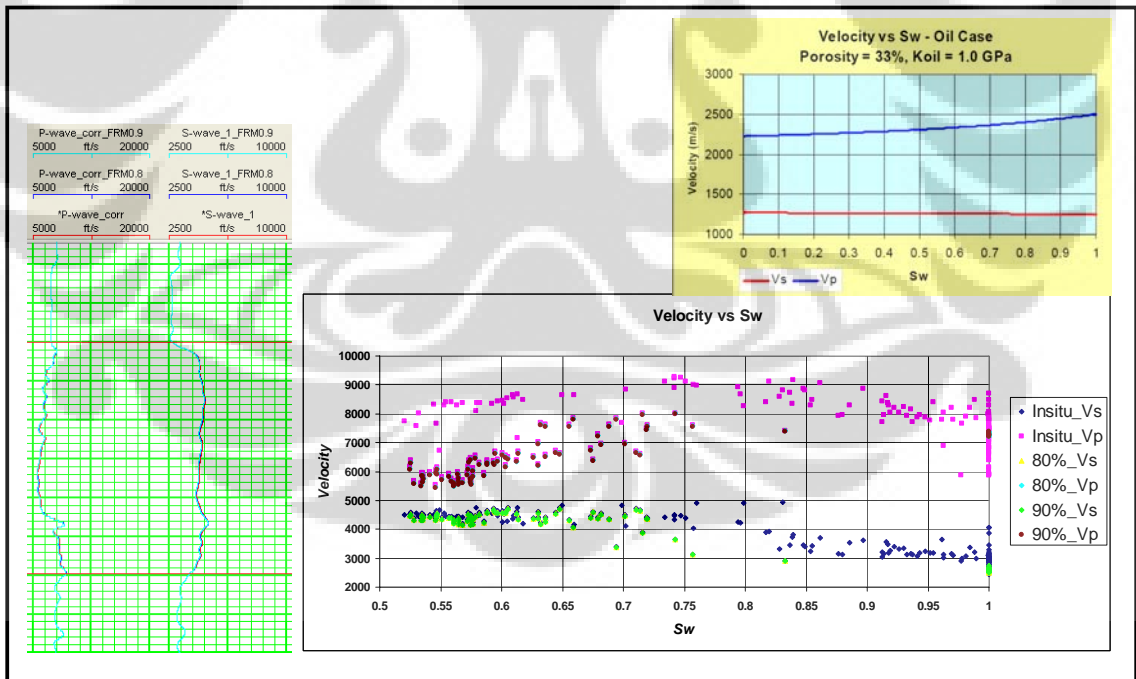


Figure 4.16 Crossplot Velocity – Water Saturation (80% & 90%)_YM-232 Well

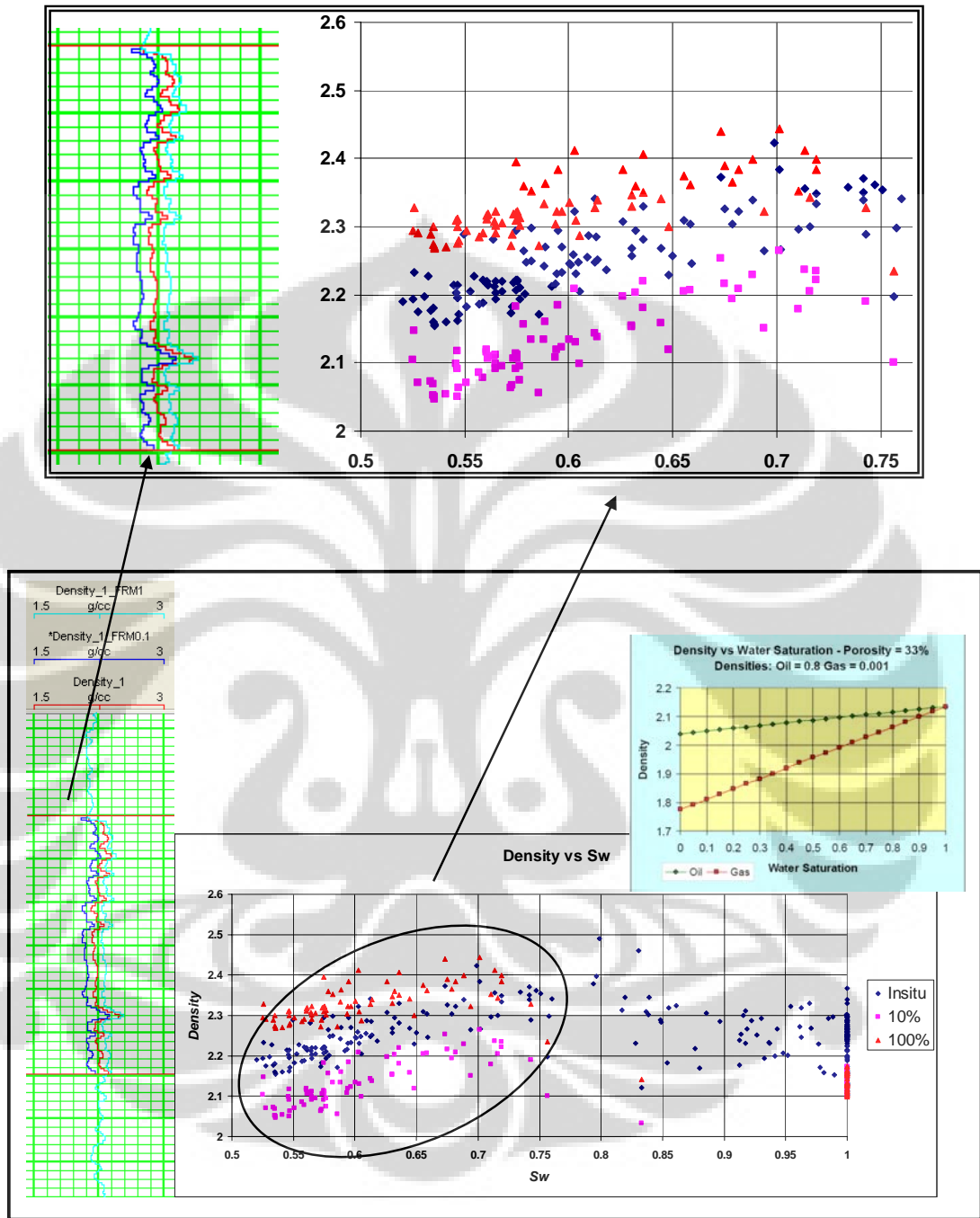


Figure 4.17 Crossplot Density – Water Saturation (10% & 100%)_YM-232 Well

From YM-247 well, the range P-imp is about 18000 to 21000 ft/s*g/cc for the original case. And also when it was completely oil saturated. But when it was substituted with 100% water saturation, the P-imp increases, the value is 22000 to 24000 ft/s8g/cc. And the porosity that we used from the original case (constant). To observe the changes of the fluid density (oil) and Vp to the actual the changes of water saturation at YM-232 well, we will use fluid substitution by Gassmann. The result indicates that the changes in density and vp fluida in the Telisa Sand reservoir in this well is responsive to the gradually changing of 10%, 40%, 70%, 80%, 90% and 100% water saturation. Analysis that is done is to create some crossplot of rock properties that have been achieved from the previous analysis.

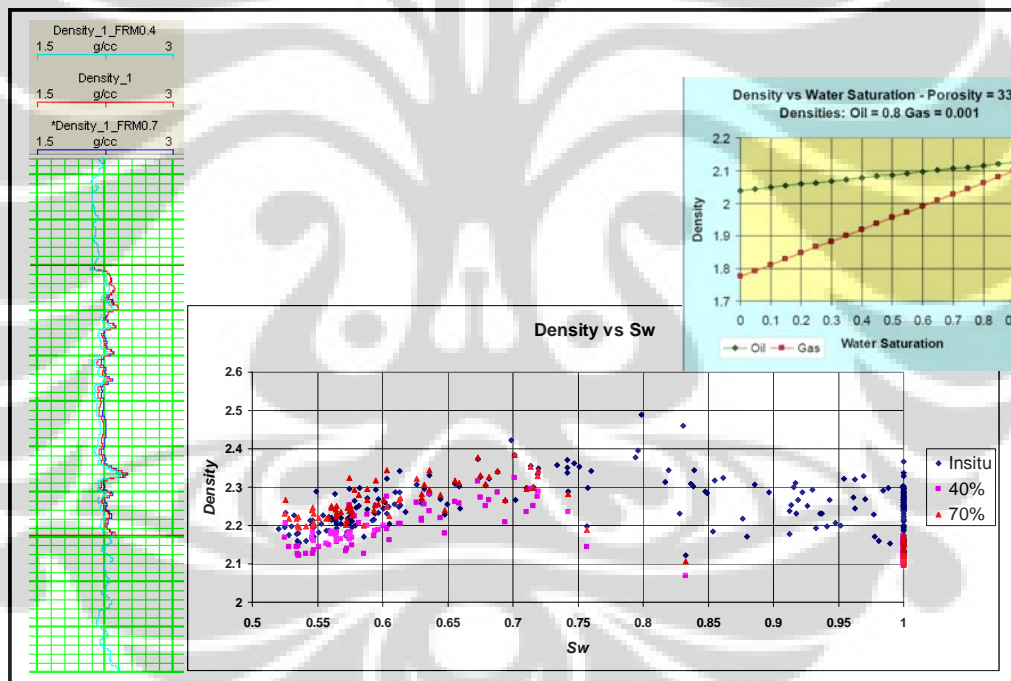


Figure 4.18 Crossplot Density – Water Saturation (40% & 70%) YM-232 Well

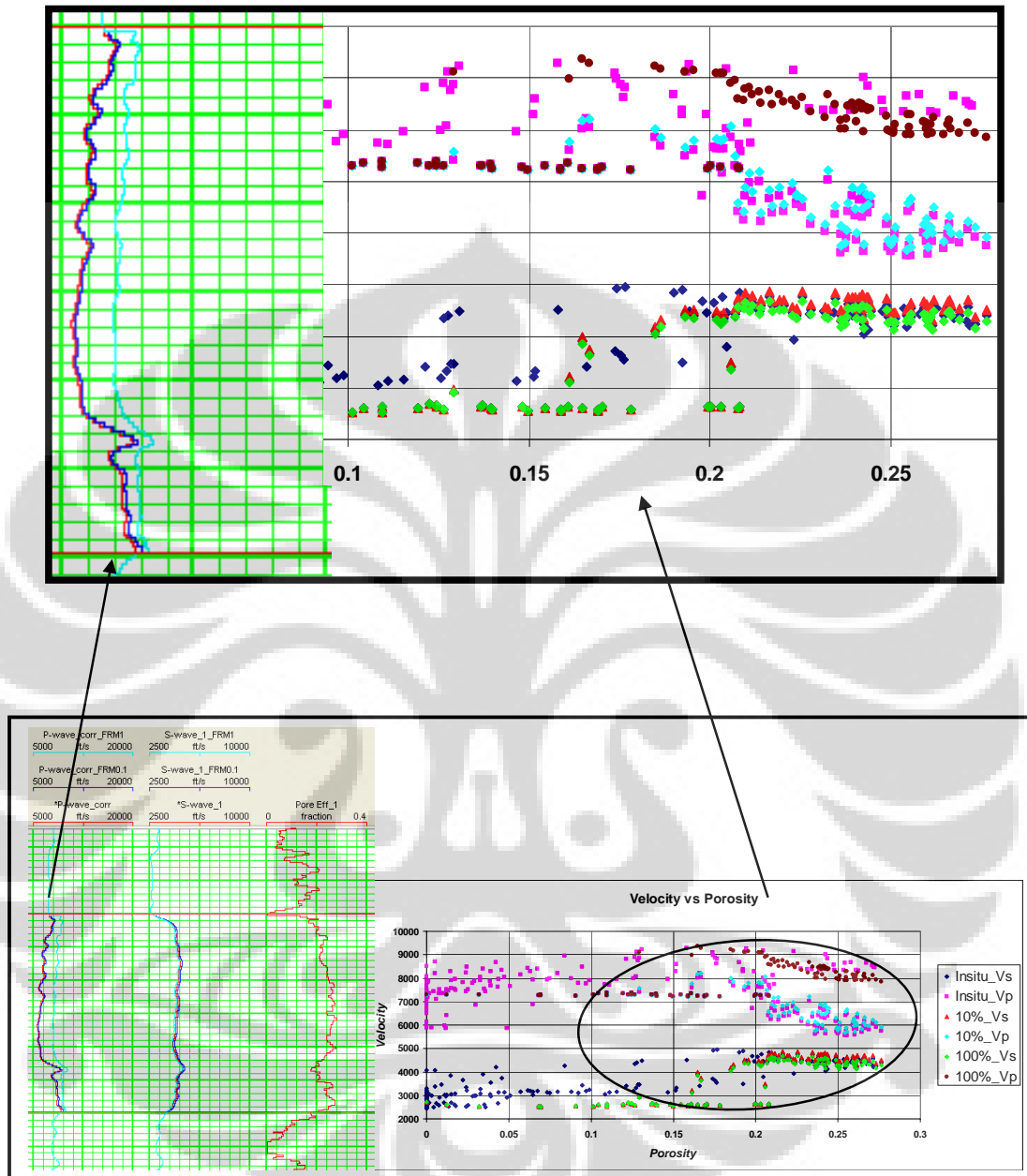


Figure 4.19 Crossplot Velocity – Porosity (10% & 100% water saturation) YM-232 Well

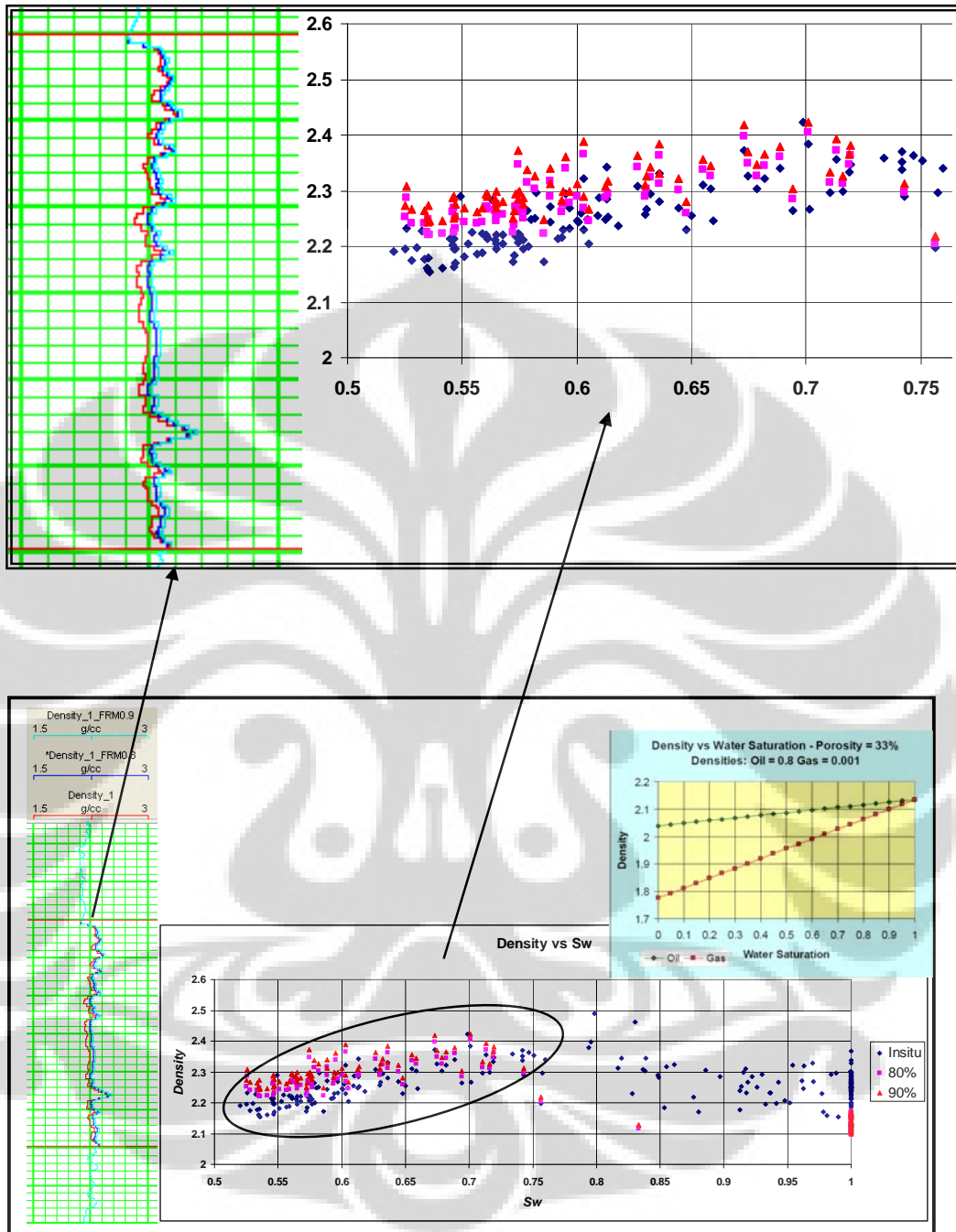


Figure 4.20 Crossplot Density – Water Saturation (80% & 90%) YM-232 Well

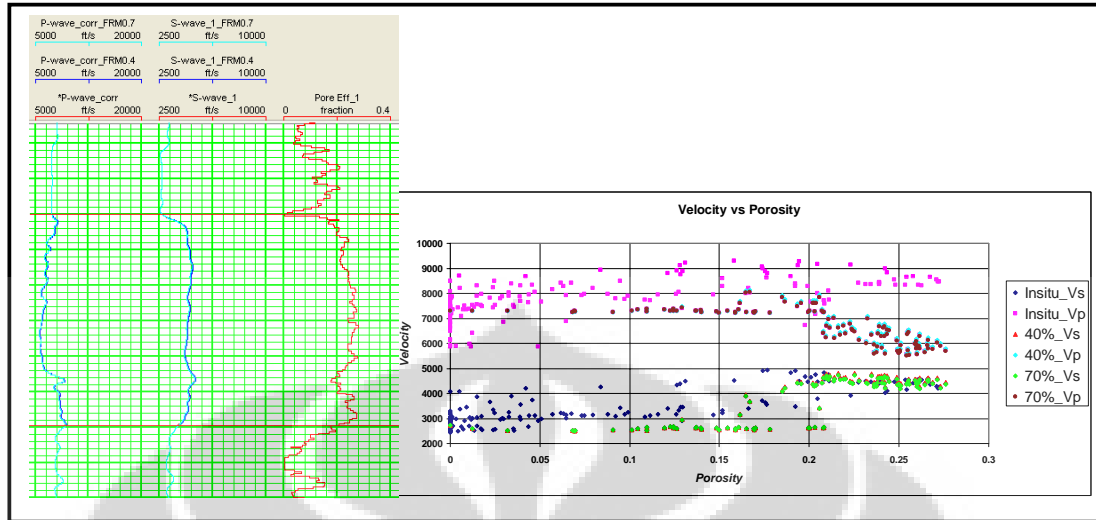


Figure 4.21 Crossplot Velocity – Porosity (40% & 70% water saturation) YM-232 Well

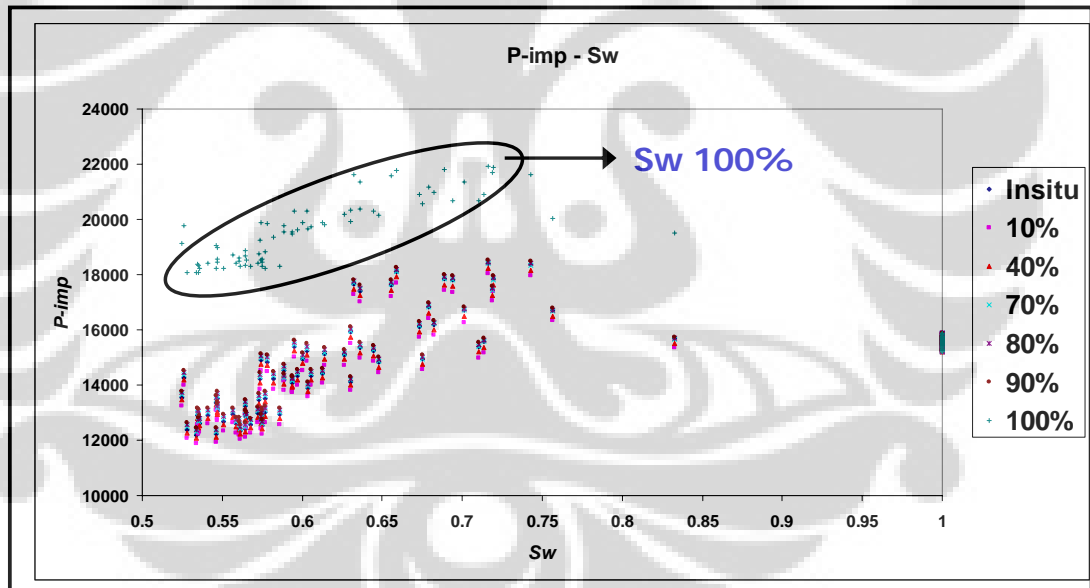


Figure 4.22 Crossplot P-impedance – Water Saturation YM-232 Well

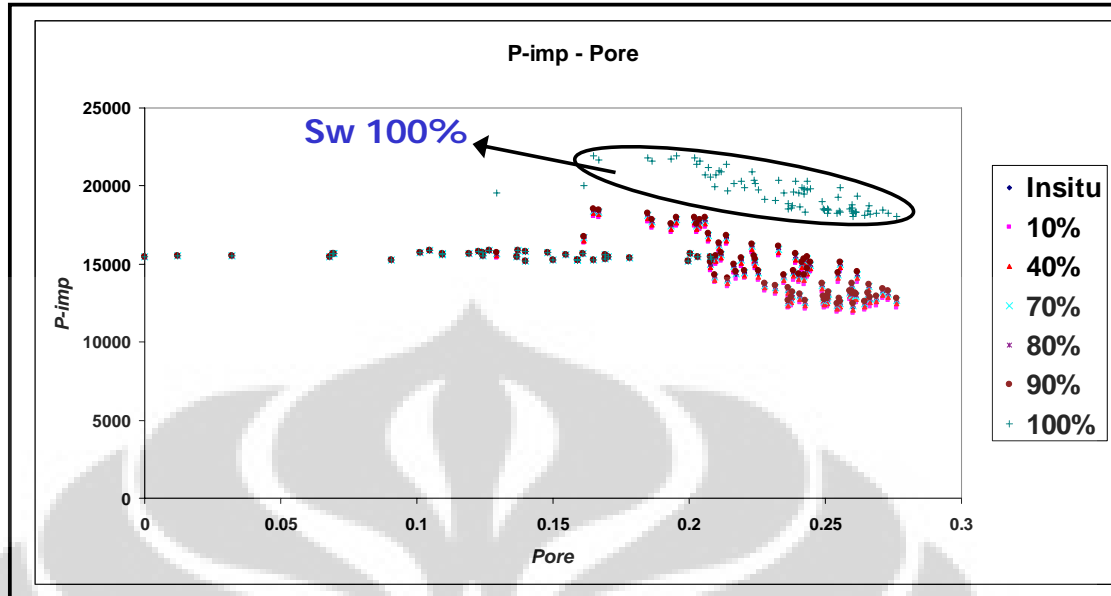


Figure 4.23 Crossplot P-impedance – Porosity YM-232 Well

Then performed the same synthetic seismic routine and the results are shown. Synthetic Offset Gathers made with the various variations offsets, 4500, 4000, 3500, 3000, 2500 and 2000 ft until resolved the pay zone. Actually, the strong response can only be seen when it was completely oil or water saturated. Compared to the insitu case, can be seen that the offset response is very similar, however the reflection amplitudes increases that it was completely water saturated. On the contrary, the reflection amplitudes decrease that assumed 10% water saturation and clean sand.

Next, computed new V_p , V_s , and density values for the pay zone assuming that it was completely water saturated. The synthetic seismic (figure 4.32 & 4.34) shows a major change in character at all offsets. The polarity of the reflections are completely reversed indicating that the hydrocarbons are a major factor only in this model (at YM-232 well).

4.5.2 The Analysis of The Telisa Sand Reservoir at YM-247 Well

The porosity of Telisa Sand reservoir at YM-247 well is 20% to 30%, based on petrophysical analysis. The reservoir quality is relatively good than Telisa Sand reservoir at YM-232 well. The Gamma Ray log is 40 – 55 API. The mudlog indicates that the lithology in this reservoir is fine to medium grain, while the gas readings is 32 to 35 units. No MDT data in this well.

The P-imp in this reservoir is 18500 – 22000 gr/cc*ft/sec. This value is higher than P-imp at the same reservoir with oil content at YM-232 well (figure 4.17). The V_p/V_s Ratio is 2.25 to 2.75, this value is higher than YM-232 well. And this phenomena is related to the physics of fluid (oil) is quite low (35.2 API) and the reservoir rock itself.

This well contains a hydrocarbon (oil) from about 2810 to 2873 ft. Next by assuming that the fluid was brine and the mineralogy was clean sand (figure). And from fluid substitution analysis we can see the increases of water saturation (10%, 40%, 70%, 100%) affects the changing of V_p (fluid) that it was sensitive.

The V_p , V_s , and density from fluid substitution analysis will be applied on seismic amplitude or called its as Synthetic Offset Gathers. It is made with various variations offsets 4500, 4000, 3500, 3000 and 2000 ft. This analysis will compare to insitu case. This figure shows taht the near offset response is very similar. When computed new V_p , V_s , and density values for the pay zone assuming that it was completely water saturated. The synthetic seismic shows a major change in character at all offsets (figure 4.32 & 4.35).

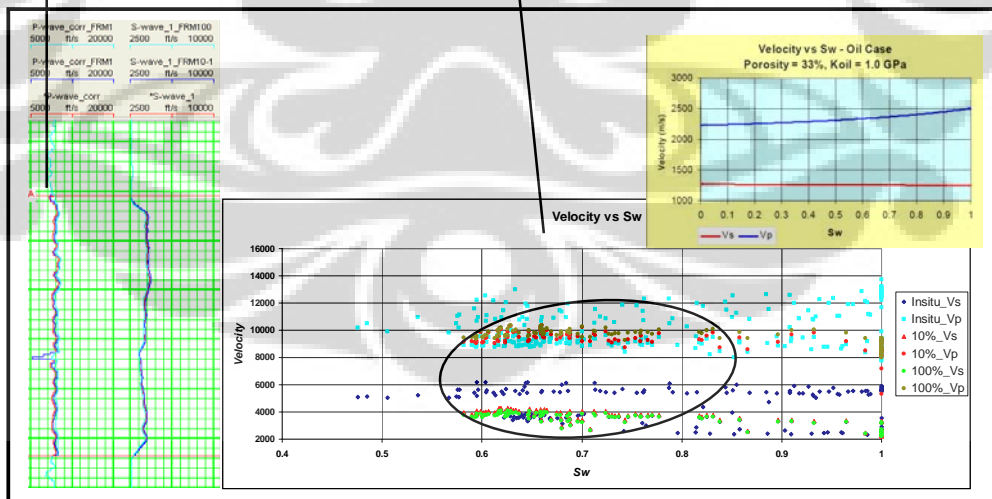
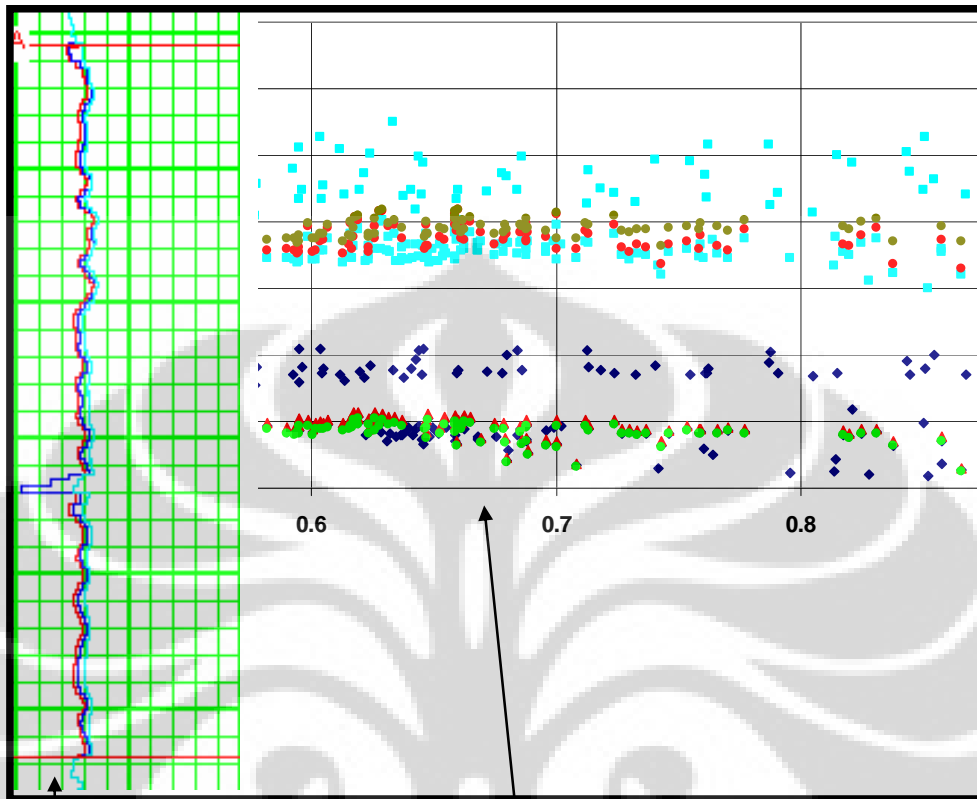


Figure 4.24 Crossplot Velocity – Water Saturation (10% & 100%)_YM-247 Well

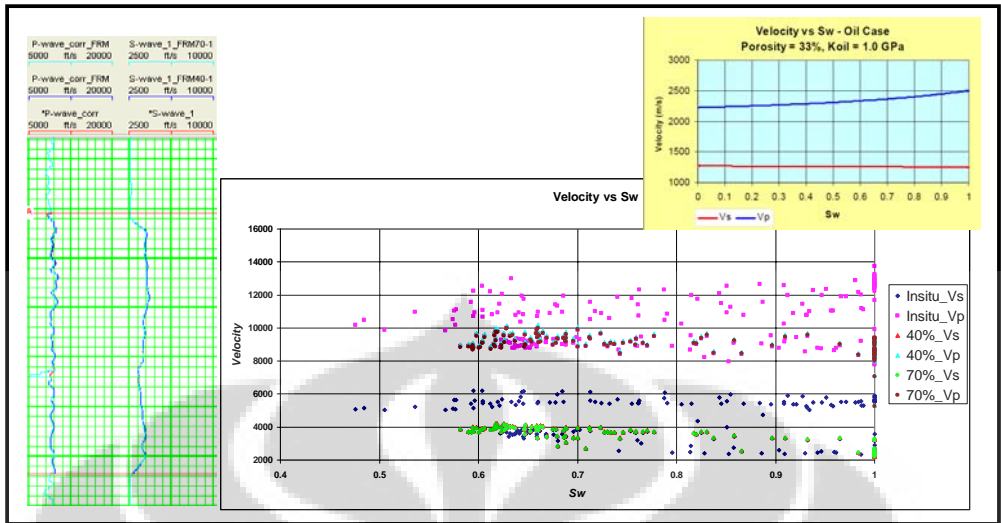


Figure 4.25 Crossplot Velocity – Water Saturation (40% & 70%)_YM-247 Well

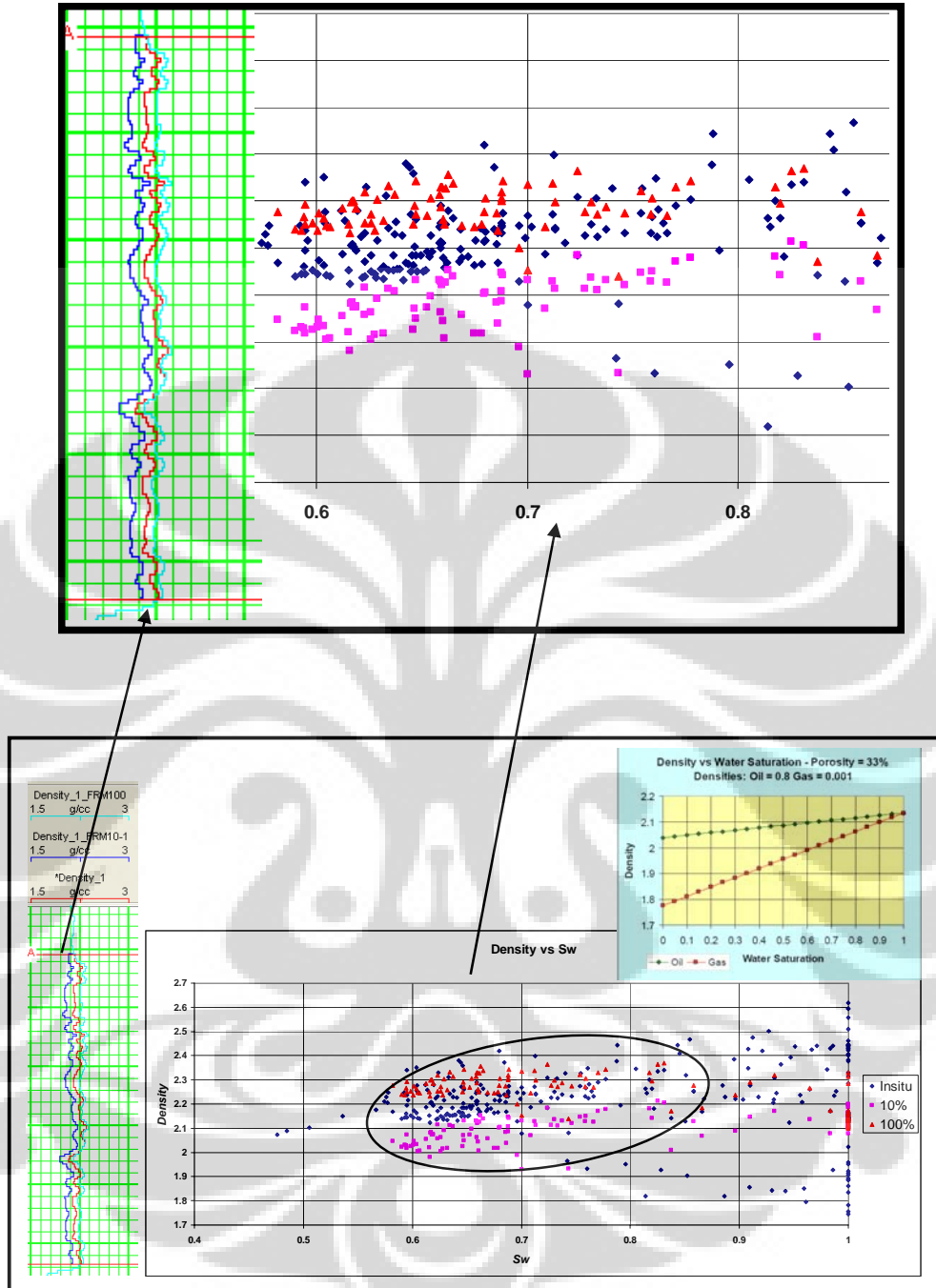


Figure 4.26 Crossplot Density – Water Saturation (10% & 100%)_YM-247 Well

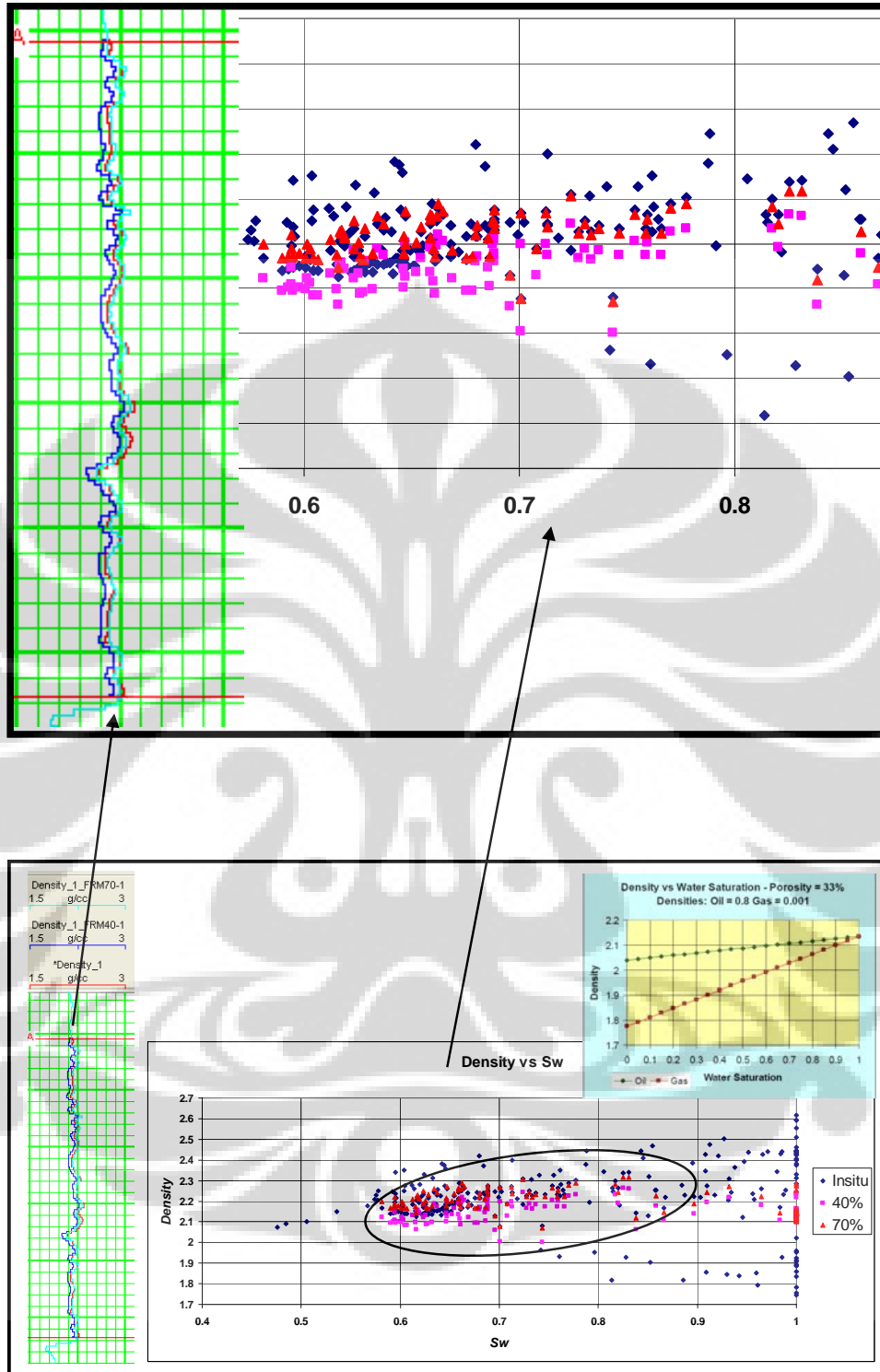


Figure 4.27 Crossplot Density – Water Saturation (40% & 70%)_YM-247 Well

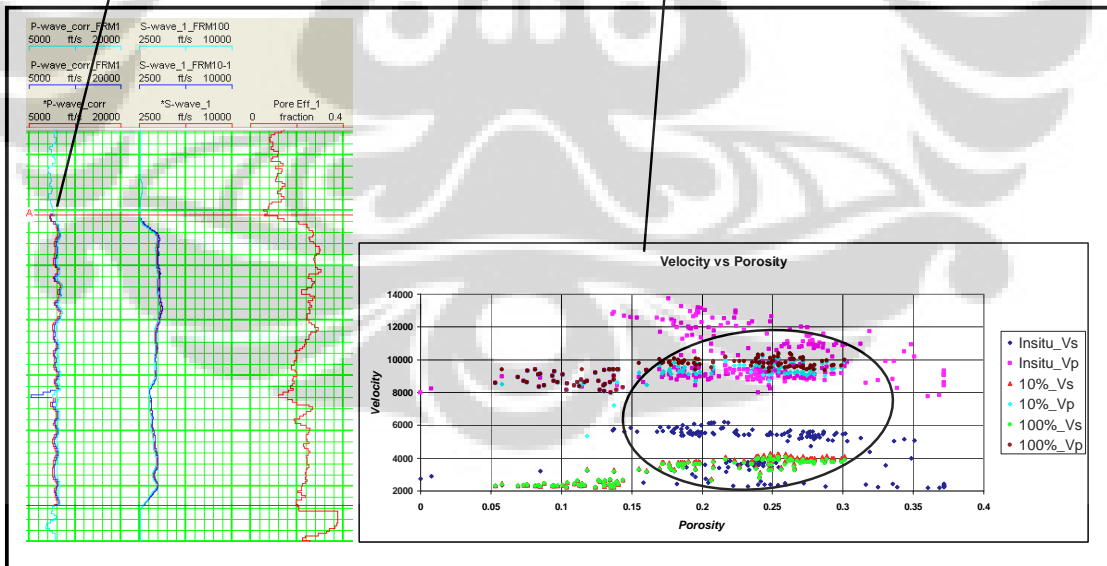
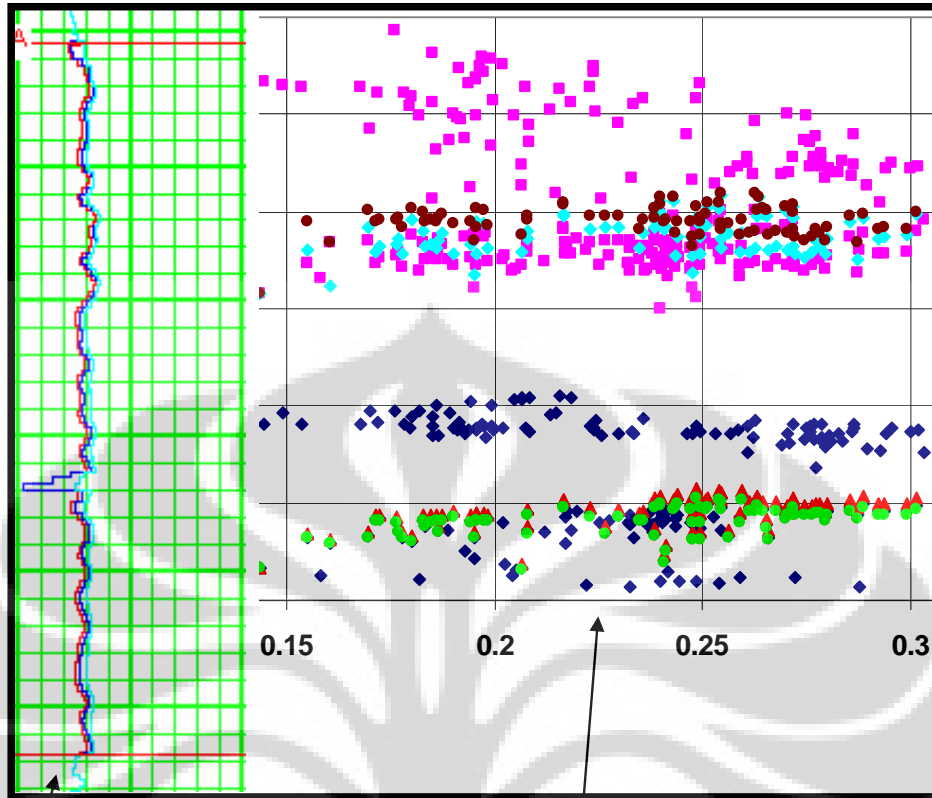


Figure 4.28 Crossplot Velocity – Porosity (10% & 100% water saturation)_YM-247 Well

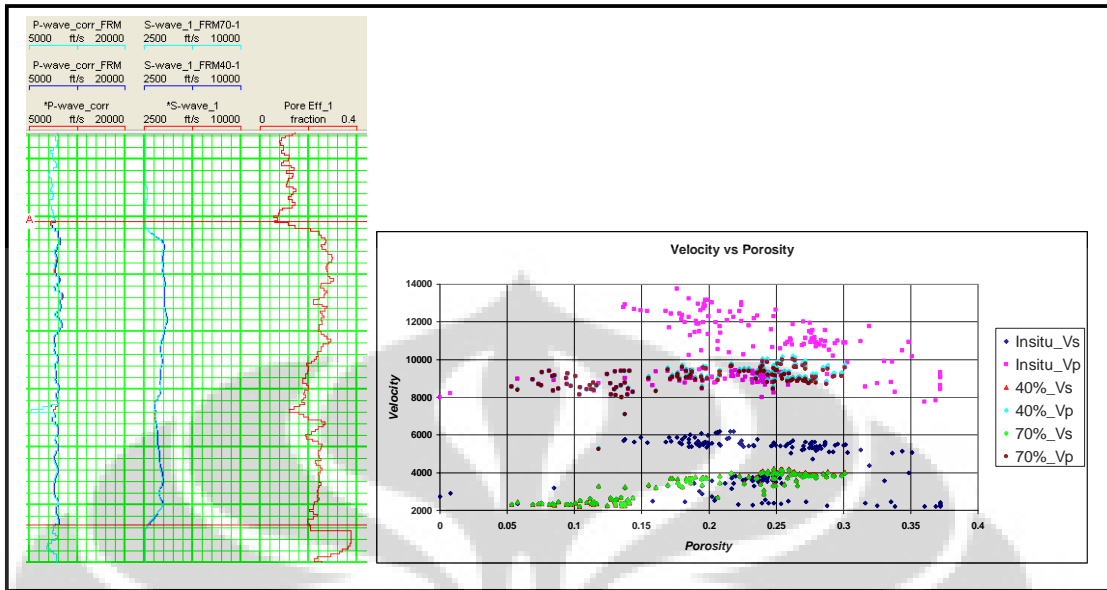


Figure 4.29 Crossplot Velocity – Porosity (40% & 70% water saturation)_YM-247 Well

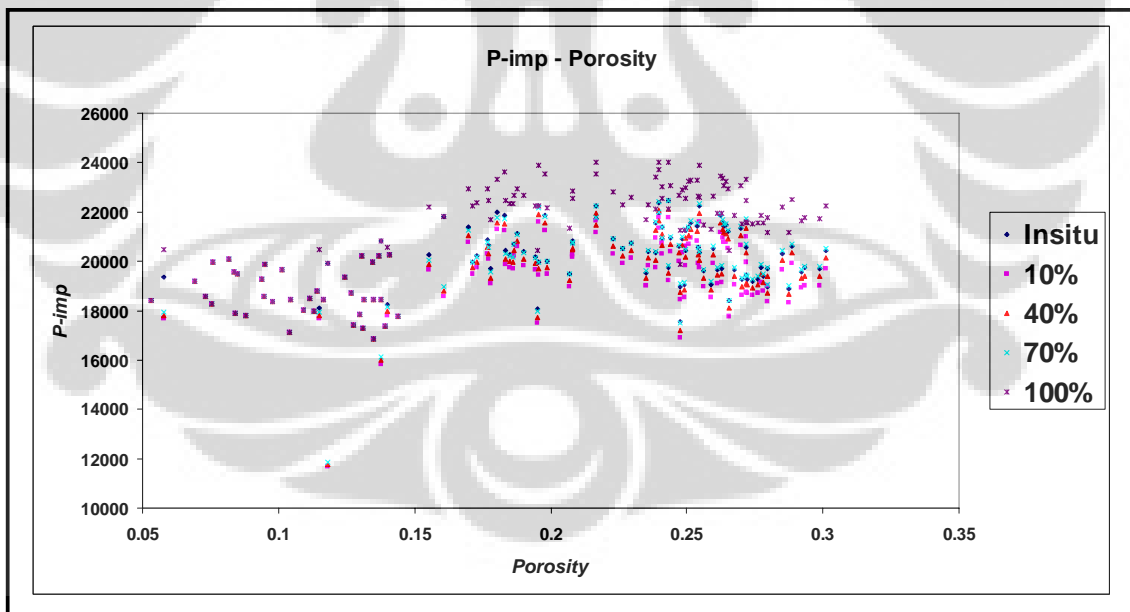


Figure 4.30 Crossplot P-impedance - Porosity YM-247 Well

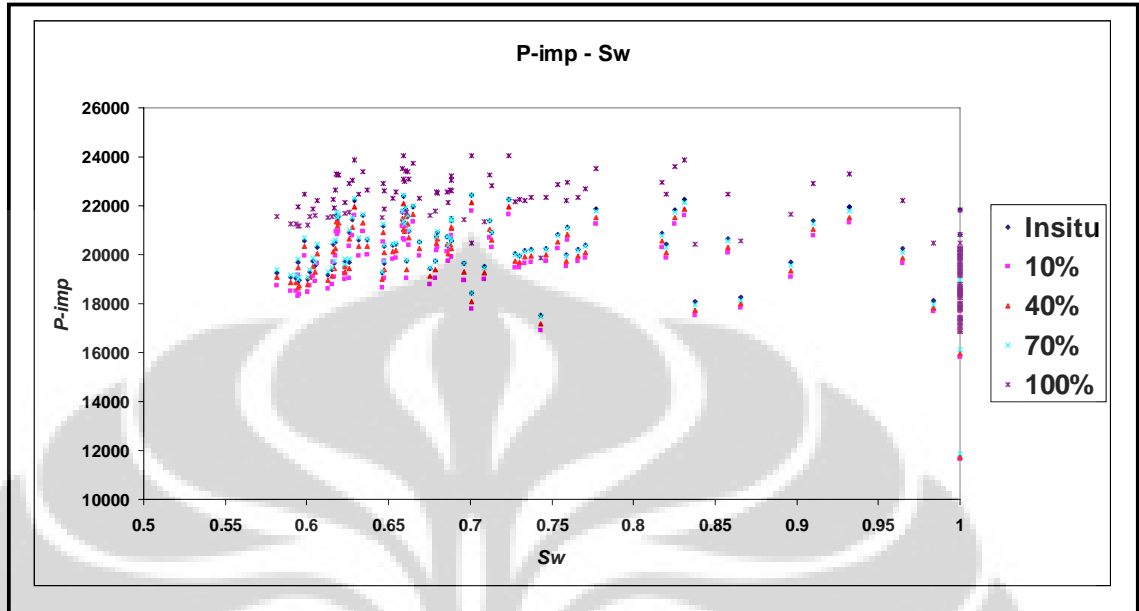


Figure 4.31 Crossplot P-impedance – Water Saturation YM-247 Well

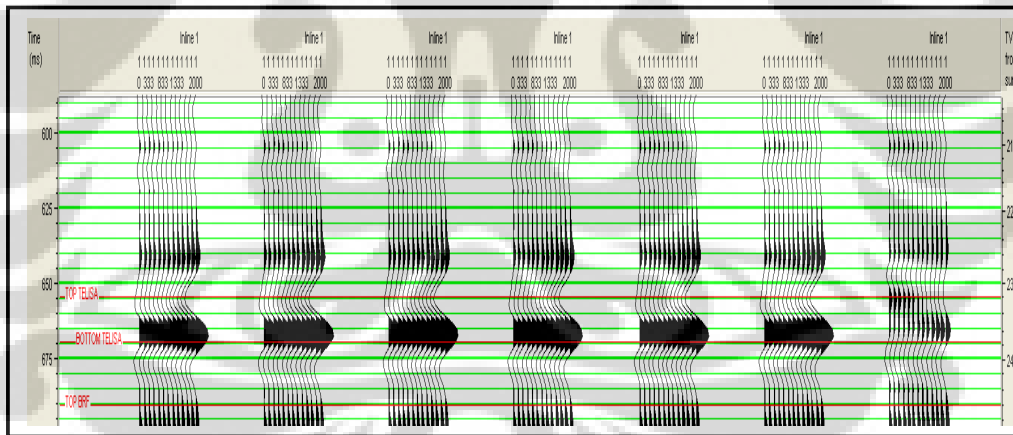


Figure 4.32 Synthetic Seismic at YM-232 Well with offset 2000 ft (insitu case, after substituted with 10%, 40%, 70%, 80%, 90%, & 100% water saturation)

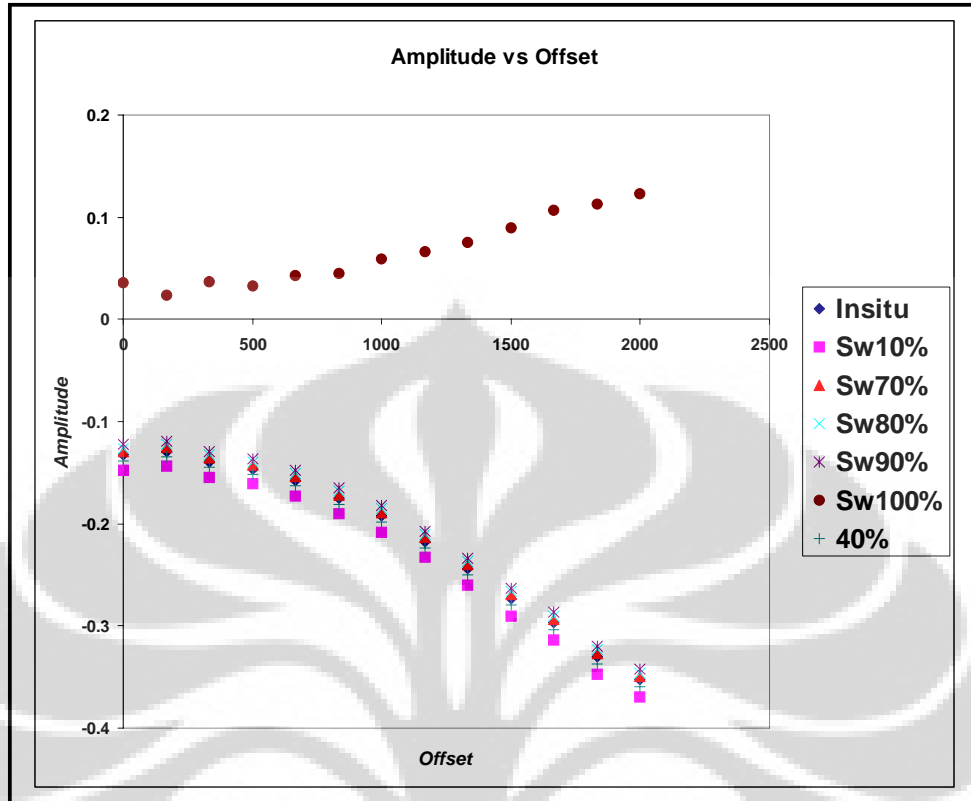


Figure 4.33 AVO Crossplot at YM-232 Well with offset 2000 ft (insitu case, after substituted with 10%, 40%, 70%, 80%, 90%, & 100% water saturation)

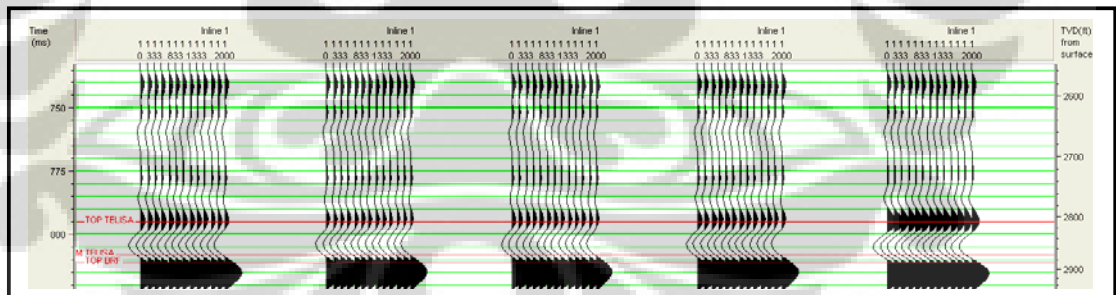


Figure 4.34 Synthetic Seismic at YM-247 Well with offset 2000 ft (insitu case, after substituted with 10%, 40%, 70%, & 100% water saturation)

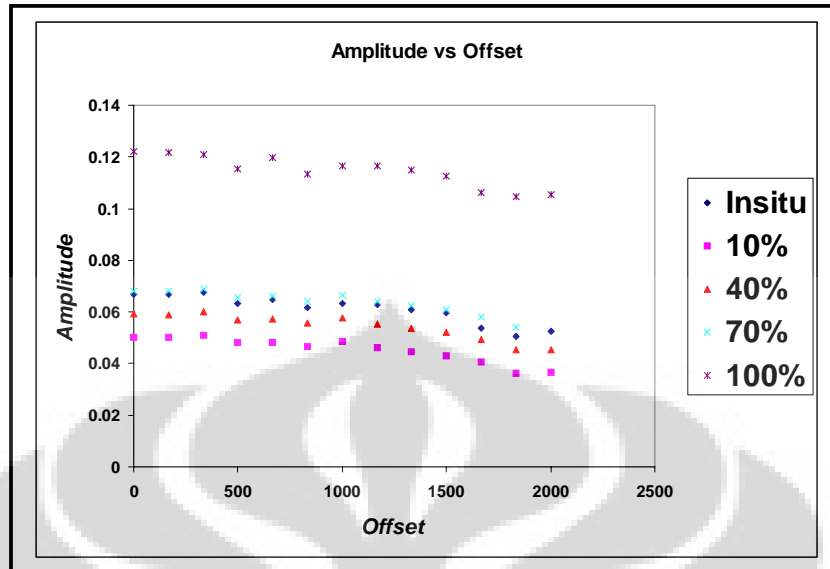


Figure 4.35 AVO Crossplot at YM-247 Well with offset 2000 ft (insitu case, after substituted with 10%, 40%, 70%, & 100% water saturation)

Synthetic seismic from YM-232 & YM-247 wells show a major change of amplitude response (substituted with 10% & 100% water saturation) in character at all offsets, indicating that the hydrocarbons are a major factor in this model, as opposed to simply changes in lithology.

We assumed that the amplitude response close related to sonic wave propagation (DT). The oil content affects the sonic wave propagation (DT), in a specific manner: at low interval oil content, the sonic transit time decreases gradually & drops suddenly at a specific value, above this value the sonic transit time seems does not change with the increase of oil content. The water content affects the sonic wave propagation in a specific interval of water saturation (figure 4.36).

And the second assumption, that, the pore space (porosity Φ) is filled with a fluid of density ρ_{fl} & bulk modulus K_{fl} . In other words, the bulk modulus of saturated rock equals the bulk modulus of the skeleton plus a term which depends on the fluid.

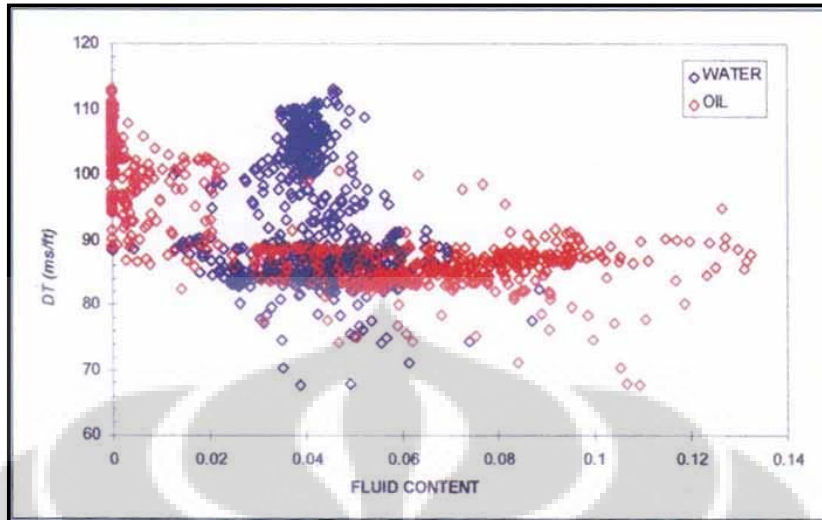


Figure 4.36 The Behavior of Sonic Transit Time in The Reservoir Rock as Fluid Content Increases. Red Indicates Oil & Blue Indicates Water.

(Suprajitno Munadi, 2007)

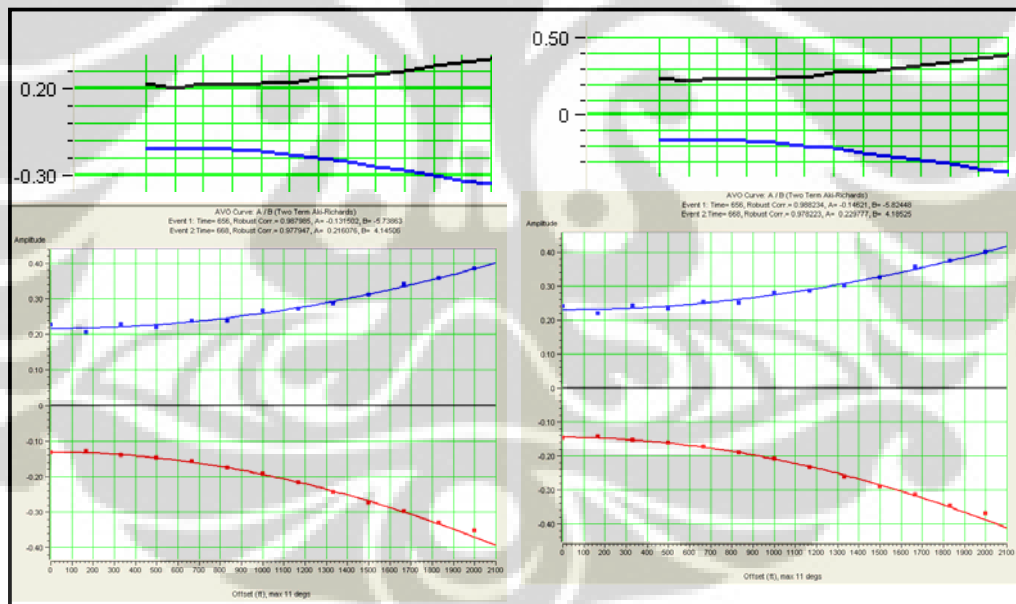
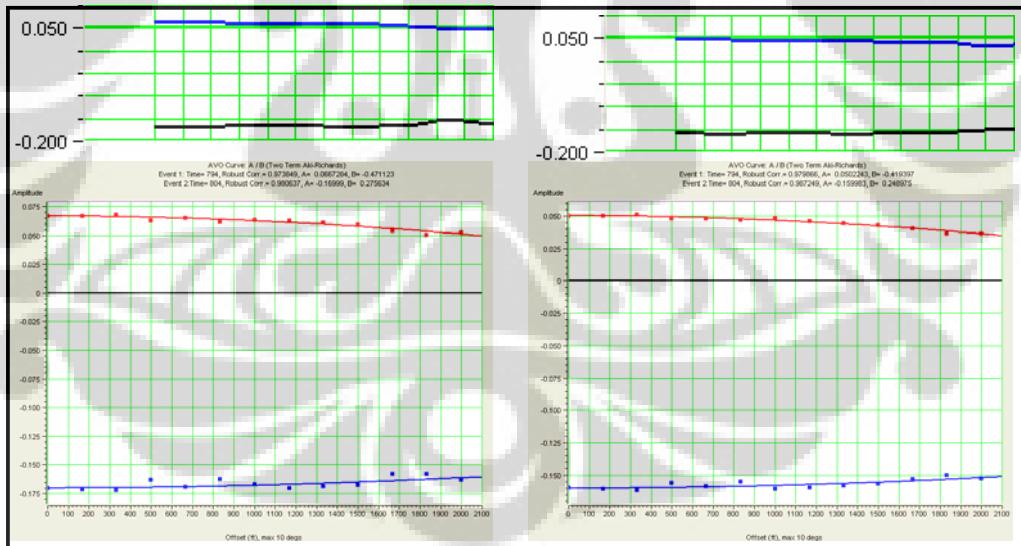
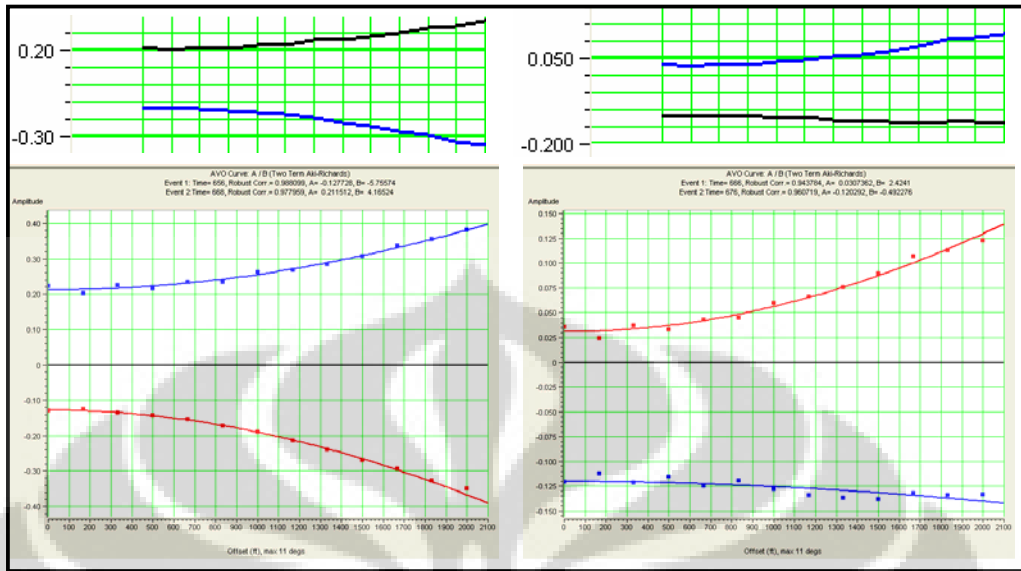


Figure 4.37 AVO Analysis (Intercept & Gradient of Top & Bottom Telisa Sand)

for Synthetic of YM-232 Well

(insitu case & substituted with 10% water saturation)



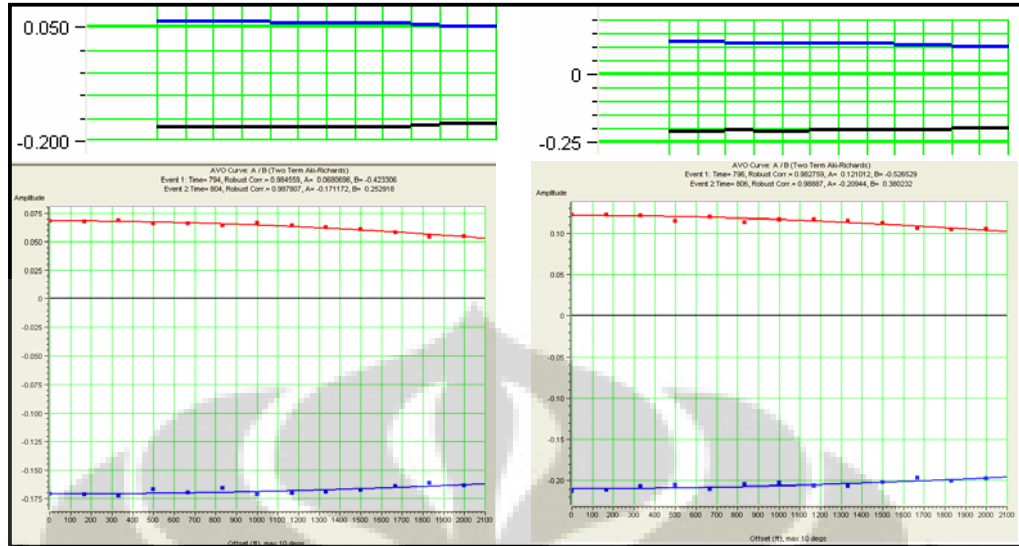


Figure 4.40 AVO Analysis (Intercept & Gradient of Top & Bottom Telisa Sand) for Synthetic of YM-247 Well (substituted with 70% & 100% water saturation)

From YM-232 well at figure 4.33, 4.37 & 4.38 can be interpreted that the synthetic after substituted with 10% & 70% water saturation, it can be classified as near-zero impedance contrast sands. Same as the above classification, the synthetic after substituted with 100% water saturation is near-zero impedance contrast sands, but it looks like polarity change.

While, YM-247 from figure 4.35, 4.39 & 4.30 is interpreted as high impedance sand.

4.8 Comparison between Model Amplitude and Real Seismic

A problem often encountered in exploration and development geophysics is to estimate the fluid type in prospect based on amplitude information in seismic data. The method applied data on sand velocity, density, porosity, clay content and expected fluid types as input into the rock physics software for estimation of acoustic impedance and reflectivity for various types of hydrocarbon saturation. And the result is the coefficient from the model have good correlation with the real seismic, at YM-247 well.

Each of correlation coefficient from YM-232 well : when it was completely water saturated is 0.12, 0.87 for the original saturation, when it was substituted with 70% and 90% water saturation : 0.87 and 0.88 , and for 10% water saturation is 0.86.

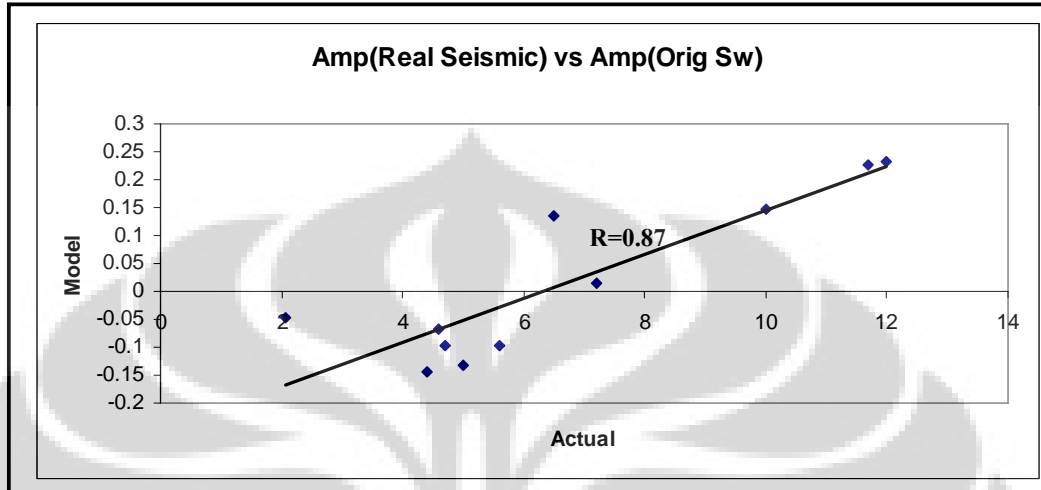


Figure 4.41 The Correlation Coefficient between Real Amplitude & Model Amplitude at Insitu Case (original Sw) _YM-232 Well

While the smallest correlation is found at YM-232 well, when it was completely water saturated.

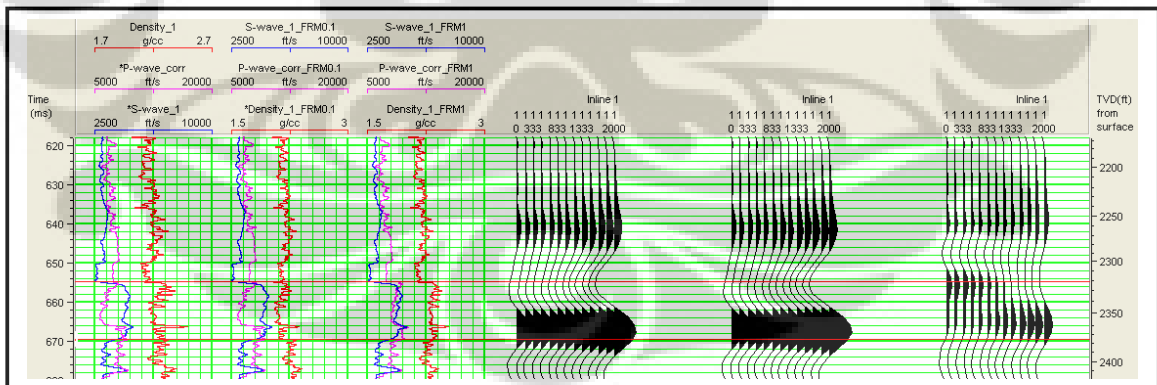


Figure 4.42 ρ , V_p , & V_s _ Synthetic Offset Gathers (insitu case, substituted with 10% & 100% water saturation) _YM-232 Well

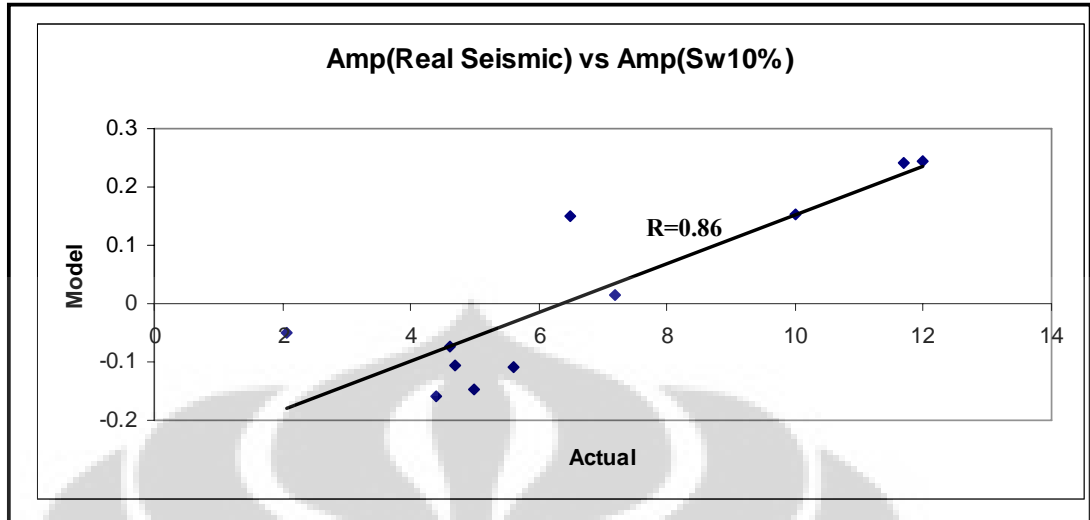


Figure 4.43 The Correlation Coefficient between Real Amplitude & Model Amplitude After Substituted with 10% Water Saturation _ YM-232 Well

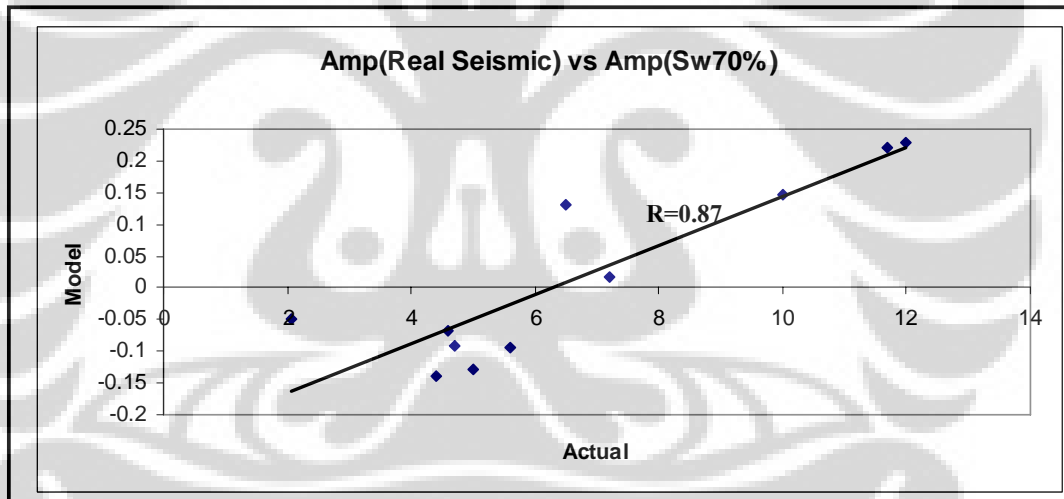


Figure 4.44 The Correlation Coefficient between Real Amplitude & Model Amplitude After Substituted with 70% Water Saturation _ YM-232 Well

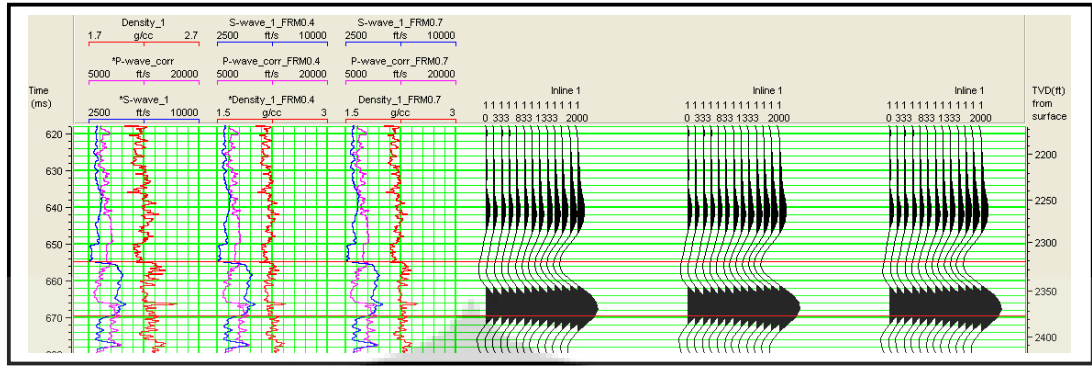


Figure 4.45 ρ , V_p , & V_s _ Synthetic Offset Gathers (insitu case, substituted with 40% & 70% water saturation) _YM-232 Well

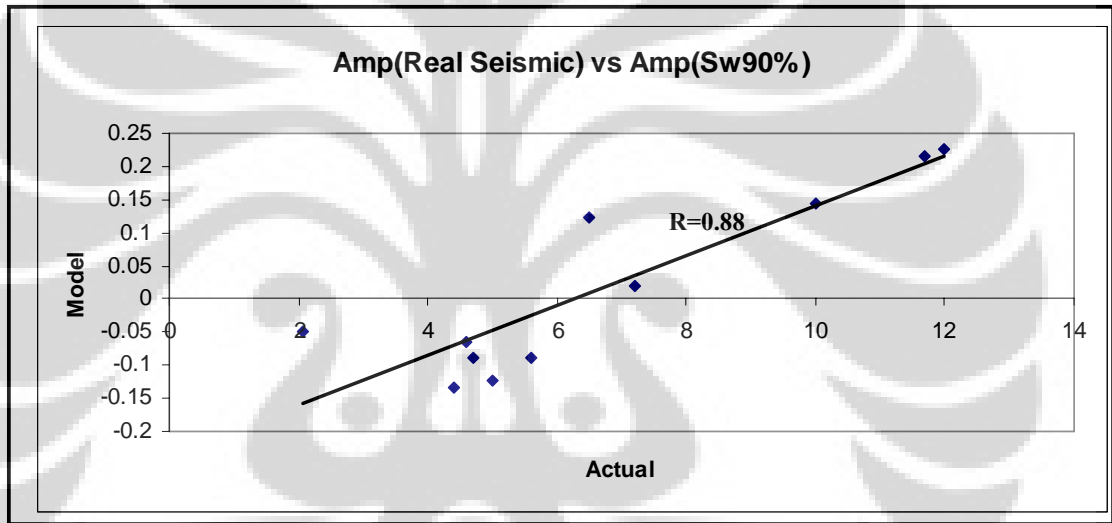


Figure 4.46 The Correlation Coefficient between Real Amplitude & Model Amplitude After Substituted with 90% Water Saturation _ YM-232 Well

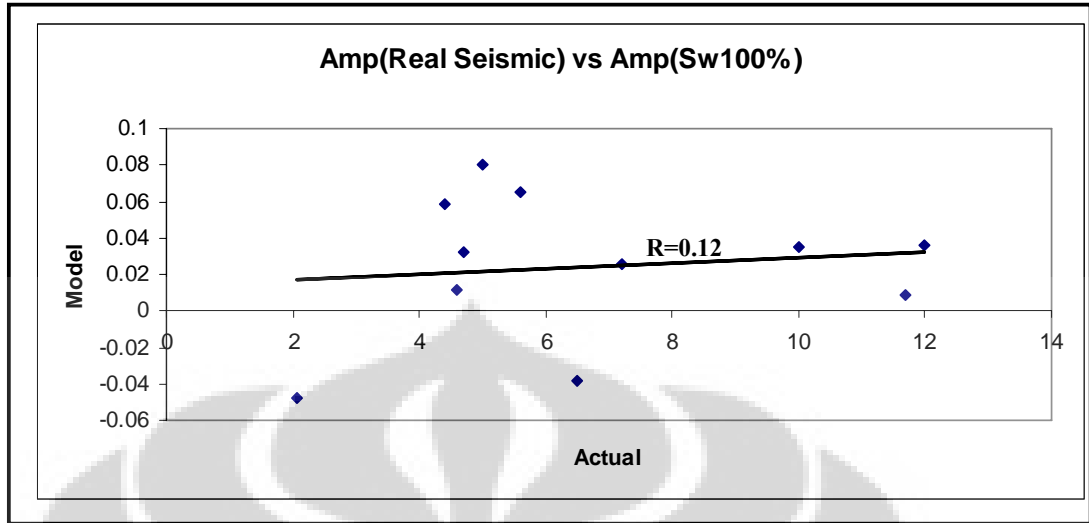


Figure 4.47 The Correlation Coefficient between Real Amplitude & Model Amplitude After Substituted with 100% Water Saturation _ YM-232 Well

Overall, model amplitude YM-232 well, close to the real seismic data, except for 100% water saturation. However, good correlation is achieved when it was substituted by water saturation.

After the model was normalized to seismic data, then, its can be applied to predict the fluid in other area within the field.

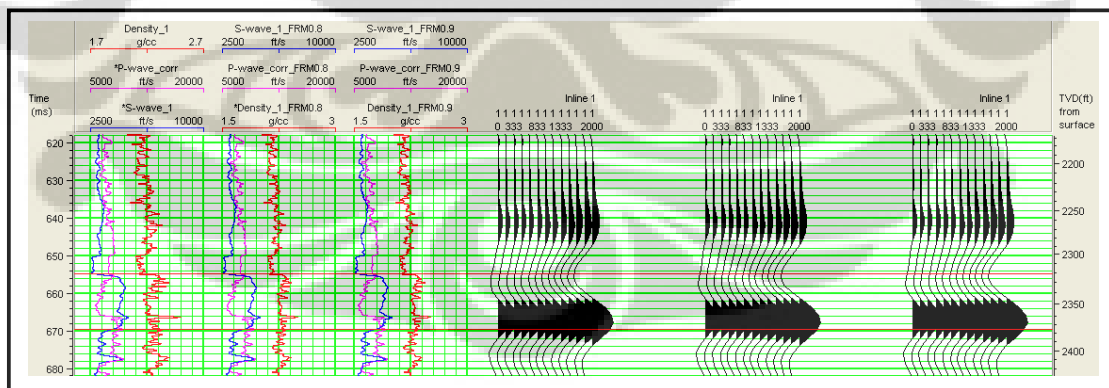


Figure 4.48 ρ , V_p , & V_s _ Synthetic Offset Gathers (insitu case, substituted with 80% & 90% water saturation) _ YM-232 Well

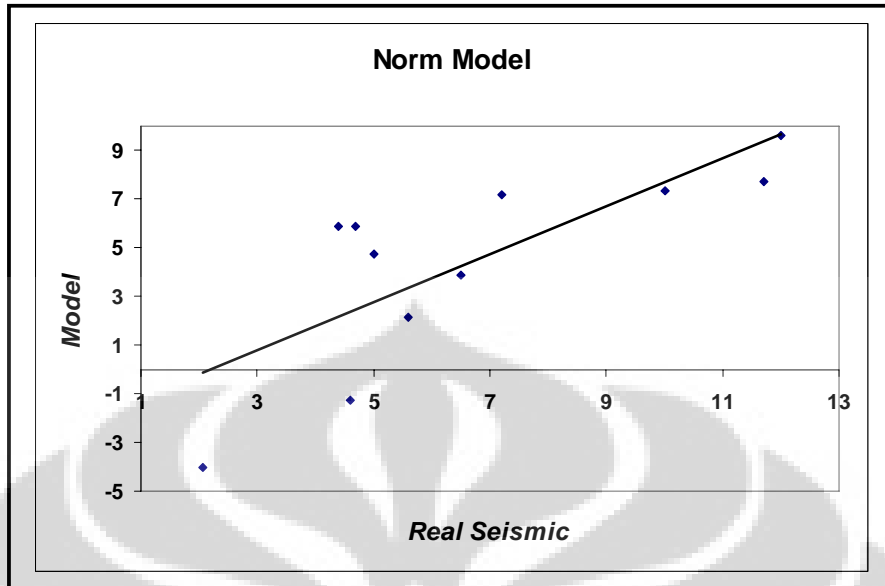


Figure 4.49 The Correlation Coefficient between Real Amplitude & Model Amplitude After Normalized _YM-232 Well

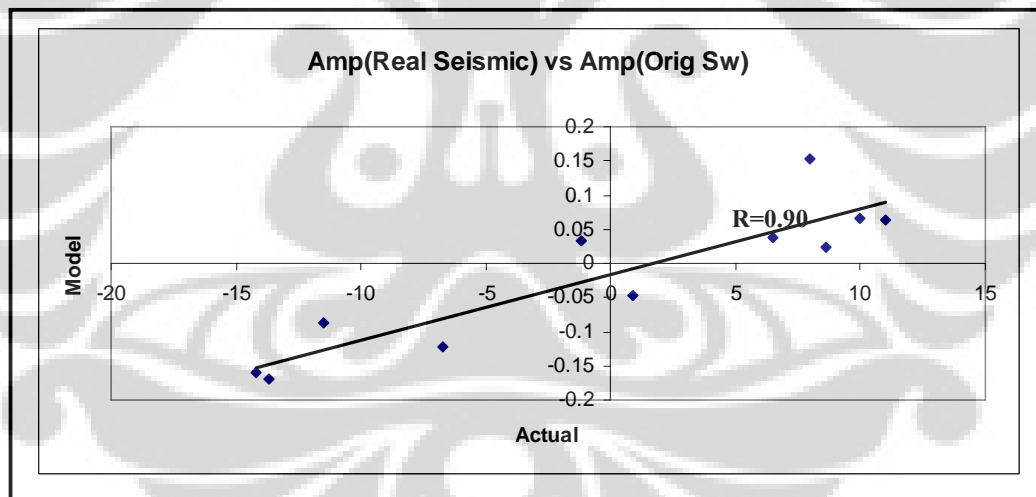


Figure 4.50 The Correlation Coefficient between Real Amplitude & Model Amplitude for Insitu Case _YM-247 Well

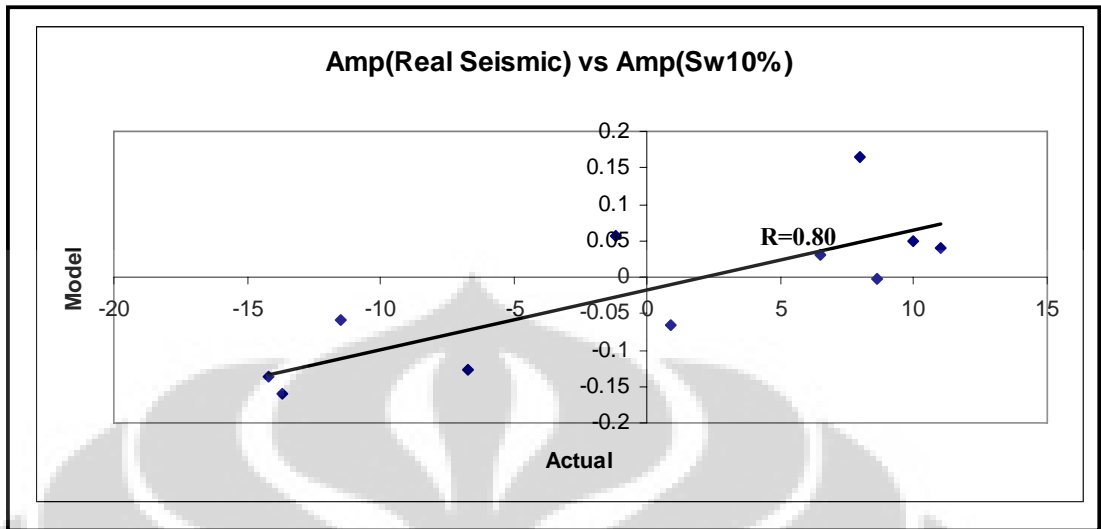


Figure 4.51 The Correlation Coefficient between Real Amplitude & Model Amplitude After Substituted with 10% Water Saturation _ YM-247 Well

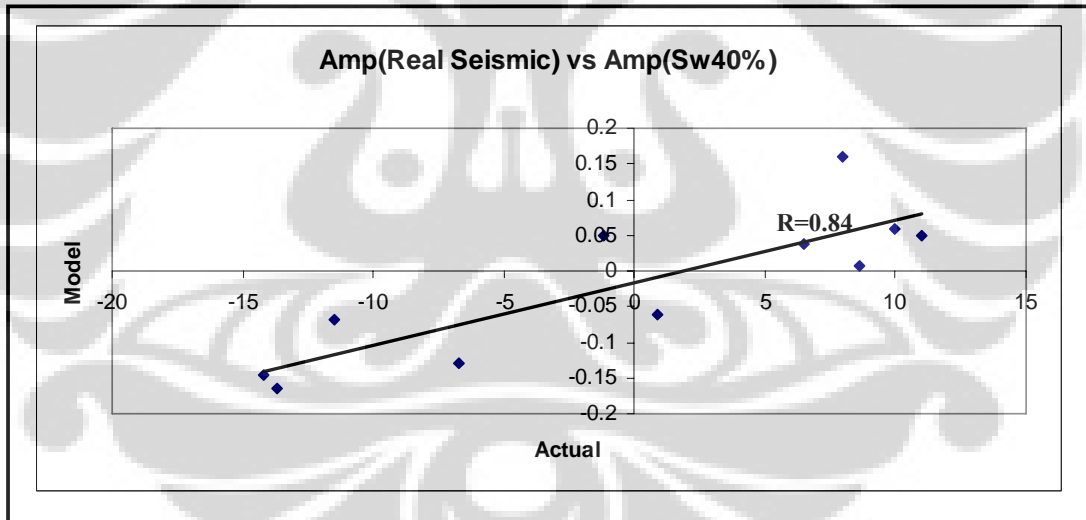


Figure 4. 52 The Correlation Coefficient between Real Amplitude & Model Amplitude After Substituted with 40% Water Saturation _ YM-247 Well

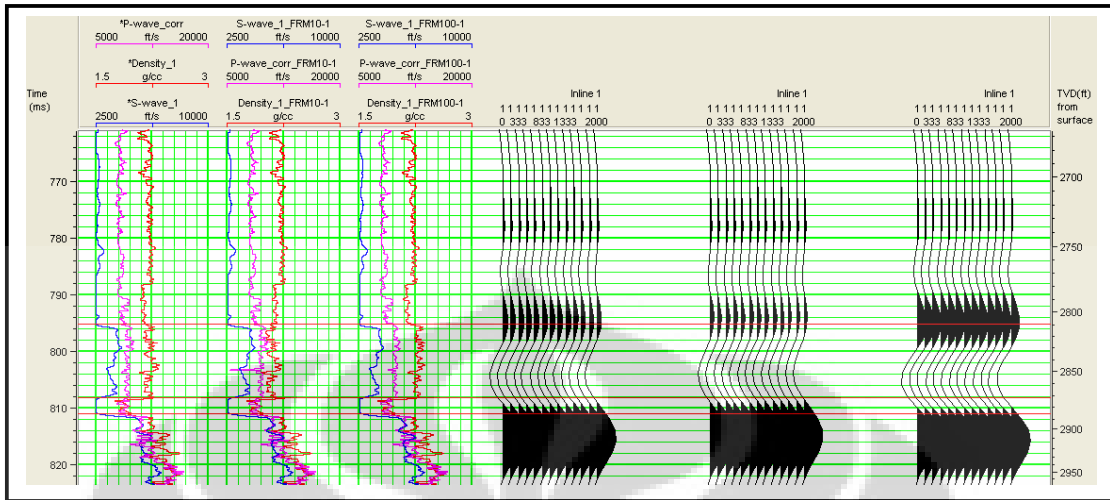


Figure 4.53 ρ , V_p , & V_s _ Synthetic Offset Gathers (insitu case, substituted with 10% & 100% water saturation) _YM-247 Well

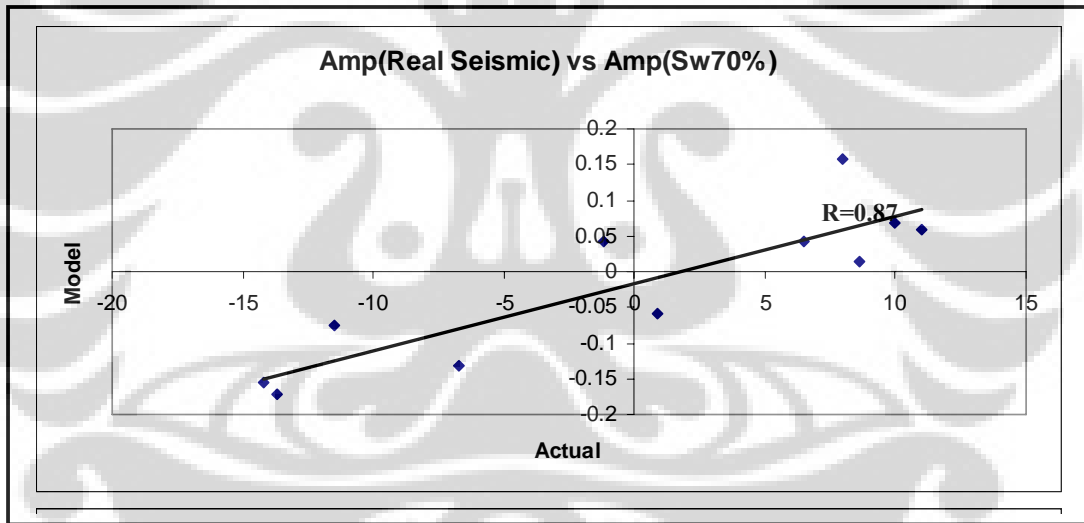


Figure 4.54 The Correlation Coefficient between Real Amplitude & Model Amplitude After Substituted with 70% Water Saturation _ YM-247 Well

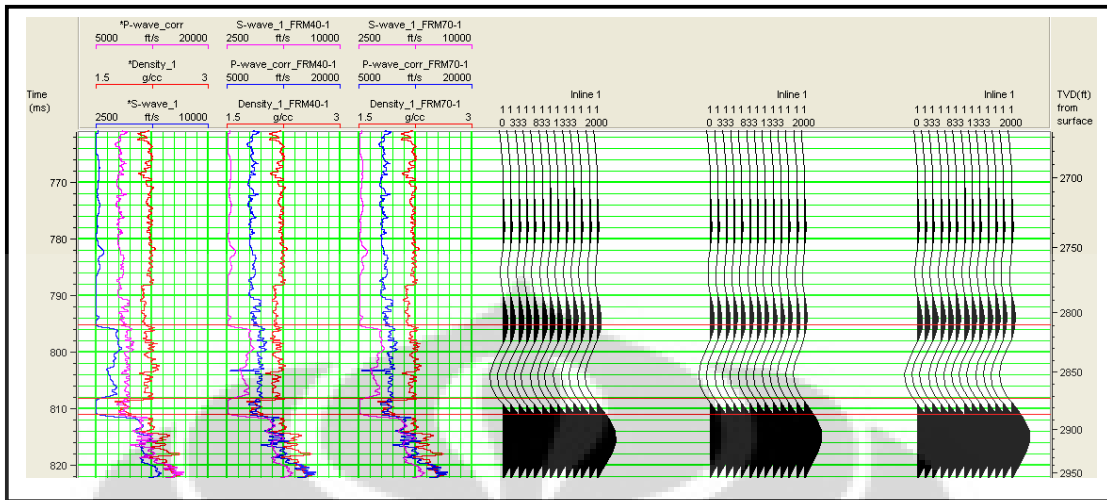


Figure 4.55 ρ , V_p , & V_s _ Synthetic Offset Gathers (insitu case, substituted with 40% & 70% water saturation) _YM-247 Well

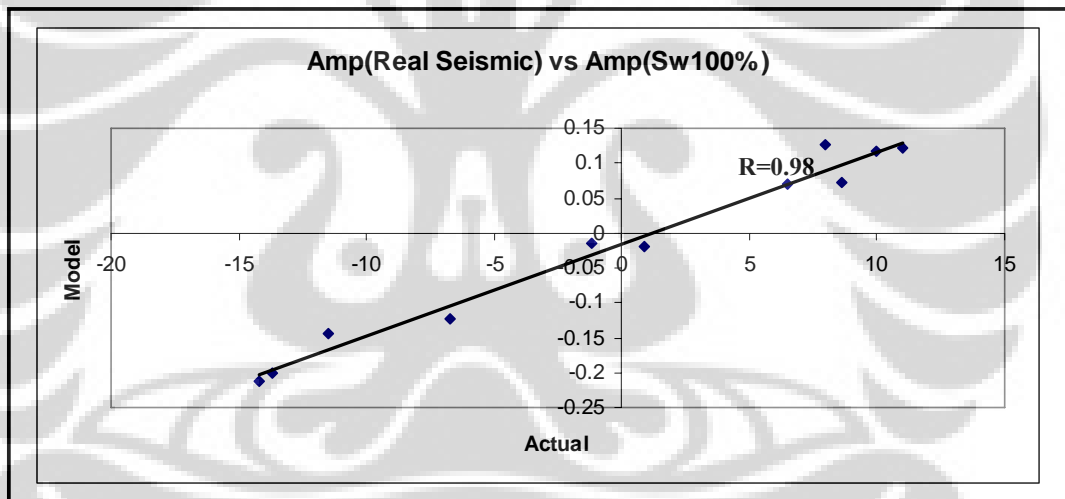


Figure 4.56 The Correlation Coefficient between Real Amplitude & Model Amplitude After Substituted with 100% Water Saturation _ YM-247 Well

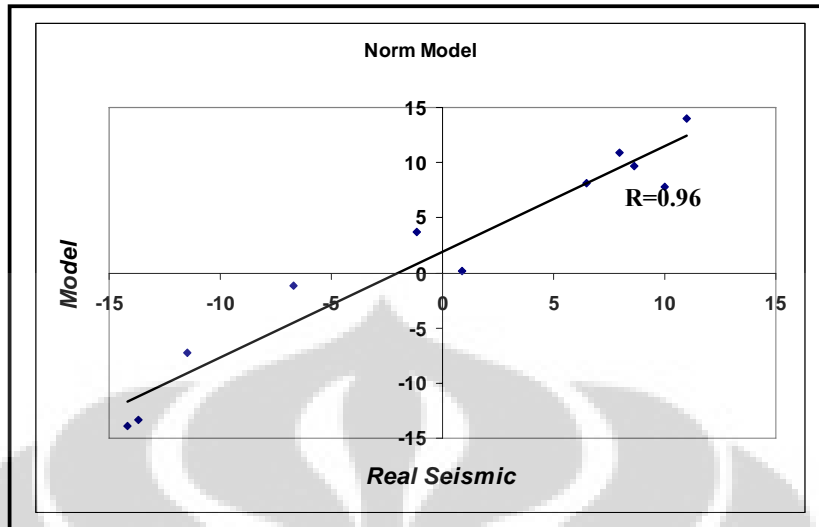


Figure 4. 57 The Correlation Coefficient between Real Amplitude & Model Amplitude After Normalized _ YM-247 Well

Also with YM-232 well, YM-247 model can be applied to predict the fluid in other area within the field. A good correlation is achieved when it was substituted by 100% water saturation, 0.98. And the second is when it was substituted by 70% water saturation, 0.87.

This is summary of correlation amplitude model with real seismic data from YM-247 well (table 4.2 & 4.3) :

The Correlation Coefficient Amplitude Model with Real Seismic (YM-232 well)	
Original Case	0.8754
Substituted with Sw 10%	0.8656
Substituted with Sw 70%	0.8793
Substituted with Sw 90%	0.8842
Substituted with Sw 100%	0.1244
Norm Model	0.7745

Table 4.2 The Correlation Coefficient Model Amplitude to Real Seismic (YM-232 Well)

The Correlation Coefficient Amplitude Model with Real Seismic(YM-247 well)	
Original Case	0.9028
Substituted with Sw 10%	0.808
Substituted with Sw 40%	0.8449
Substituted with Sw 70%	0.8756
Substituted with Sw 100%	0.9894
Norm Model	0.9691

Tabl 4.3 The Correlation Coefficient Model Amplitude to Real Seismic (YM-247 Well)

The range of model amplitude is -0.2 to 0.24. While the amplitude distribution from real seismic is -10 to 10 (figure 4.45). The amplitude model will be calibrated and correlated to real seismic, to achieve the correlation coefficient. Then, those model (normalization model) ready to be applied within field (figure 4.44 & 4.52).

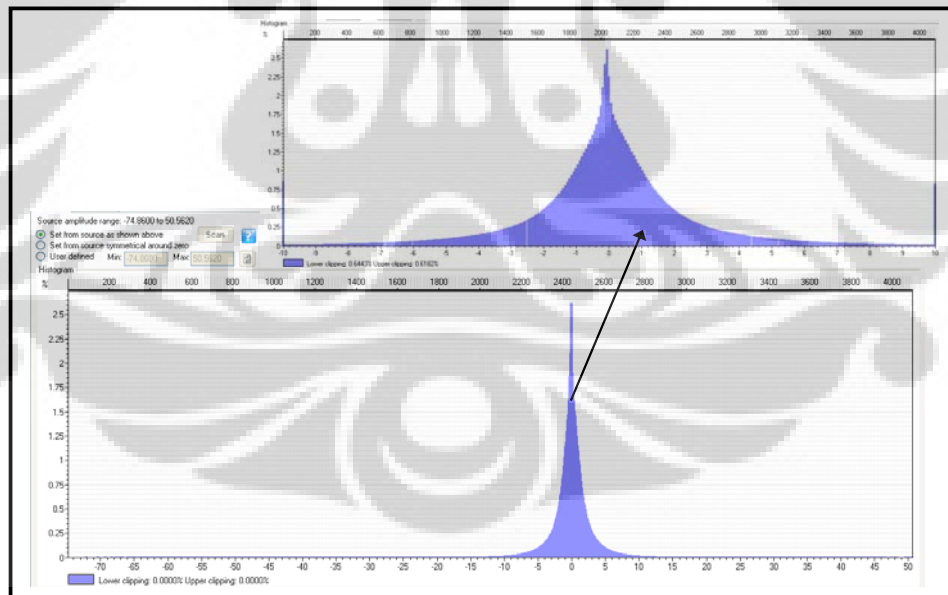


Figure 4.58 The Amplitude Distribution from Real Seismic

CHAPTER 5

Conclusions and Recommendation

The original reservoir sand interval (YM-232 & YM-247 wells) (oil filled) shows high porosity, low V_{clay} , high water saturation, decreasing P-imp. Gassmann's equation provide the seismic interpreter with a powerful framework for evaluating various fluid scenarios which might give rise to an observed seismic. When applied fluid substitution at YM-232 & YM-247 wells, the changing of V_p is sensitive to the increases of water saturation. At the time completely oil saturated, the porosity increases and P-imp decreases. When, it was completely water saturated, P-imp increases and also porosity.

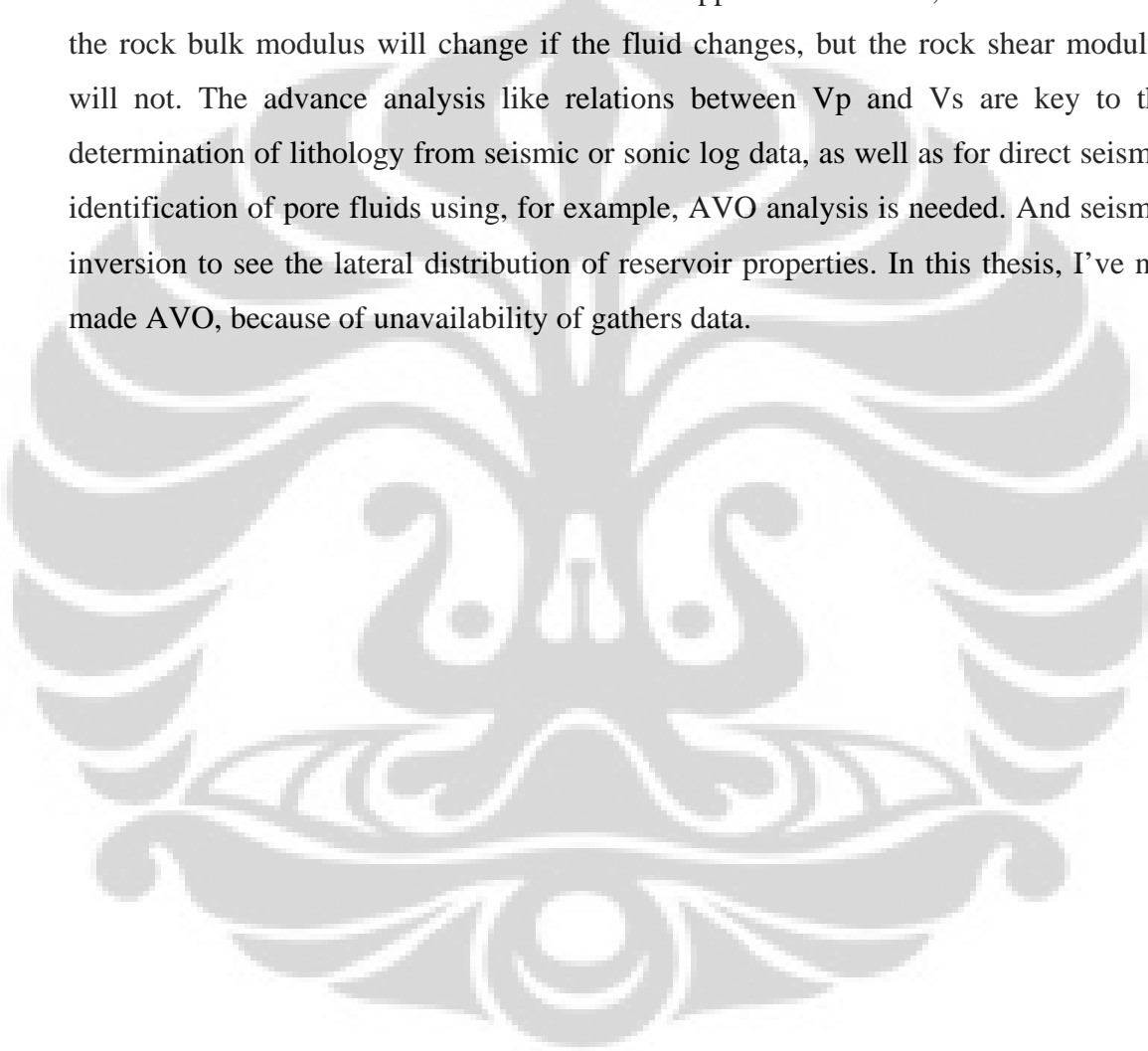
The Synthetic Offset Gathers is a way to understand the effect of hydrocarbon saturation on synthetic offset gather. From YM-232 and YM-247 wells, the offset response is very similar, however the reflection amplitudes increases that it was completely water saturated. These two examples illustrate that quantitative interpretation of fluid type can be made based on computed rock properties and seismic data. They also show the importance of fluid properties and reflections amplitudes. These amplitudes applied as a model and will be calibrated and correlated to the real seismic. The good correlation coefficient is considered to be closed to the real seismic data. And this model can be applied to predict the fluid in other area within the field.

YM-232 & YM-247 wells have good correlation, when it was substituted with 90% & 70% water saturation, the correlation coefficient are 0.88 and 0.87 . However, at YM-247 well, a good correlation is achieved when it was substituted with 100% & 70% water saturation, are 0.98 and 0.87. Actually, by knowing those model or we called as normalization model (after normalized to real seismic) : 0.77 (YM-232 well) and 0.96 (YM-247 well) can be applied within field as parameter to improve when interpreted 3D seismic data. Model amplitude of YM-232 & YM-247 wells, each of which can be a model that represents each field. Of course, after doing some test of

some well of each Y & M field. At YM-247 well, a model represents Y field, have the characters on the density log is contrast, so the rock more dominant than fluid.

This improved interpretation can reduce drilling risk and ultimately increase asset value by avoiding wet zone in this case.

The sensitivity analysis to critical reservoir parameters, has been done. Its worked at YM Field. Gassmann formula can be applied in this field, as we can see that the rock bulk modulus will change if the fluid changes, but the rock shear modulus will not. The advance analysis like relations between V_p and V_s are key to the determination of lithology from seismic or sonic log data, as well as for direct seismic identification of pore fluids using, for example, AVO analysis is needed. And seismic inversion to see the lateral distribution of reservoir properties. In this thesis, I've not made AVO, because of unavailability of gathers data.



REFERENCES

- Avseth P, Mukerji T., & Mavko G., 2005. **Quantitative Seismic Interpretation, Applying Rock Physics Tools to Reduce Interpretation Risk**. Cambridge University Press. UK
- Chaveste, Alvaro., May 2003. **Risk reduction in estimation of petrophysical properties from seismic data through well-log modeling, seismic modeling, and rock properties estimation**. Core Laboratories Reservoir Technologies Division, Houston, Texas, U.S.
- Kumar, Dhananjay., January 4, 2006. **A Tutorial on Gassmann Fluid Substitution : Formulation, Algorithm and Matlab Code**. Chevron Energy Technology Company, California
- Mavko, Gary. **Introduction to Rock Physics**. Stanford Rock Physics Laboratory.
- Munadi, Suprajitno., October, 2007. **The Effect of Oil Content on Sonic Wave Propagation (Analyses from Well Log Data)**. Lemigas Contributions Vol. 30 No. 2
- Munadi, Suprajitno, 2000. **Aspek Fisis Seismologi Eksplorasi**. Program Studi Geofisika, Jurusan Fisika, FMIPA, Universitas Indonesia, Depok.
- Pennington, W.D., 2008. **Advanced Seismic Petrophysics**. NEXT Course Note. Bandung
- M. Smith*, Tad., H. Sondergeld, Carl., S. Rai, Candra, March-April 2003. **Tutorial Gassmann Fluid Substitutions : A tutorial**. Geophysical, Vol. 68, No. 2.
- R.M.I. Argakoesoemah., Rahardja Maria., Winardhi Sonny., Tarigan Rudhy., Febriwan Tino., Aimar Amritzar, Agustus 30-September 1, 2005. **Telisa Shallow Marine Sandstone as An Emerging Exploration Target in Palembang High, South Sumatra Basin**. 30th Annual Convention & Exhibition, IPA
- D. Walls, Joel. **Fluids, AVO, and Seismic Amplitudes : field examples**. PetroSoft Inc.
- Walls, Joel., Dvorkin Jack., Carr, Matt., 2004. **Well Logs and Rock Physics in Seismic Reservoir Characterization**. Rock Solid Images. Houston, Texas, U.S.A